Received: 24 July 2017 | Accepted: 8 February 2018

DOI: 10.1002/dep2.40

ORIGINAL RESEARCH ARTICLE

WILEY The Depositional Record Open Access
The journal of the International Association of Seidmentologisits

Tectono-stratigraphic response of the Sandino Forearc Basin (N-Costa Rica and W-Nicaragua) to episodes of rough crust and oblique subduction

Goran Andjić[1] | **Claudia Baumgartner-Mora**[1] | **Peter Oliver Baumgartner**[1] | **Maria Rose Petrizzo**[2]

[1]Institut des Sciences de la Terre, Université de Lausanne, Lausanne, Switzerland

[2]Dipartimento di Scienze della Terra, Università degli Studi di Milano, Milano, Italy

Correspondence
Goran Andjić, Institut des Sciences de la Terre, Université de Lausanne, Lausanne, Switzerland.
Email: goran.andjic@unil.ch

Funding information
Swiss National Science Foundation, Grant/Award Number: 200021-134873, 200020-143894; Herbette Foundation at the University of Lausanne

Abstract

The southern Central American active margin is a world-class site where past and present subduction processes have been extensively studied. Tectonic erosion/accretion and oblique/orthogonal subduction are thought to alternate in space and time along the Middle American Trench. These processes may cause various responses in the upper plate, such as uplift/subsidence, deformation, and volcanic arc migration/shut-off. We present an updated stratigraphic framework of the Late Cretaceous–Cenozoic Sandino Forearc Basin (SFB) which provides evidence of sedimentary response to tectonic events. Since its inception, the basin was predominantly filled with deep-water volcaniclastic deposits. In contrast, shallow-water deposits appeared episodically in the basin record and are considered as tectonic event markers. The SFB stretches for about 300 km and varies in thickness from 5 km (southern part) to about 16 km (northern part). The drastic, along-basin, thickness variation appears to be the result of (1) differential tectonic evolutions and (2) differential rates of sediment supply. (1) The northern SFB did not experience major tectonic events. In contrast, the reduced thickness of the southern SFB (5 km) is the result of at least four uplift phases related to the collision/accretion of bathymetric reliefs on the incoming plate: (i) the accretion of a buoyant oceanic plateau (Nicoya Complex) during the middle Campanian; (ii) the collision of an oceanic plateau (?) during the late Danian–Selandian; (iii) the collision/accretion of seamounts during the late Eocene–early Oligocene; (iv) the collision of seamounts and ridges during the Pliocene–Holocene. (2) The northwestward thickening of the SFB may have been enhanced by high sediment supply in the Fonseca Gulf area which reflects sourcing from wide, high relief drainage basins. In contrast, sedimentary input has possibly been lower along the southern SFB, due to the proximity of the narrow, lowland isthmus of southern Central America. Moreover, two phases of strongly oblique subduction affected the margin, producing strike-slip faulting in the forearc basin: (1) prior to the Farallon Plate breakup, an Oligocene transpressional phase caused deformation and uplift of the basin depocenter, triggering shallowing-upward of the Nicaraguan Isthmus in the central and northern SFB; (2) a Pleistocene–

Holocene transtensional phase drives the NW-directed motion of a forearc sliver and reactivation of the graben-bounding faults of the late Neogene Nicaraguan Depression. We discuss arguments in favour of a Pliocene development of the Nicaraguan Depression and propose that the Nicaraguan Isthmus, which is the apparent rift shoulder of the depression, represents a structure inherited from the Oligocene transpressional phase.

KEYWORDS
Late Cretaceous–Cenozoic, Nicaragua, oblique subduction, Sandino forearc basin, seamount/plateau collision, tectonic uplift

1 | INTRODUCTION

The construction of the Central American land bridge represents a long-term process that initiated in Cretaceous time (Bundschuh & Alvarado, 2007; Dengo & Case, 1990; Figure 1). Since that time, collision/accretion, subduction and strike-slip processes operated in association with arc volcanism, building a complex geological puzzle (Mann, 2007). The present-day terrane collage consists mainly of a northern province (from Guatemala to N-Nicaragua), made of Precambrian–Mesozoic continental terranes of North America-affinity (Chortis Block *s.s.*), and a southern province (from S-Nicaragua to Panama) made of Mesozoic–Cenozoic oceanic assemblages (Baumgartner, Flores, Bandini, Girault, & Cruz, 2008; Buchs, Arculus, Baumgartner, Baumgartner-Mora, & Ulianov, 2010; Denyer & Gazel, 2009; Flores, 2009; Rogers, Mann, & Emmet, 2007; Figure 1b). The oceanic assemblages reveal the long-lived influence of the Galápagos hotspot on the geologic history of southern Central America. The latter has been shaped by the collision/subduction of seamounts, ridges and plateaus since the Late Cretaceous. In addition, the fore-, intra- and backarc basins deposited on these provinces recorded the tectonic evolution of the active margin (Figure 1c). Tectonic events led to major facies changes, unconformities, deformations and variations in the supply of arc-derived material (Barat et al., 2014; Baumgartner, Baumgartner-Mora, & Andjić, 2016; Baumgartner, Baumgartner-Mora, Andjić, Salazar Ortiz, & Rincon Martinez, 2015; Brandes, Astorga, Littke, & Winsemann, 2008; Kolarsky, Mann, Monechi, Meyerhoff, & PessagnoJr, 1995; Krawinkel, Seyfried, Calvo, & Astorga, 2000; Rogers, Mann, Emmet, & Venable, 2007; Rogers, Mann, Scott, & Patino, 2007).

The Sandino Forearc Basin (SFB; Figures 1–5) represents a natural laboratory where the sedimentary response to tectonic events may be investigated. The onland geology of the SFB has been studied since the earliest 20th century (see Bundschuh & Alvarado, 2007; Hoffstetter et al., 1960; Weyl, 1980; Zoppis Bracci & Del Giudice, 1958; and references therein). Since the 1990s, few sedimentological contributions were published, especially regarding the Nicaraguan part of the basin (Elming, Widenfalk, & Rodriguez, 1998; Kolb & Schmidt, 1991; Krawinkel & Kolb, 1994; Lang, Brandes, & Winsemann, 2017; Struss, Artiles, Cramer, & Winsemann, 2008; Struss, Brandes, Blisniuk, & Winsemann, 2007; Winsemann, 1992). At the same time, most of the basin studies focused on geophysical data acquisition and modelling (Berhorst, 2006; Cailleau & Oncken, 2008; DeMets, 2001; Elming, Layer, & Ubieta, 2001; Elming & Rasmussen, 1997; Funk, Mann, McIntosh, & Stephens, 2009; McIntosh et al., 2007; Noda, 2016; Ranero et al., 2000; Sallarès et al., 2013; Stephens, 2014; Turner et al., 2007; Walther, Flueh, Ranero, Von Huene, & Strauch, 2000).

The general arrangement of the formations in the onshore basin was already mapped in the 1960s–1970s (Dengo, 1962; Weyl, 1980). Yet, it appears that the onshore SFB hosts sedimentary units that have been overlooked in the past decades. The age and facies of these new units may shed a new light on the basin evolution. In a recent paper, we updated the stratigraphy of the Costa Rican part of the SFB, with the description of two new, shallow-shelf formations (Andjić, Baumgartner-Mora, & Baumgartner, 2016; Figures 3 and 4). In this study, we present facies descriptions and biostratigraphic data of previously undescribed lithologies. Altogether, these new data allow us to propose a rather detailed tectono-stratigraphic evolution of the SFB, which is refined by recent offshore, seismic reflection data (Berhorst, 2006; Funk et al., 2009; McIntosh et al., 2007; Ranero et al., 2000; Stephens, 2014). Eventually, the evolution of the basin is discussed with reference to regional tectonic events and subduction processes that affected the active margin of southern Central America.

2 | THE SANDINO FOREARC BASIN

The SFB extends over a distance of 300 km, from the Santa Elena Peninsula (Costa Rica) to the Fonseca Gulf (Honduras-El Salvador-Nicaragua triple point; Figures 1–3). Over 85% of the SFB is located offshore (Figure 2).

Offshore western Nicaragua, the basin presents a km-thick depocenter which coincides with the present-day shelf (<500 m water depth; Ranero et al., 2000; Figures 2 and 3). In its southeastern part, the depocenter is filled with 5 km of sediments (Figure 5c), whereas its thickness reaches ~16 km towards the Gulf of Fonseca (McIntosh et al., 2007; Figure 5a). The depocenter is separated from the trench slope by an outer high where the sediment thickness is reduced (<2–3 km; Figures 2a and 5). A narrow strip of coastal outcrops in southwestern Nicaragua and northwestern Costa Rica accounts for ~10% of the total area of the forearc basin. Onshore exposures of the basin are located in the vicinity of the Santa Elena Peninsula and in part along the 300-km-long Nicaraguan Isthmus (Zoppis Bracci & Del Giudice, 1958; Figures 2 and 3). The latter is bordered to the east by a half-graben, the fault-bounded Nicaraguan Depression, which hosts the active volcanic front (Funk et al., 2009; Weyl, 1980; Figure 3).

The Santa Elena Peninsula provides a glimpse into what could be the oceanic basement of the southern SFB (Figure 3). It consists of a tectonic stack of two distinct assemblages originating from the same intraoceanic edifice: (1) the Santa Elena Ophiolite is made of abyssal and supra-subduction zone peridotites intruded and overlain by arc gabbros (Escuder-Viruete, Baumgartner, & Castillo-Carrión, 2015; Madrigal et al., 2015; Whattam, Gazel, Yi, & Denyer, 2016); (2) the ophiolite thrusts over a serpentinite-matrix mélange embedding remnants of an island arc (Nancite Layered Complex, ~124 Ma) and the Santa Rosa Accretionary Complex, made of stacked Jurassic–Early Cretaceous oceanic floor units (Bandini, Baumgartner, Flores, Dumitrica, & Jackett, 2011; Baumgartner & Denyer, 2006; Buchs et al., 2013; Escuder-Viruete & Baumgartner, 2014; Hauff, Hoernle, van den Bogaard, Alvarado, & Garbe-Schönberg, 2000). In middle Cretaceous time, the two assemblages were superposed during the accretion of the intraoceanic arc to the Mesquito Composite Oceanic Terrane (MCOT; Figure 1b). The latter possibly floors most of Nicaragua and corresponds to a serpentinite-matrix mélange containing oceanic floor and arc-derived rocks, including radiolarites of Triassic–Jurassic age (Baumgartner et al., 2008; Flores, 2009; Flores et al., 2015). The MCOT is thought to have accreted to the Chortis Block during the latest Jurassic–earliest Cretaceous. The limit between the MCOT and the Santa Elena arc is not exposed. In the southern Nicaraguan Isthmus, a basaltic basement was sampled in the Rivas-1 borehole (near the city of Rivas; Ranero et al., 2000; Figure 3). However, there is no sufficient data to tie this basement to a specific terrane.

Considering geochronologic, isotopic and geochemical data, Geldmacher, Hoernle, van den Bogaard, Hauff, and Klügel (2008) showed the similarity between the forearc basement off Guatemala and the Santa Elena arc (DSDP Legs 67 and 84; Figure 1c). Moreover, seismic data suggest the presence of a mantle wedge beneath the depocenter of the southern SFB (at ~10 km depth), in the prolongation of the Santa Elena Peninsula (Berhorst, 2006; Sallarès et al., 2013; Figure 5c). Towards the NW, a mantle wedge is also detected in an outer high position (Figure 5b) and may represent an oceanic plateau remnant (Walther et al., 2000) or alternatively a lateral equivalent of the Santa Elena accreted arc.

The SFB hosts various sedimentary formations which were deposited through Late Cretaceous-Neogene times (Figures 3–5). The oldest sediments in contact with the basement are poorly known. They were only recovered in the Rivas-1 and El-Ostional-1 boreholes and correspond to volcaniclastic turbidites and cherts (pre-Campanian "Loma Chumico Fm."; Barbosa et al., 1993; Ranero et al., 2000). In the Santa Elena Peninsula, middle Campanian neritic limestones (El Viejo and Santa Ana fms.) unconformably overlie the Santa Elena Ophiolite (Denyer, Aguilar, & Montero, 2014; Pons, Vicens, & Schmidt-Effing, 2016; Schmidt-Effing, 1974; Seyfried & Sprechmann, 1985). These limestones were rapidly replaced by globotruncanid-rich, pelagic limestones of the upper Campanian–upper Maastrichtian Piedras Blancas Fm. (~50 m thick; Baumgartner et al., 1984; Di Marco, Baumgartner, & Chanell, 1995; Flores, 2003). The lateral extent of the Piedras Blancas Fm. towards the north is unknown. Its northernmost occurrence is in the El-Ostional-1 borehole (Figures 3 and 4). The pelagic limestones are overlain by arc-derived, deep-water turbidites of the upper Maastrichtian-Palaeocene Rivas Fm. (=Curú Fm. in Costa Rica, 500–1,000 m thick; Astorga, 1987; Darce & Duarte, 2002; Joy, 1941; Struss et al., 2008; Winsemann, 1992). In the southern Nicaraguan Isthmus, the upper Danian–early Selandian, shallow-water Sapoá limestones unconformably overlie the Rivas Fm. (see next section; Figures 3 and 4). The Sapoá limestones present facies and age characteristics similar to those of the Costa Rican upper Palaeocene Barra Honda Fm. (Baumgartner-Mora & Baumgartner, 2016; Jaccard, Münster, Baumgartner, Baumgartner-Mora, & Denyer, 2001). In the southern Nicaraguan Isthmus and in northern Costa Rica, the Rivas–Curú turbidites are overlain by the siliceous pelagic limestones of the upper Palaeocene–lower Eocene Buenavista Fm. (~250 m thick; Baumgartner et al., 1984). The overlying Eocene Brito Fm. (=Descartes Fm. in Costa Rica) is the thickest forearc formation of the SFB (up to 4,000 m in the offshore depocenter; Ranero et al., 2000; Figure 5). It consists of basin-plain, thin-bedded volcaniclastic turbidites and siliceous pelagics interstratified with laterally and vertically stacked coarse-grained channel-levee complexes (Astorga, 1987; Darce & Duarte, 2002; Hayes, 1899; Lang et al., 2017; Struss et al., 2007;

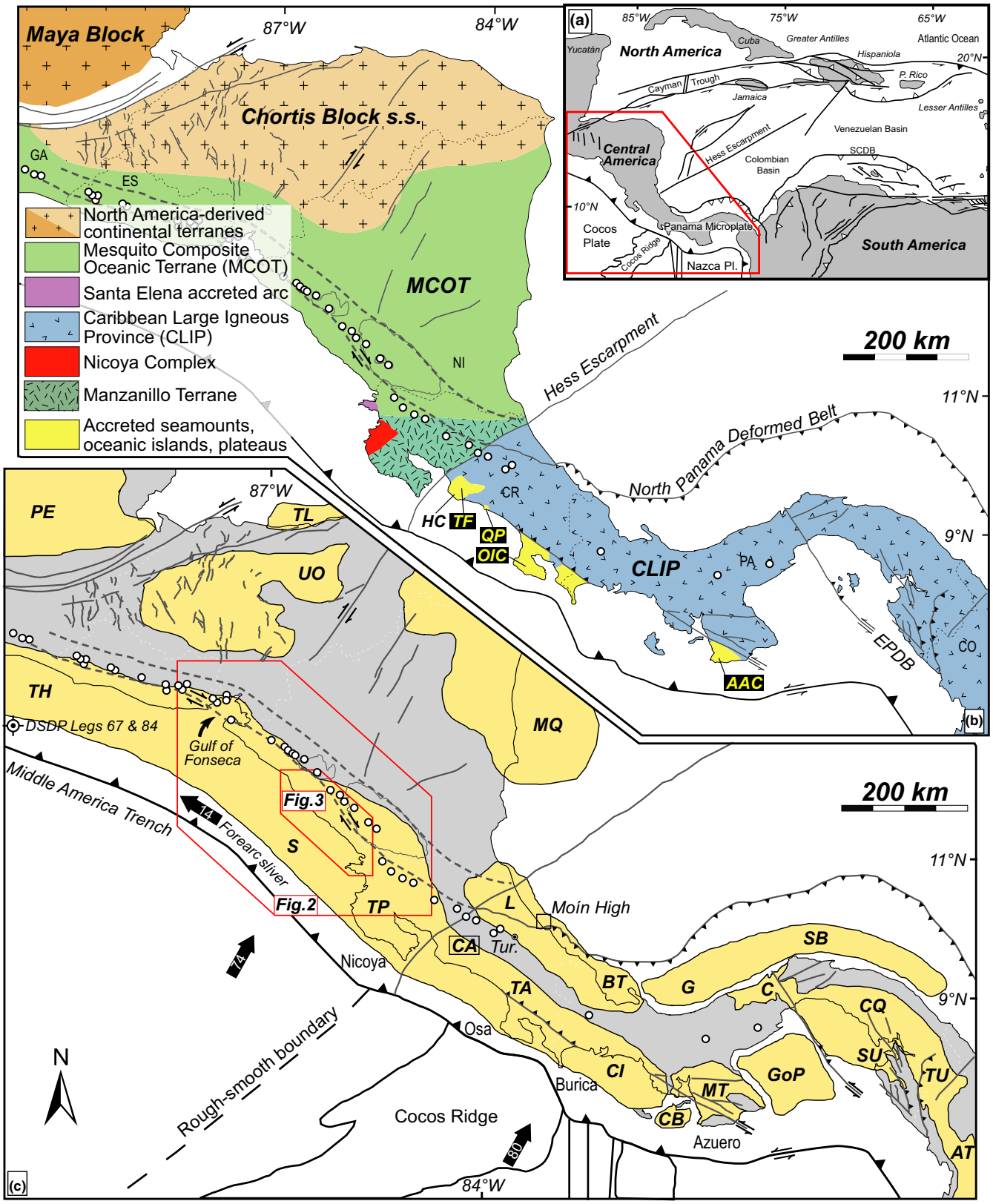

Winsemann, 1992). In the southern Nicaraguan Isthmus and in northern Costa Rica, the Brito-Descartes formations are overlain by volcaniclastic tempestites (Junquillal Fm. in Costa Rica, El Astillero Fm., herein described, in Nicaragua; Andjić et al., 2016). The formations of the southern SFB are very similar to those exposed in the Tempisque Forearc Basin, located further to the south (Alvarado et al., 2007).

FIGURE 1 (a) Tectonic map of the Caribbean Plate (modified after Pindell & Kennan, 2009). The studied area is indicated with the red polygon. SCDB-South Caribbean Deformed Belt. Black triangles: subduction zones. White triangles: thrust belts. (b) Terrane map displaying the major structural features of the western Caribbean Plate (modified after Barat et al., 2014; Baumgartner et al., 2008; Buchs et al., 2010; Flores, 2009; Rogers & Mann, 2007). Dashed grey lines represent the Nicaraguan Depression. AAC, Azuero Accretionary Complex; HC, Herradura Complex; TF, Tulín Formation; OIC, Osa Igneous Complexes; QP, Quepos; GA, Guatemala, ES, El Salvador, HS, Honduras, NI, Nicaragua, CR, Costa Rica, PA, Panama, CO, Colombia, EPDB, East Panama Deformed Belt. (c) Mesozoic–Cenozoic basins of Central America (after Alvarado et al., 2007; Barat et al., 2014; Dengo, 2007; Escalante, 1990; Kolarsky et al., 1995; Mann, 1995; Mann & Kolarsky, 1995; Rogers & Mann, 2007; Morell, 2015). Velocities (mm/year): Cocos Plate after Kobayashi et al. (2014); forearc after DeMets (2001). Basin names abbreviations, from NW to ESE: PE, Péten; TL, Tela; MQ, Mosquitia; UO, Ulua-Olancho; TH, Tehuantepec; S, Sandino; TP, Tempisque; L, Limón; CA, Candelaria; TA, Térraba; BT, Bocas del Toro; CI, Chiriquí; CB, Cebaco; MT, Macaracas, Tonosí; G, Gatun; SB, San Blas; C, Canal; GoP, Gulf of Panama; CQ, Chucunaque; SU, Sambu; TU, Tuira; AT, Atrato. Other abbreviations: Tur., Turrialba

In contrast, in the central Nicaraguan Isthmus, the Brito Fm. is overlain by fine-grained volcaniclastic turbidites and hemipelagics of the Oligocene–lower Miocene Masachapa Fm. (1,500-2,000 m thick; Kuang, 1971; Weyl, 1980; Wilson, 1941a). Towards the top of the Masachapa Fm. the proportion of sand is higher, marking the transition to the overlying shallow-shelf Miocene El Fraile Fm. The El Fraile Fm. is composed of fine- to coarse-grained, deltaic, volcaniclastic deposits (1,200–1,800 m; Kolb & Schmidt, 1991; Krawinkel & Kolb, 1994; Ranero et al., 2000; Struss, 2008; Wilson, 1942). Towards the NW, the El Fraile Fm. is interbedded with the middle Miocene, volcanic Tamarindo Fm., which consists of massive, subaerial tuffs alternating with lavas (900 m thick; McBirney & Williams, 1965; Wilson, 1941b; Zoppis Bracci & Del Giudice, 1958; Figures 3 and 4). Finally, the shallow-shelf, Pliocene El Salto Fm. unconformably overlies older formations and shows alternations of carbonate-bearing, tuffaceous volcaniclastics and mollusc-rich, neritic carbonates (100 m thick onshore, up to 1,000 m offshore; Kirby & Jackson, 2004; Ranero et al., 2000; Wilson, 1941a; Zoppis Bracci & Del Giudice, 1958).

3 | NEW STRATIGRAPHIC AND BIOCHRONOLOGIC DATA OF THE SANDINO BASIN (NICARAGUA)

3.1 | Sapoá limestones

3.1.1 | Facies description

The Sapoá limestones crop out in a series of quarries 2 km southwest of the town of Sapoá, near the Costa Rican border (Cárdenas quadrangle; Figures 3, 4 and 6). The Sapoá limestones represent shallow-water deposits exposed in a small area (2 km^2; Figure 6a,b) with a total thickness of ~30 m (Figure 6c).

The Sapoá limestones unconformably overlie a deeply scoured, 2 m thick, highly weathered andesitic flow (N11°13′48.6″/W085°38′31.4″). The andesite presents a porphyritic texture and contains weathered, subeuhedral feldspars (lengths 0.25–0.75 mm) which often display cruciform twinning (Figures 6c and 7j–l). The groundmass is composed of much smaller feldspars and opaque grains (<0.03 mm). The andesitic flow is underlain by two poorly preserved facies. The lower one corresponds to black, hemipelagic limestones rich in planktonic Foraminifera. It is overlain by a dark grey, recrystallized, wackestone containing a few distinguishable shallow-water bioclasts (green algae, echinoid spines, miliolids). A centimetric bed of inversely graded, matrix-supported breccia rests with a sharp erosional surface (locally cut-and-fill) on the wackestone (Figures 6c and 7i). The breccia is composed of millimetric, angular clasts of the underlying, wackestone as well as clasts of black, hemipelagic wackestone. The matrix of the breccia was recrystallized to microspar, pseudospar and drusy calcite. However, an original, plane-parallel lamination is preserved in its lower, fine-grained part.

The Sapoá limestones consist of several different facies, from bottom to top (Figures 6c and 7):

1. 3 m of dark grey, nodular miliolid-mollusc-dasycladacean wackestones overlying the andesitic flow (Figure 7l).
2. 20 m of irregularly bedded, beige to white, wackestones presenting a micrite-microspar matrix. The bioclastic content consists of miliolids and fine to coarse sand-sized fragments of dasycladacean alga, peyssonnelid alga, corallinacean red alga, mollusc and echinoderm. The peyssonnelid algae may appear as crusts binding the sediment and as unilayered rhodoliths (Figure 7h). Locally, the wackestones alternate with peloidal-green algal grainstones (udoteaceans, dasycladaceans) and coral-red algal rudstones-floatstones (peyssonnelids, solenoporaceans, corallinaceans; Figure 7f). In the upper part, fenestral, non-laminated, red wackestones occur (northeasternmost quarry; Figures 6b and 7g). The fenestral cavities are filled with microspar and drusy sparite. Voids are present along unconformities with the underlying grainstones and were filled with muddy, red sediment containing ostracods and oxidized anomuran

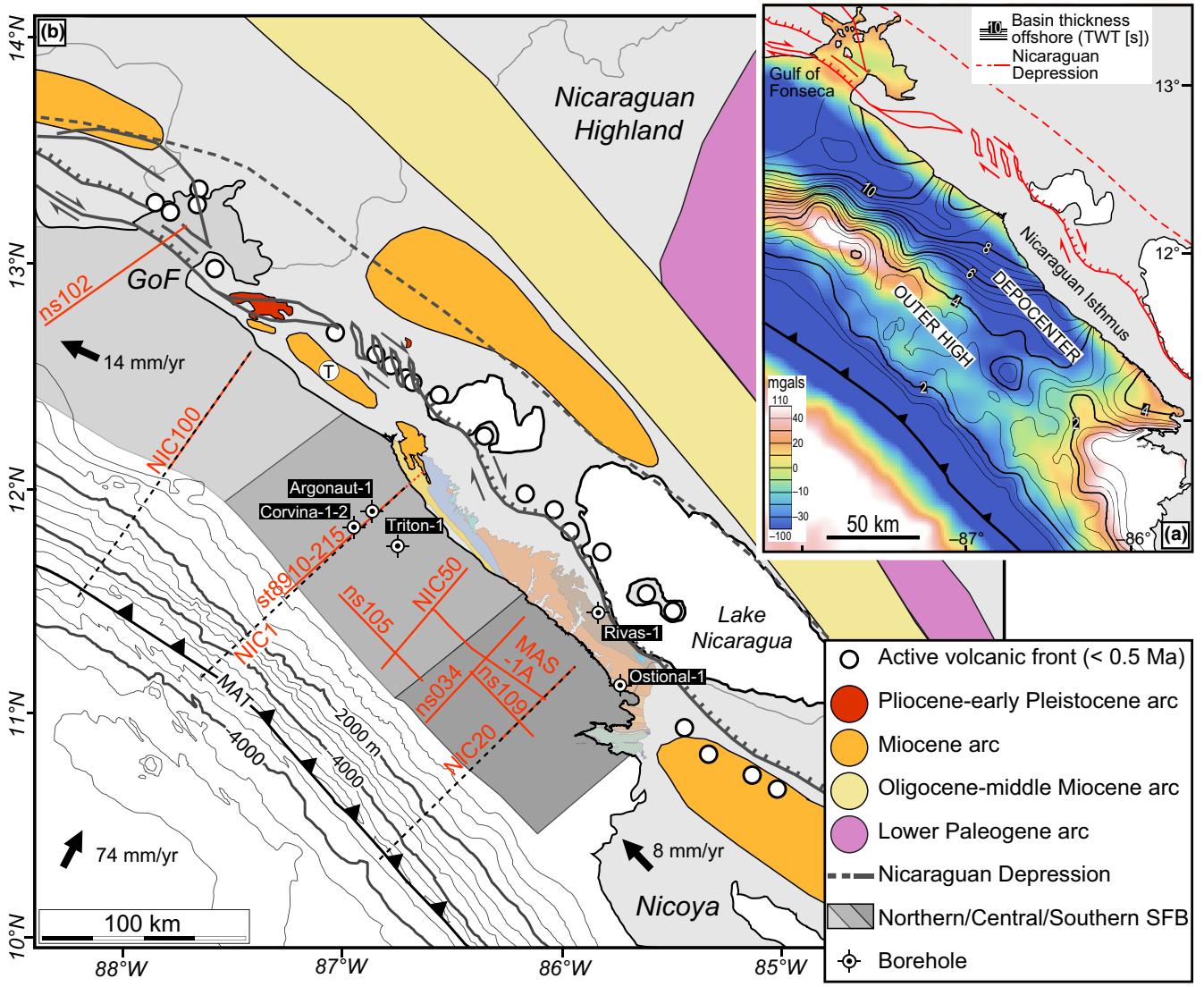

FIGURE 2 Maps of onshore and offshore areas located between northern Costa Rica and the Gulf of Fonseca. (a) Onshore: the Nicaraguan Depression is after Funk et al. (2009). Offshore: satellite free-air gravity map after Sandwell and Smith (1997), extracted from GeoMapApp; basin thickness in TWT[s] after Stephens (2014). (b) Onshore: the locations of ancient and modern volcanic fronts are indicated (after Alvarado et al., 2007; Saginor, Gazel, Condie, & Carr, 2013) together with the Nicaraguan Depression (after Funk et al., 2009). Note the trenchward migration of the successive volcanic fronts through the Neogene. Onland geology of the Sandino Forearc Basin is displayed in transparency along the southern Nicaraguan Isthmus. See Figure 3 for the detailed geological map. Offshore: seismic lines correspond to the seismic profiles depicted in Figure 5 (dashed black lines) and in Figure 19 (continuous red lines; after Funk et al., 2009; McIntosh et al., 2007; Ranero et al., 2000; Stephens, 2014). From the NW to the SE, the three grey boxes correspond to the northern, central and southern Sandino Basin. Onshore and offshore wells are also indicated (after Ranero et al., 2000). Offshore bathymetry is after McIntosh et al. (2007). GPS velocities are after DeMets (2001), Montero and Denyer (2011), and Kobayashi et al. (2014). GoF, Gulf of Fonseca; T, Tamarindo Fm.; MAT, Middle American Trench

coprolites. Bioclastic grains are scarce (<10%) and comprise miliolids and fragments of gastropod and alga.

3. 5 m-thick sponge patch reef consisting of tubular demosponges in a massive, dark grey-blue limestone. The sponge tubes grew in random directions and show centimetric sizes (1–10 cm long, 1–4 cm thick). The skeletons structure corresponds to a delicate, three-dimensional framework of interlocking sponge spicules with an axial canal, the whole being filled with mud (Figure 7d,e). Delicate, branched coral frameworks with millimetric, vertically growing polyps are also present in places (Figure 7c). The sponges and the corals are recrystallized in calcite and embedded in a mudstone matrix containing rare smaller benthic Foraminifera. Locally, small scale fractures are filled with hemipelagic, brown sediment. The latter contains smaller benthic Foraminifera, planktonic Foraminifera and plagioclase crystals.

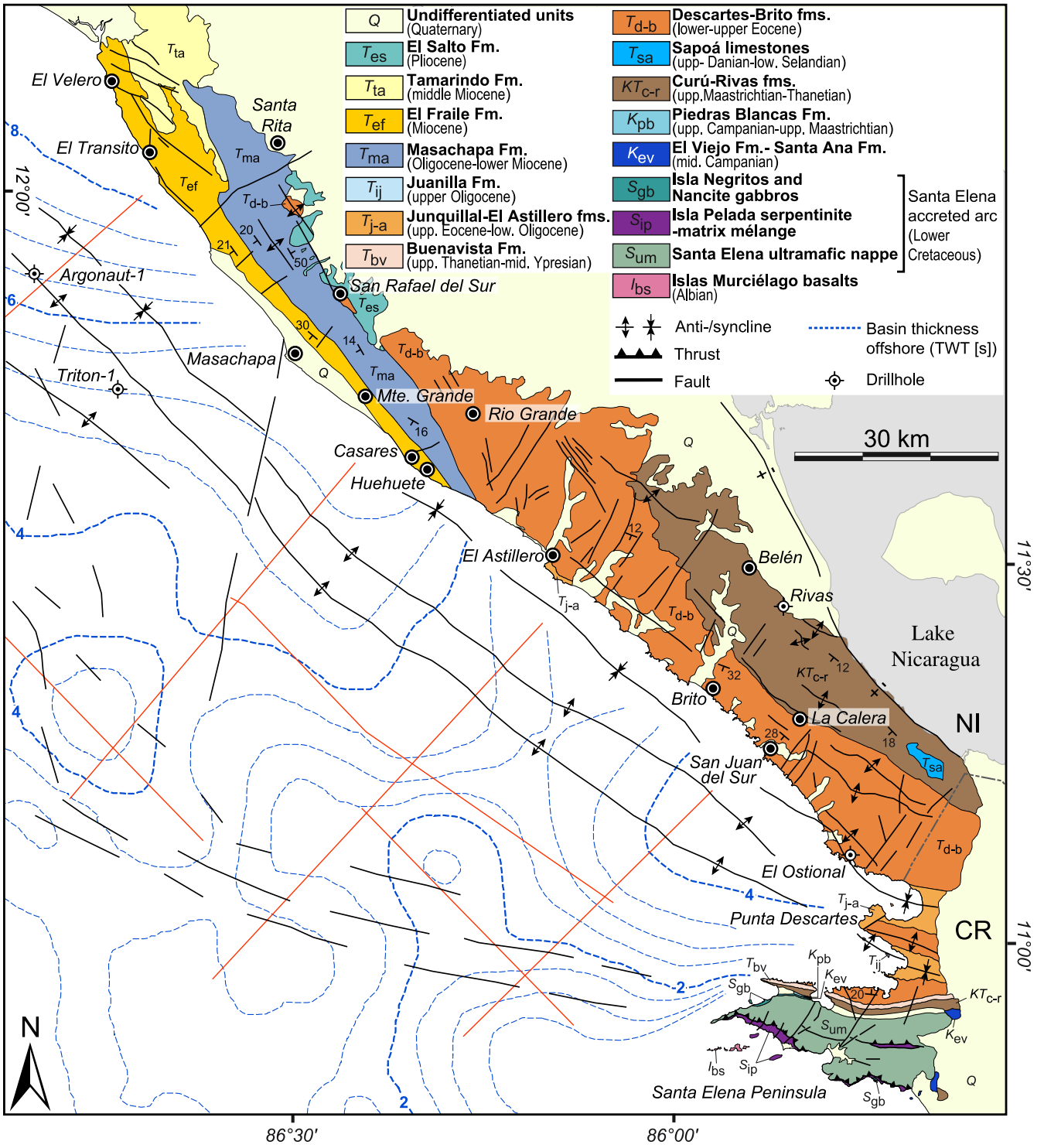

FIGURE 3 Geological map of the Sandino Forearc Basin in the southern Nicaraguan Isthmus (modified after Andjić et al., 2016; Astorga, 1987; Baumgartner et al., 1984; Darce & Duarte, 2002; Dengo, 1962; Denyer & Alvarado, 2007; Escuder-Viruete et al., 2015; Weyl, 1980). Offsore isopachs represent the thickness of the sedimentary infill (after Stephens, 2014). See Figure 2b for the locations of the seismic lines (in red). CR, Costa Rica; NI, Nicaragua

4. 2 m of massive wackestones and packstones, containing miliolids and fragments of dasycladacean, peyssonnelid, and corallinacean red alga, and echinoderm.

In the southeasternmost quarry (Figure 6a,b), the Sapoá limestones are overlain along an erosional unconformity by 1.5–2 m of massive, matrix-supported, dark green-

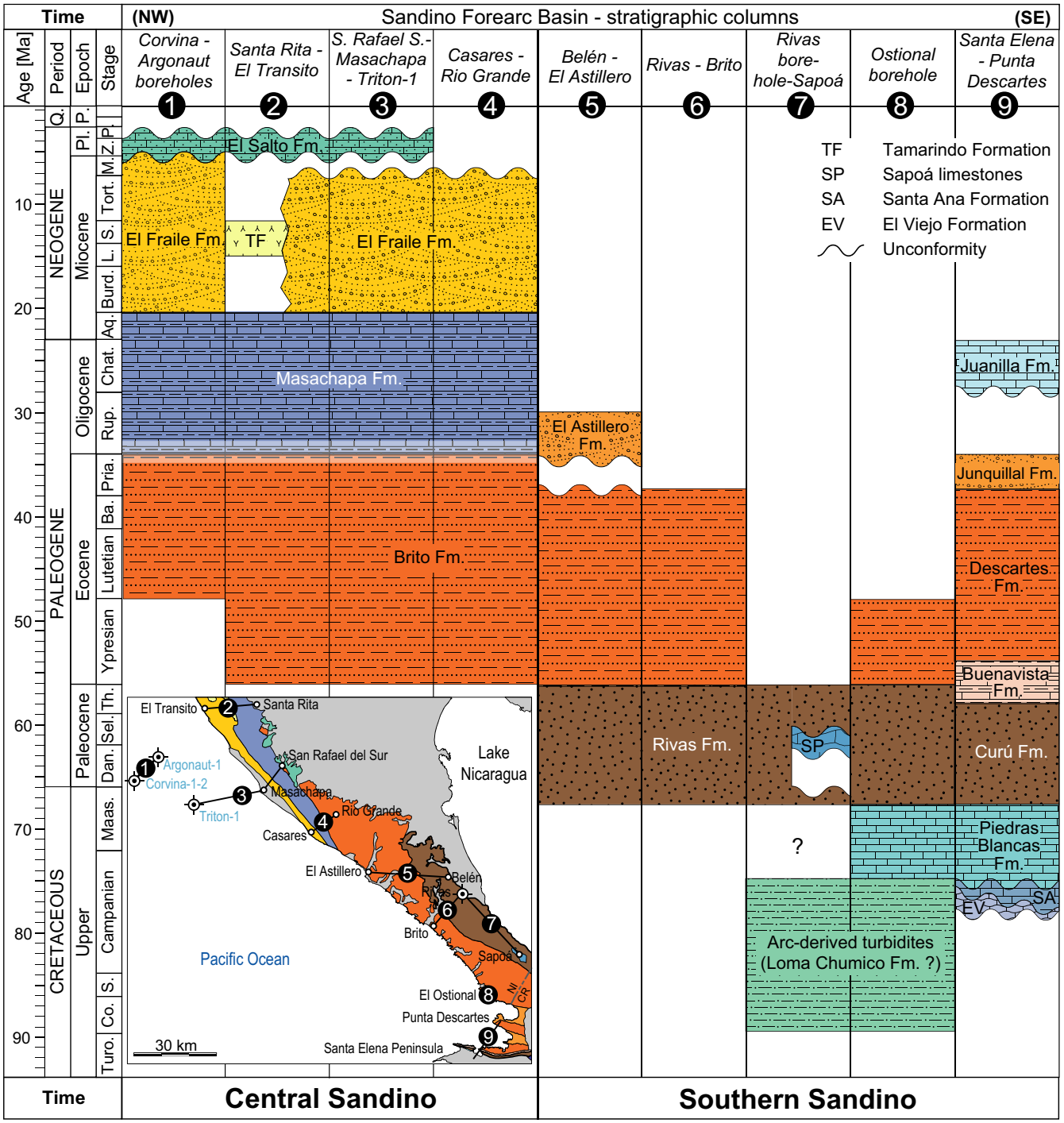

FIGURE 4 Updated chronostratigraphic chart of the Sandino Forearc Basin (stratigraphic data from: Andjić et al., 2016; Astorga, 1987; Baumgartner et al., 1984; Dengo, 1962; Di Marco et al., 1995; Hoffstetter et al., 1960; Joy, 1941; Pons et al., 2016; Ranero et al., 2000; Weyl, 1980; Wilson, 1941a, 1941b, 1942; Zoppis Bracci & Del Giudice, 1958; this study). Localities indicated in the upper part of the figure are depicted in the map (lower left) and in Figures 2 and 3. For the distinction between northern, central and southern Sandino see also Figure 2. The white transparent rectangle highlights a lack of age constraint for the Brito-Masachapa boundary

black conglomerates. This polymict, pebble conglomerate facies consists of sands to pebbles of Sapoá limestones and volcanic rocks in equal proportions, all embedded in a carbonate-bearing, arkosic wacke matrix (Figure 7a,b). The protoliths of the volcanic clasts include crystal tuffs as well as holocrystalline and porphyritic, intermediate rocks. All these clasts mainly contain subeuhedral to euhedral, plagioclase crystals. The matrix exhibits individual plagioclase crystals with identical characteristics (25%–35% of the rock matrix). Other less common minerals (<10% of the matrix) consist of green clinopyroxene and opaque grains.

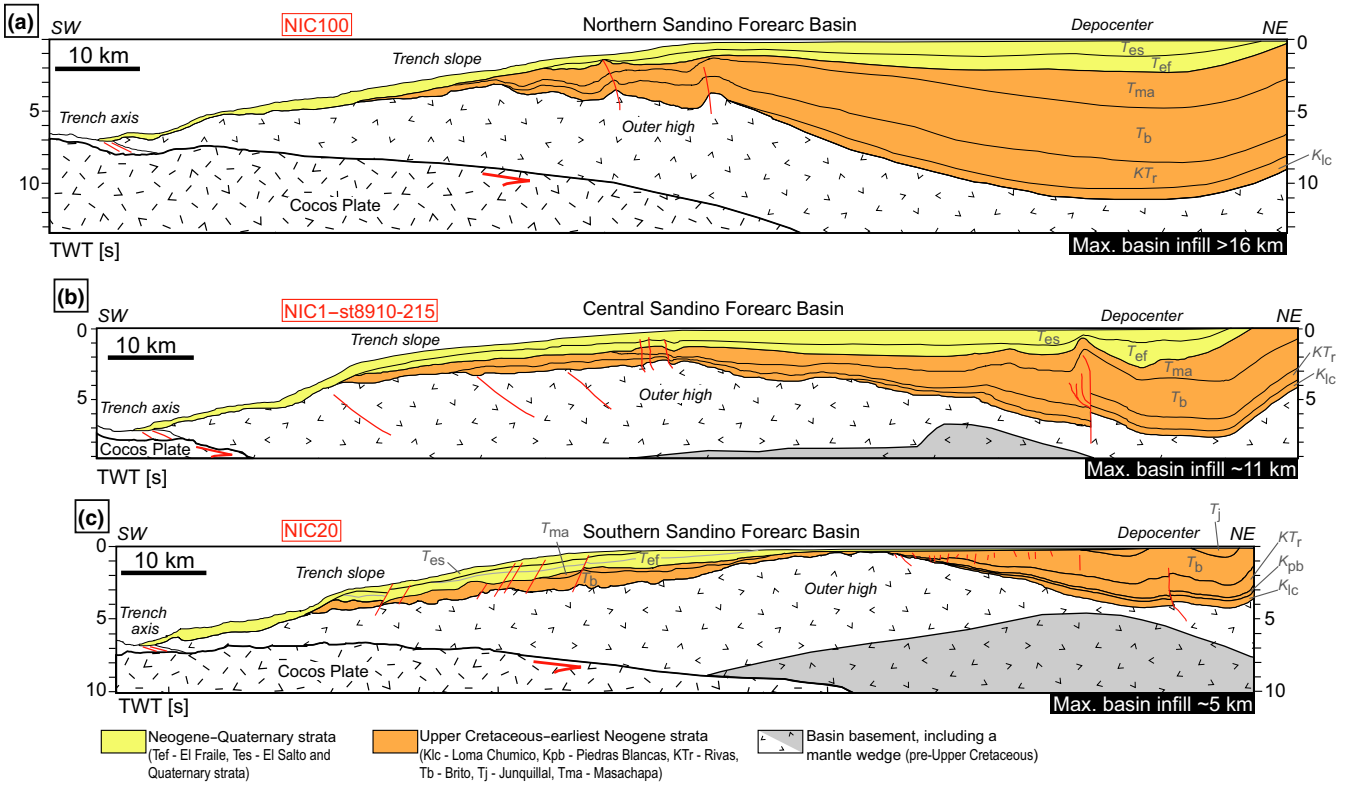

FIGURE 5 Seismic profiles of the northern (a; McIntosh et al., 2007), central (b; Ranero et al., 2000) and southern (c; Berhorst, 2006; Sallarès et al., 2013) Sandino Forearc Basin. See Figure 2b for profile locations. Pre-Miocene and post-Miocene strata are distinguished to evidence the change in basin morphology around the Oligocene–Miocene boundary (i.e. Noda, 2016)

The conglomerate facies grades progressively upward into a black, sandy wackestone which is only observed in the La Pita river, 380 m northwest of the said quarry (Figure 6a,b). The biogenic component is dominant (up to 20%) and corresponds to globigerinids (Figure 8) and scarce shallow-water bioclasts. Common detrital grains correspond to anhedral to subeuhedral plagioclases, anhedral green amphiboles and opaque grains.

3.1.2 | Age of the Sapoá limestones

The Sapoá limestones are stratigraphically set between hemipelagic limestones. We recovered one sample in the underlying hemipelagic limestones (SA14-15) and one sample in the overlying hemipelagic limestones (SA14-11; Figures 6c and 8). In both samples, Foraminifera are poorly preserved and the shell is completely recrystallized, preventing the identification of the wall textures. However, genera and some species can be identified according to their morphological features and to the thickness of the shell even if it is recrystallized. Planktonic Foraminifera are mainly represented by specimens belonging to the genera *Subbotina* and *Parasubbotina* and by trochospiral and planispiral benthic Foraminifera (Figure 8).

Based on the occurrence of *Subbotina* spp., *Subbotina triloculinoides* (Plummer), *Subbotina trivialis* (Subbotina), *Parasubbotina* spp., *Parasubbotina pseudobulloides* (Plummer), *Praemurica pseudoinconstans* (Blow), *Praemurica uncinata* (Bolli), *Morozovella praeangulata* (Blow), *Globanomalina compressa* (Plummer) and a single specimen of *Igorina* sp., the assemblages from both samples could be assigned to the stratigraphic interval between the upper part of Zone P2 and the lower part of Zone P3, which corresponds to a late Danian to early Selandian age. In comparison, the base of the coeval shallow-water unit of Costa Rica (Barra Honda Fm.) may not be older than the middle Selandian, with the presence of *Morozovella velascoensis* (Cushman) (Baumgartner-Mora & Baumgartner, 2016; Jaccard et al., 2001), the first occurrence of which lies in the upper part of Zone P3.

3.1.3 | Depositional environment

The different lithologies described in the Sapoá area indicate rapid changes in the depositional palaeoenvironment of the southern SFB during the earliest late Palaeocene. The observed facies evolution registered successively a subaerial emergence of basinal or deep shelfal lithologies on which a short-lived, carbonate bank developed, followed by the drowning of the latter to hemipelagic environments.

In a first step, black hemipelagic wackestones, initially accumulated in bathyal environments, were brought to the

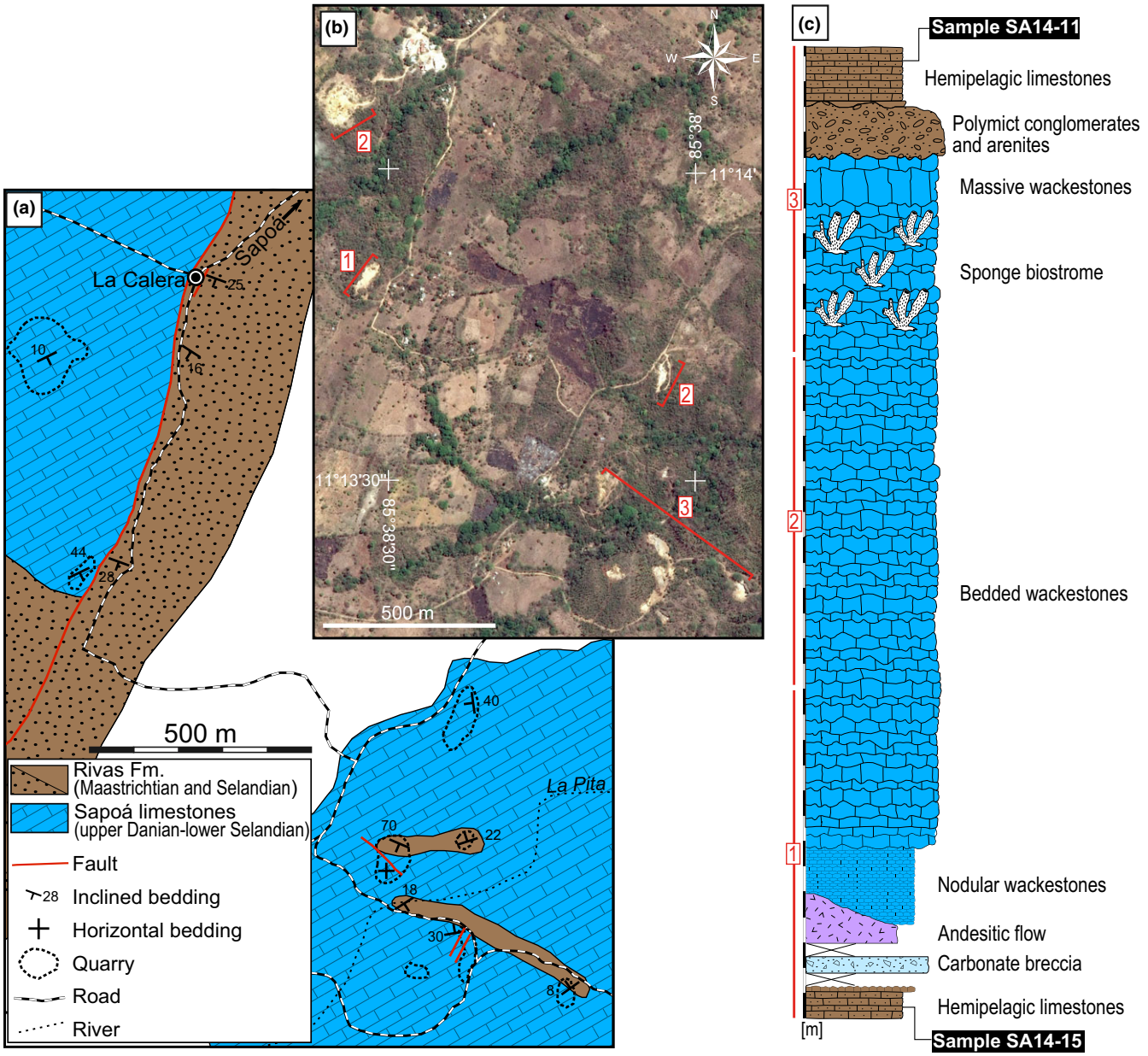

FIGURE 6 (a) Simplified geological map of the Sapoá area (Cardenas quadrangle). (b) Google Earth view of the area depicted in (a). The numbers 1–3 correspond to parts of the general column depicted in (c). (c) General column of the late Danian–early Selandian Sapoá limestones and encompassing deposits. The column is based on the facies descriptions made in the quarries depicted in (a) and (b). Dated samples are indicated (SA14-11 and SA14-15)

neritic zone, with the subsequent deposition of shallow-water bioclast-bearing wackestones. Then, these lithologies were uplifted, eroded, and reworked in a syn-tectonic breccia. Subaerial environments were reached as it is deduced from the occurrence of a subaerial andesitic flow upsection. Interestingly, Jaccard et al. (2001) and

FIGURE 7 Key facies of the Sapoá area. (a) Top of the late Danian–early Selandian Sapoá limestones. Unconformable contact between massive wackestones (Sapoá limestones) and overlying polymict conglomerates (Rivas Fm.). Hammer length is 31 cm. (b) Arkosic wacke representing the matrix of the conglomerate illustrated in (a). (c) Small coral colony embedded in a muddy matrix and locally occurring in the sponge biostrome. (d and e) Cm-sized sponge tubes occurring in the sponge biostrome. (f) *Solenopora* floatstone with a peloid-skeletal grainstone matrix. (g) Peloid-skeletal wackestone with fenestral fabrics. Fenestral cavities up to 4 mm in size. (h) Peysonnelid bindstone with mm-thick, cm-long algal crusts. (i) Unconformable contact between a dark wackestone and an overlying matrix-supported carbonate breccia. See Figure 6c. (j and k) Cruciform twinning in euhedral feldspars recovered from the andesitic flow shown in (l). Scale bars are 0.1 mm. (l) Base of the Sapoá limestones. Unconformable contact between nodular limestones and underlying andesitic flow. See text and Figure 6 for locations

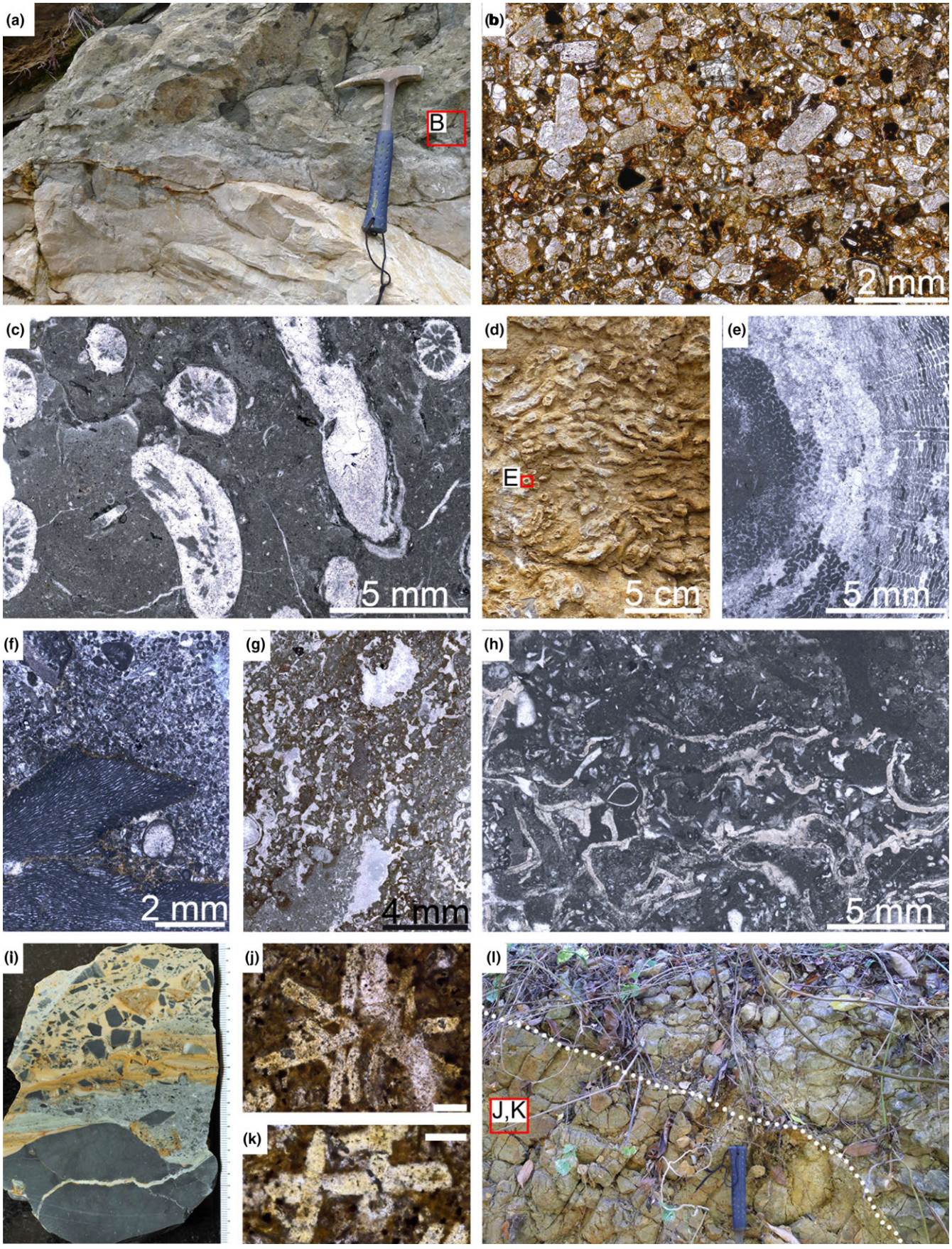
(a)
B
(b)
2 mm
(c)
5 mm
(d)
E
5 cm
(e)
5 mm
(f)
2 mm
(g)
4 mm
(h)
5 mm
(i)
(j)
(k)
(l)
J,K

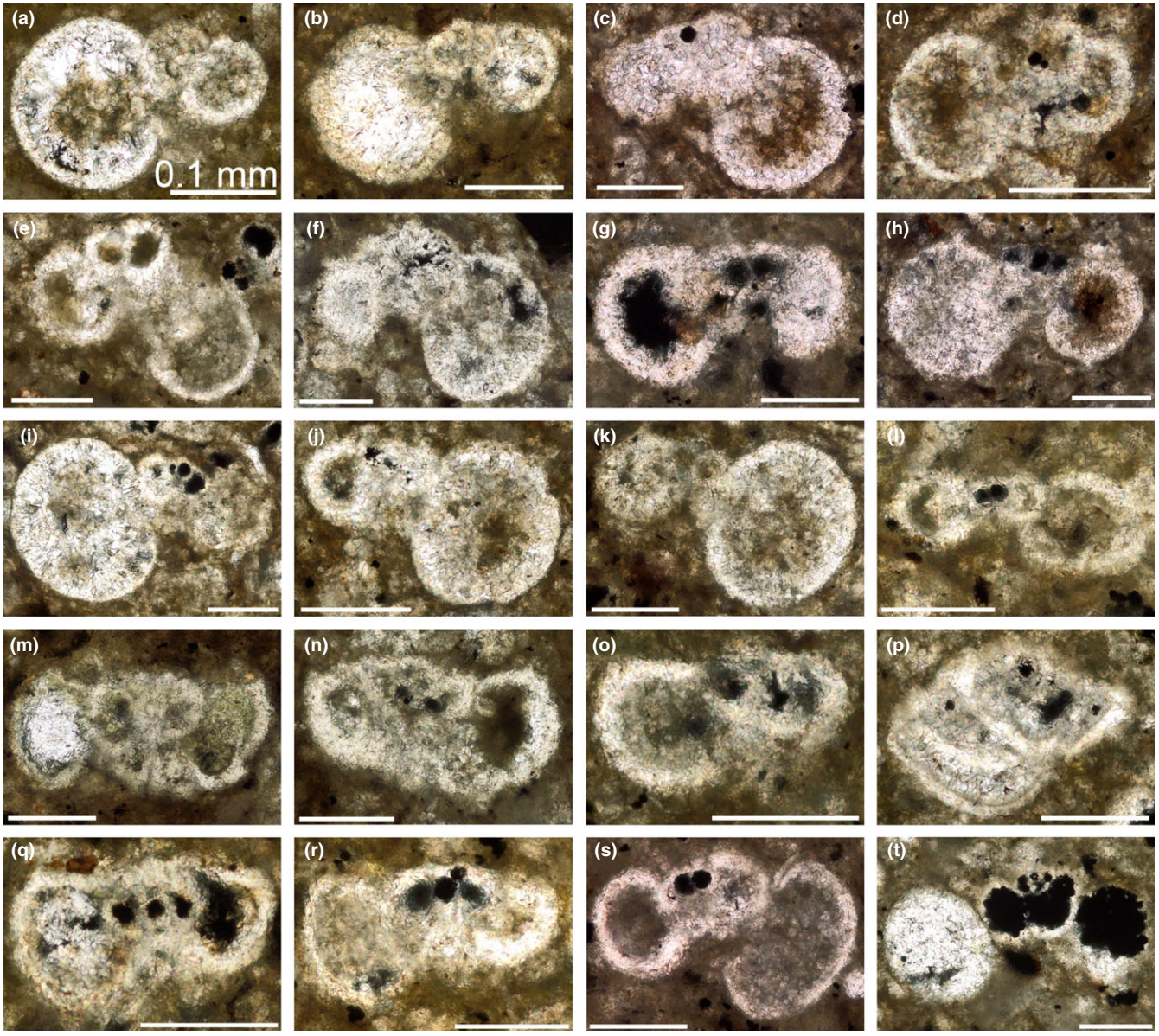

FIGURE 8 Late Danian–early Selandian planktonic Foraminifera of the Sapoá area (see Figure 6). Scale bars are 0.1 mm. (a and b) *Subbotina triloculinoides* (Plummer). (c and d) *Subbotina* cf. *triloculinoides* (Plummer). (e) *Subbotina trivialis* (Subbotina). (f) *Subbotina* cf. *trivialis* (Subbotina). (g–j) *Parasubbotina pseudobulloides* (Plummer). (k) *Parasubbotina* cf. *pseudobulloides* (Plummer). (l) *Globanomalina compressa* (Plummer). (m and n) *Morozovella praeangulata* (Blow). (o) *Morozovella uncinata* (Bolli). (p) *Igorina* sp. (q and r) *Praemurica uncinata* (Bolli). (s) *Praemurica inconstans* (Subbotina). (t) *Praemurica pseudoinconstans* (Blow). Samples: SA14-15 (N 11°13′48.6″/W 85°38′31.4″) (c), (d), (f)–(k); SA14-11 (N 11°13′26.9″/W 85°38′06.9″) (a), (b), (e), (l)–(t)

Baumgartner-Mora and Baumgartner (2016) report also evidence of emersion (palaeosol and littoral conglomerates, erosion of Upper Cretaceous pelagics) prior to the development of the late Palaeocene Barra Honda platform (Costa Rica); the latter may represent a lateral equivalent of the Sapoá limestones. Finally, a relative sea-level rise occurred to accommodate the deposition of the Sapoá limestones.

The development of the Sapoá carbonate bank took place in lagoonal conditions. Such conditions are evidenced by the mud-rich, fossil-poor content of the limestones. The co-occurrence of miliolids, green algae, gastropods and peloids in mud-rich facies is indicative of lagoonal, subtidal environments of open to restricted inner platforms (Flügel, 2010; Jaccard et al., 2001; Sadeghi, Vaziri-Moghaddam, & Taheri, 2011; Saller, Richard, La Ode, & Glenn-Sullivan, 1993; Sartorio & Venturini, 1988; Wilson, 1975). Evidence for intertidal conditions is scarce and was registered by rare occurrence of fenestral fabrics. The local prevalence of peyssonnelid algae is possibly due to their ability to grow on soft substrates (Rasser, 2001; Wray, 1977) which dominated in this mud-rich environment. Protected, low-energy environments with muddy substrates favoured also the

growth of siliceous sponges which produced important biostromes (Gammon & James, 2001; Wiedenmayer, 1977). The general low faunal diversity was locally increased by the input of higher energy deposits (grainstones, rudstones) which brought debris of organisms growing in more open marine, oligotrophic conditions, such as corals and various red algae. The latter may indicate occurrences of coral-algal patch reefs in the vicinity. The reef debris was possibly transported in the inner platform by currents and storms. In contrast with the Barra Honda platform, no Larger Benthic Foraminifera (LBF) has been found in the Sapoá limestones.

The demise of the short-lived Sapoá carbonate bank during the early Selandian is marked by an erosional unconformity overlain by volcanoclastic conglomerates. The very well preserved arc-derived crystals suggest a proximal source of intermediate volcanic rocks. The drowning of the carbonate bank is evidenced by the deposition of hemipelagic facies, under the influence of a reduced detrital input.

3.2 | Brito formation

3.2.1 | Facies description

The Brito Fm. represents a turbiditic sequence the thickness of which reaches 4 km in the basin depocenter (offshore; Figure 5; Ranero et al., 2000); much thinner exposures occur onshore, along the southern Nicaraguan Isthmus. This formation is composed of various deep-water facies, which are not exhaustively reviewed here. Instead, we present observations made at localities which remained undescribed so far.

The base of the Brito Fm. was observed in two locations of the southern Nicaraguan Isthmus. In El Ostional (Figure 3; El Ostional quadrangle), a 500 m long, exceptional coastal outcrop shows deep-water, seaward-tilted lithologies. The first 80 m of the section are composed of brown turbidites alternating with grey, pelagic and tuffaceous hemipelagic limestones containing abundant planktonic Foraminifera and fewer radiolarians; these limestone beds resemble much the lithologies of the upper Palaeocene–lower Eocene Buenavista Fm. described 18 km southward (Baumgartner et al., 1984; Figure 3). The rest of the section consists of thick packages alternating, as follows; up to 50 m thick channel-levee packages consisting of stacked, dm- to m-thick coarse-grained arenites (Figure 9b), sometimes containing abundant *Nummulites* spp.; up to 120 m thick packages consisting of mm to cm alternances of (hemi)pelagic mudstones and turbiditic, fine-grained sandstones and siltstones (Figure 9a,c). In general, channel-levee and thin pelagic/turbiditic alternances (Figure 9b–d) are the most common facies of the formation.

Further inland, a comparable section is observed in the area of La Calera (abandoned rock quarries, San Juan del Sur quadrangle; Figure 3). The limit between the Brito and the underlying, less competent Rivas Fm. appears clearly in the landscape morphology; in the area, the base of the Brito Fm. coincides with a 40-km long range of hills. The base of the section consists of 40 m of pelagic limestones alternating with minor turbiditic and tuffaceous beds; the outcrops are located in the river (N 11°17′30.8″/W 085°50′15.5″) as well as along the road. The pelagic limestones display very thin, graded laminations containing shallow-water benthos fragments (red and green algae, molluscs). Upsection, turbidites dominate and correspond to cm- to dm-thick siltstones and fine-grained sandstones. La Calera presents also one of the most intriguing features of the basin; along the strike of the pelagic limestones, a hill shows massive cliffs (N11°17′15.7″/W085°50′02.1″) including coral framework with dm-sized colonies of corals (*Montastrea* sp.?; Figure 9f) and hydrozoans (?). No distinct polarity is visible, but the framework seems to be in place, or is part of a big (>100 m sized) block. The limestones correspond mainly to udoteacean packstones and well-washed grainstones; miliolids, other smaller benthic Foraminifera, and fragments of red alga and mollusc are a minor component. Moreover, the top of the block displays a very thin *Nummulites* rudstone facies (Figure 10), which is described in the age section (see below).

Resedimented shallow benthos occurs in all the levels of the formation. In Las Parcelas (N11°13′19.0″/W085°47’10.8″) and 23 de Octubre (N11°27′13.9″/W086°02′52.5″) quarries, dm- to m-thick, isolated to stacked channels (Figure 9e) consist of carbonates ranging from grainstones-packstones with shallow benthos to packstones with mixed pelagic/shallow-water components. They contain LBF such as *Nummulites*, *Discocyclina, Amphistegina*, and *Eoconoloides*, and fragments of mollusc, udoteacean green alga, red alga, coral and echinoid spine.

The upper part of the formation is well-exposed in two localities. In the Rio Grande (central SFB; Figure 3), a km-thick section is exposed and encompasses the limit between the Brito and Masachapa formations (see the description of the Masachapa Fm.). The uppermost Brito Fm. displays alternances of thin-bedded, brown-grey sandy mudstones and graded arkosic-lithic, sometimes tuffaceous wackes. The latter exhibit graded laminae which contain scarce LBF, such as *Nummulites, Actinocyclina and Helicostegi-noides*. In El Astillero (southern SFB; Figures 3 and 12), the Brito Fm. is unconformably overlain by the stacked, shallow-shelf volcaniclastics of the El Astillero Fm. (see below).

3.2.2 | Age of the Brito Formation

An Eocene age was assigned to the Brito Fm. in the early studies of the basin (Auer, 1942; Cushman, 1920; Green,

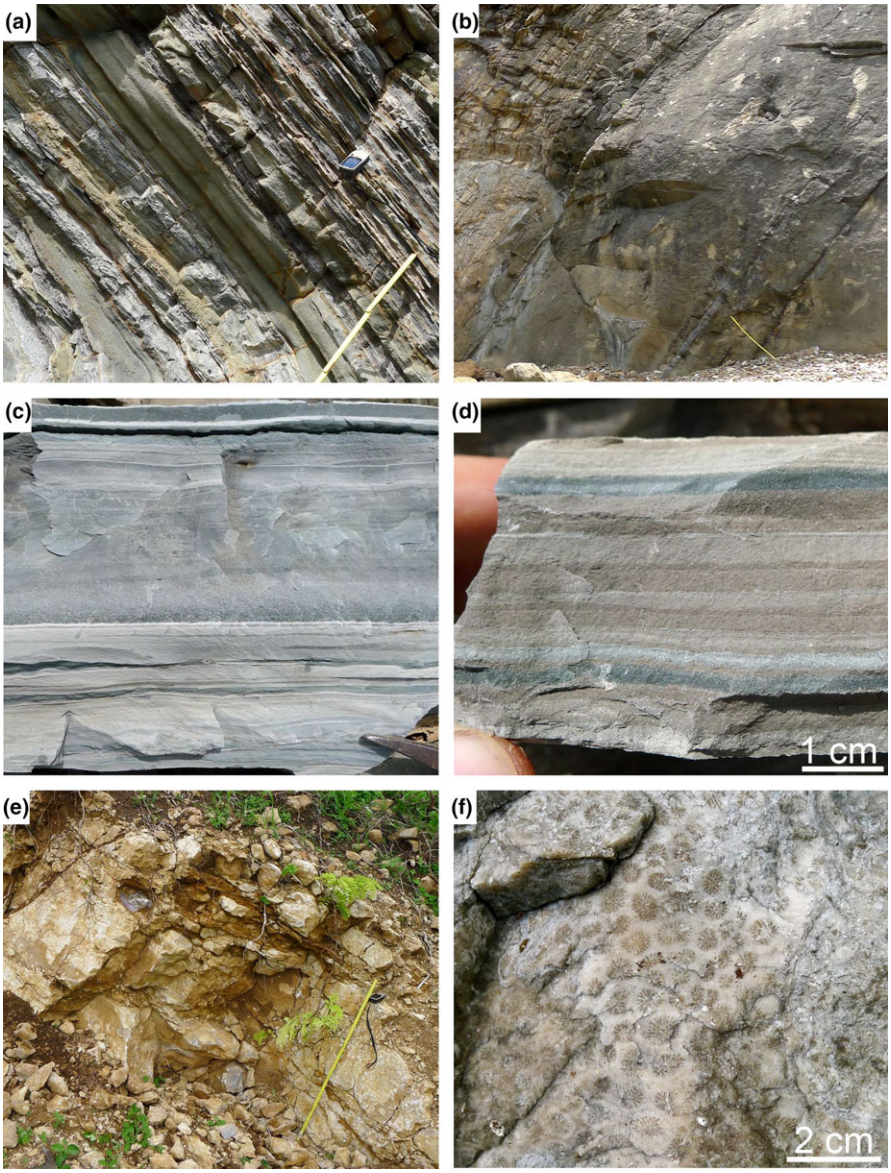

FIGURE 9 Field photographs of the Eocene Brito Fm. (a), (c) Mm- to cm-alternances of (hemi)pelagic mudstones and turbiditic, fine-grained sandstones and siltstones (El Ostional). In (a), meter stick length is 40 cm. (b) Thick channel-levee packages consisting of stacked, dm- to m-thick coarse-grained arenites (El Ostional). Meter stick length is 1 m. (d) Mm- to cm-scale turbidites, which grade from silt to siliceous mud (Popoyo beach, La Virgen Morena quadrangle). (e) Carbonate channel rich in shallow-water material (Las Parcelas). Meter stick length is 1 m. (f) Hermatypic coral colony from La Calera massive, shallow-water limestone exposures. See text for locations

1930; Hayes, 1899; Vaughan, 1918; Zoppis Bracci & Del Giudice, 1958) as well as in more recent ones (Clowser, Cutler, Girges, Laing, & Wall, 1993; Winsemann, 1992).

In Nicaragua, the age of the base of the formation has remained poorly constrained, whereas the base of the equivalent Descartes Fm. was dated as earliest Eocene in northern Costa Rica (Clerc, 1998).

At the base of the formation, hemipelagic facies occur in the vicinity of the La Calera shallow-water limestones (Figure 3), without a visible, but possibly unconformable contact. One sample of this facies contains abundant planktonic Foraminifera (Figure 11) including *Morozovella gracilis* (Bolli). At El Ostional, *Morozovella subbotinae* (Morozova) was observed in two samples collected from the pelagic limestones (Figure 11). These three samples may be assigned to the stratigraphic interval between the upper part of Zone P5 and Zone E5, indicating a latest Palaeocene to early Eocene age. The nummulitid rudstones/floatstones from La Calera section (Figures 3 and 10) provide some additional biostratigraphic information. They contain abundant 2–3 mm sized *Nummulites* sp. consisting mostly of megalospheric, thick lenticular, tightly coiled, involute forms, with a protoconch of >100 μm in diameter. Up to 3 cm sized microspheric forms of tightly coiled *Nummulites* sp. occur less frequently. These forms can be related to *Nummulites* (*Palaeonummulites*) *macgillavryi* (Rutten). This taxon was originally described as *Camerina* by Rutten (1935) from Cuba. The Calera specimens have very similar morphological features and the presence of trabecules in the complete involute specimens permits to treat them as true *Nummulites* Lamark. This population will be reexamined for the establishment of a new species. This assemblage may represent one of the earliest *Nummulites* of the American realm. Other LBF include *Eofabiania* cf.

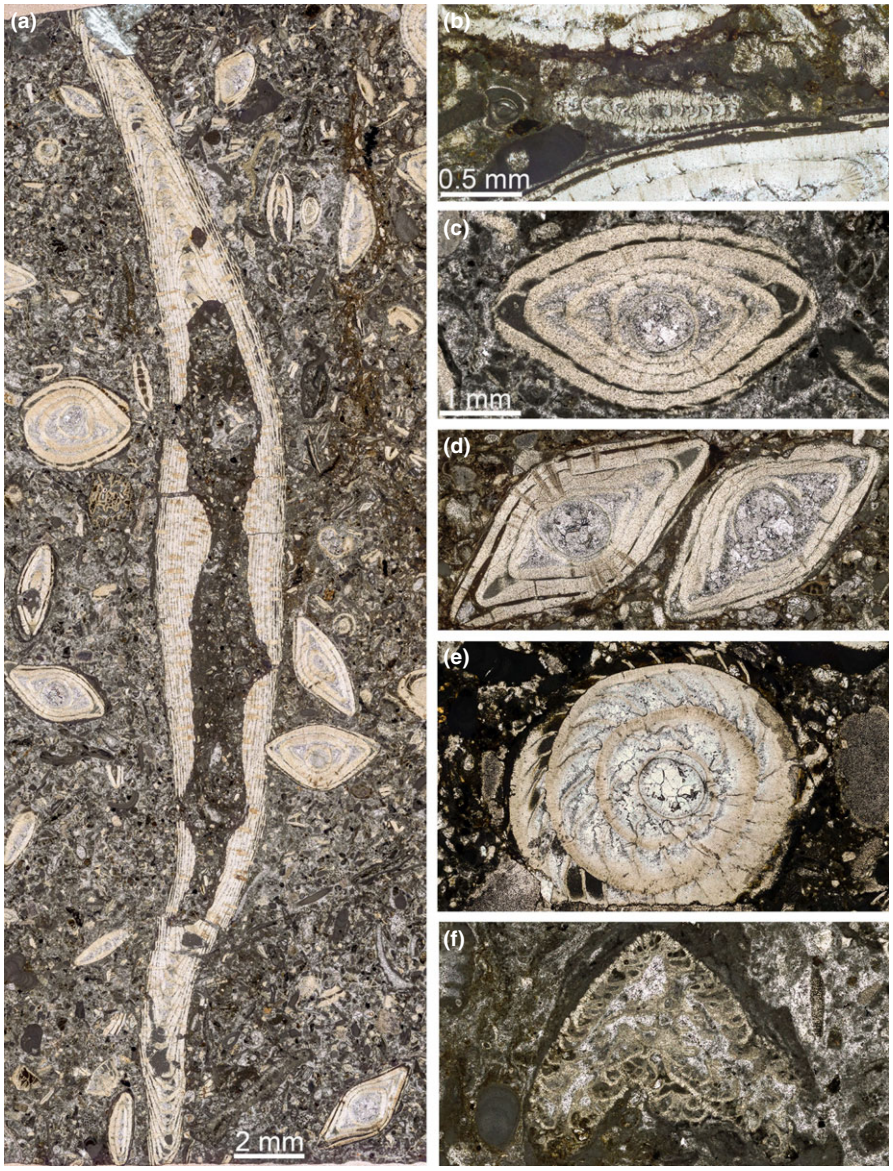

FIGURE 10 Early-middle Eocene Larger Benthic Foraminifera from the reefal limestone at La Calera. Scale bar is 2 mm for (a), 0.5 mm for (b), 1 mm for (c–f). (a) Vertical section of microspheric form and several macrospheric forms of *Nummulites macgillavryi* (Rutten) set in a fine grained sediment of micro-bioclastic hash, mainly composed of geniculate coralline algae and *Distichoplax* aff. *biserialis* (Dietrich). (b) *Linderina floridensis* Cole. (c and d) Vertical-oblique sections of macrospheric forms with inflated center of *Nummulites macgillavryi*. (e) Equatorial macrospheric section of *N. macgillavryi*. (f) *Fabiania cubensis* (Cushman & Bermudez). See text and Figure 3 for location

grahami Küpper, *Fabiania cubensis* (Cushman & Bermudez), *Linderina floridensis* Cole, *Amphistegina* spp., small discocyclinids, *Pseudophragmina* and *Rupertia*. This association is known from the early-middle Eocene. Compared to younger Eocene LBF occurrences, the chief difference of this *Nummulite*-bank is the absence of *Lepidocyclina* spp., generally abundant in middle-upper Eocene shallow-water limestones of Central America. Hence, the La Calera limestone may be of early to early–middle Eocene age. The rudstones contain also melobesian algal oncoids, and miliolids which float in a matrix of micro-bioclastic hash, composed of geniculate corallinaceans, a new species of *Distichoplax* aff. *D. biserialis* (Dietrich), and other bioclasts, as well as some planktonic Foraminifera. Many bioclasts are bio-corroded and show micritic crusts. Among the planktonic foraminifera, we distinguished *Morozovella* cf. *formosa* (Bolli), which seems to be restricted to the early Eocene, acarininids and globigerinids.

In the 23 de Octubre quarry (N11°27′13.9″/W086°02′52.5″) and in the vicinity, we found LBF typical of the early-middle Eocene epoch, such as *Nummulites willcoxi* Heilprin and *Eoconoloides wellsi* Cole & Bermudez.

The upper part of the Brito Fm. was dated as late Eocene with LBF recovered from shallow-water clasts reworked in turbidites (Punta Brito; Rivas quadrangle); Auer (1942) described a rich upper Eocene fauna, including the genera *Actinocyclina, Amphistegina, Asterocyclina, Discocyclina, Helicolepidina, Heterostegina, Lepidocyclina, Operculina, Operculinoides, Pliolepidina, Polylepidina, Proporocyclina*; Zoppis Bracci and Del Giudice (1958) indicated the occurrence of the *Lepidocyclina chaperi* Lemoine & Douvillé.

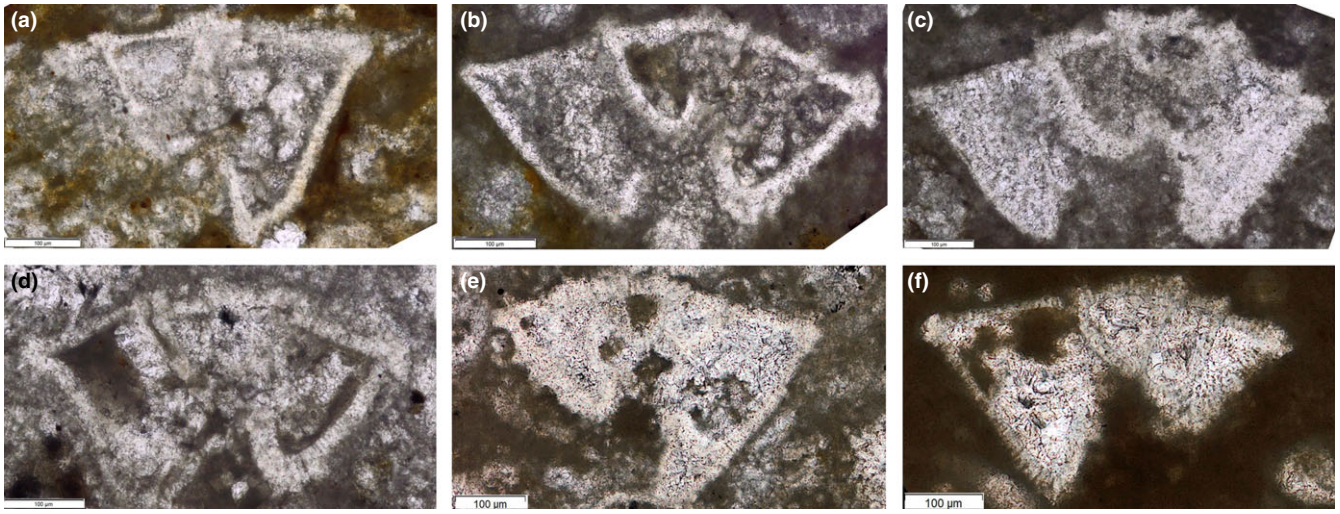

FIGURE 11 Thin section photomicrographs of planktonic Foraminifera recovered in pelagic levels from the lowermost Brito Fm. (late Palaeocene–early Eocene). Scale bars are 0.1 mm. (a) *Morozovella* sp. (b–d) *Morozovella gracilis* (Bolli). (e and f) *Morozovella subbotinae* (Morozova). Samples: LCRA1.5 (a–d) from La Calera; OST3 (e) and OST2 (f) from El Ostional. See text and Figure 3 for locations

Based on the data exposed here, the Brito Fm. is of late Palaeocene/earliest Eocene to late Eocene age in the southern Nicaraguan Isthmus.

3.2.3 | Depositional environment

The Brito Fm. consists of thick packages accumulated in deep-marine environments. Deep-basin, submarine fan environments are attested by the occurrences of thick, coarse-grained channel-levee complexes (Lang et al., 2017; Struss et al., 2007; Winsemann, 1992; Figure 9b). Deposition far from the channels resulted in thin alternations of (hemi)pelagics and fine-grained turbidites (Figure 9d). Based on palaeobathymetric data from offshore industry wells, Struss et al. (2008) indicate depositional depths reaching 3,000 m for the Brito Fm. The pelagic limestones package that occurs at the base of the formation may represent a regional marker level for the Palaeocene–Eocene boundary; it occurs in both Nicaraguan and Costa Rican sections of the basin (Buenavista Fm. in Costa Rica; Baumgartner et al., 1984).

La Calera limestones seem to rest with an unknown contact on late Palaeocene–earliest Eocene deep-water hemipelagic and turbidite facies of the Brito Fm. The shallow-water reefal lithologies are associated with nummulitid rudstones of early Eocene age. Local tectonic uplift into the photic zone could have created the conditions favourable to the formation of an ephemerous carbonate shoal during the early Eocene. Alternatively, the Calera limestones could represent an olistolith derived from an unknown carbonate platform that may have existed along the island arc or on an unknown accreted seamount. However, no island arc material has been recovered in the shallow-water facies. Isolated outcrops of lower Eocene shallow-water limestones are also reported from northern Costa Rica (Baumgartner-Mora & Baumgartner, 2016; Jaccard et al., 2001; Figure 20) and may be considered as remnants of the Barra Honda platform.

3.3 | El Astillero Formation (new lithostratigraphic unit)

3.3.1 | Facies description

The El Astillero Fm. corresponds to a new, 50 m-thick formation which crops out near the El Astillero village, located in the southern Nicaraguan Isthmus (70 km S-SW of Managua; Rio Escalante quadrangle; Figures 3 and 12). It represents a facies equivalent of the Junquillal Fm., which we previously described in northwestern Costa Rica (Andjić et al., 2016).

In two localities, a major angular unconformity with the underlying Brito Fm. is observed. The angle between the two formations reaches 35° in a quarry located 2.5 km southeast of the El Astillero village (N11°29′10.1″/W086°09′08.5″; Figure 13a), whereas it is 30° in the sea cliff located at the southern entrance of the village (Figure 13b). The lithological difference between the Brito and the El Astillero Fm. is conspicuous in outcrop and is outlined by the scarcity of muddy/silty lithologies in the El Astillero Fm. The latter exhibits mainly amalgamated, dm- to m-bedded, fine- to coarse-grained arenites locally alternating with conglomerates.

In the quarry outcrop, the Brito Fm. exhibits thin-bedded turbidites which are slumped at the formation top (Figure 13a). They are unconformably overlain by

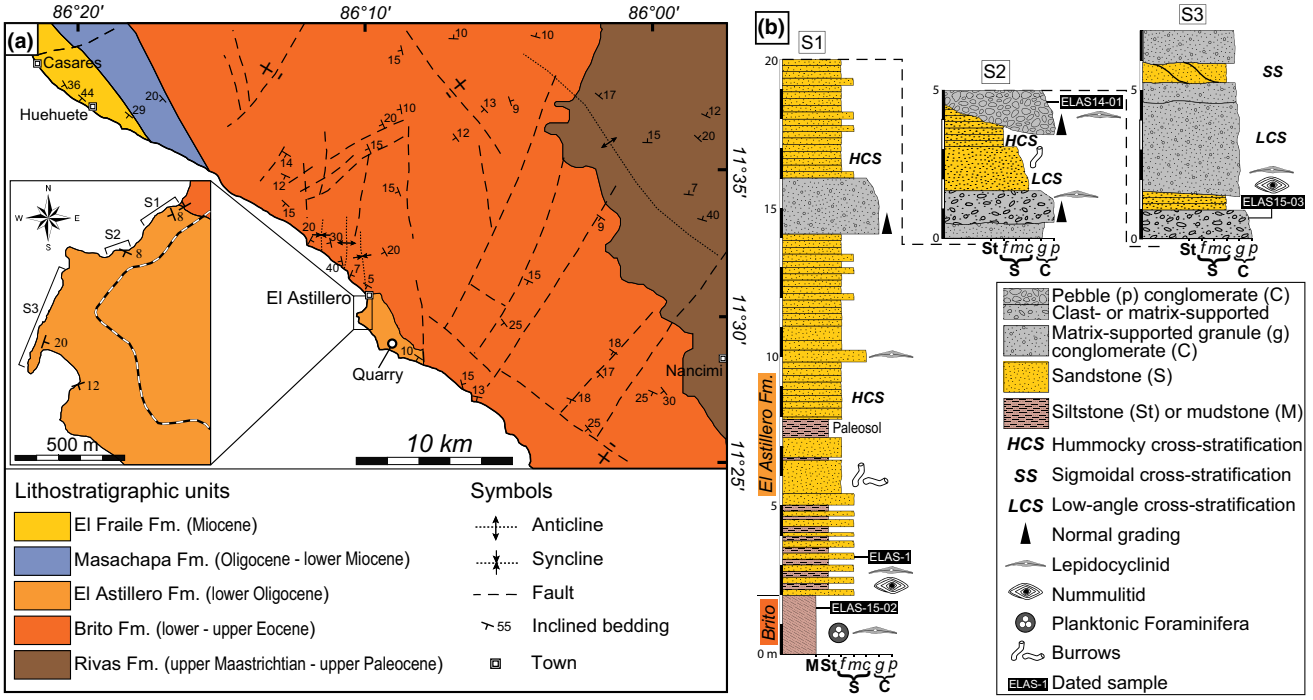

FIGURE 12 (a) Geological map of the El Astillero area (modified after Cruden, 1989; Darce & Duarte, 2002). The sections S1, S2 and S3 are depicted in (b). (b) Stratigraphic logs of the lower Oligocene El Astillero Fm. The unconformable contact with the underlying Eocene Brito is exposed in the section S1. Dated samples are indicated

sandstones and conglomerates containing cm-sized lepidocyclinids and cm- to dm-sized coral fragments (El Astillero Fm.). The formation boundary consists of a highly irregular unconformity along which the El Astillero Fm. onlaps the Brito Fm. The formations show opposite dip angles.

In the sea cliff section, the Brito Fm. shows 5 m of northwest-dipping, dark grey hemipelagic mudstones exhibiting light grey carbonate nodules (Figure 13b). The bioclastic content of the mudstones comprise mainly planktonic Foraminifera, with local, minor proportions of shallow-water, sand-sized detritus consisting of lepidocyclinids, molluscs and echinoid spines (Figure 14a–g).

The lowermost El Astillero Fm. consists of a landward-thinning, southwest-dipping, 5 m-thick package onlapping the hemipelagics (Figure 13b). It corresponds to a coarsening-upward package made of centimetric alternations of dark grey siltstones and grey lithic-arkosic arenites. Microscopically, the arenites consist of moderately sorted, subrounded volcaniclastic lithoclasts with a minor proportion of anhedral to subeuhedral plagioclase crystals. When present, the bioclastic, shallow-water component (up to 30%) is composed of *Lepidocyclina*, nummulitids, smaller benthic Foraminifera and fragments of mollusc, red alga, green alga and echinoderm (Figures 14h–l and 15a). This heterolithic facies is overlain by the first massive bed of the formation which corresponds to a medium-grained arenite showing centimetric burrows of large *Chondrites*, *Ancorichnus*, *Scolicia, Phycodes* and fewer *Zoophycos* and *Ophiomorpha*. The arenite is overlain by a reddish, brittle, 60 cm-thick sandy interval presenting a heterolithic aspect and sharply truncated by an erosional unconformity. Closer examination of the middle part reveals networks which are characteristic of a palaeosol (Figure 13c, Supporting information; Retallack, 2001): cm-sized, grey sandy peds are enclosed within a tabular, iron(?)-stained alteration framework composed of brown cutans. Thin sheets of silicate(?) crystals are associated with the carbonate-free cutans. White nodules and lenses of organic matter are observed in places. Three levels with tabular networks were recognized within the reddish bed.

Upsection, the formation exhibits a clear coarsening-upward trend with increasing upward occurrences of coarse-grained arenites and conglomerates, and decreasing trace fossils occurrences (rare *Thalassinoides* and *Ophiomorpha*). The coarsest lithologies generally bear lepidocyclinids and petrified wood.

The middle part of the El Astillero Fm. exhibits fining-upward, dm- to m-thick tempestites. They often present a basal, massive, lag deposit, made of conglomerates with rip-up clasts, resting generally on a scoured surface and grading upsection into coarse-grained arenites. Large-scale, low-angle cross-stratifications are observed in these deposits. The basal deposit underlies fine-grained arenites developing Hummocky cross-stratifications (HCS; Figure 13d), sometimes overlain in turn by very thin-bedded siltstones.

Locally, clast-supported, polymict, pebble to boulder conglomerates crop out in metric, channelized deposits

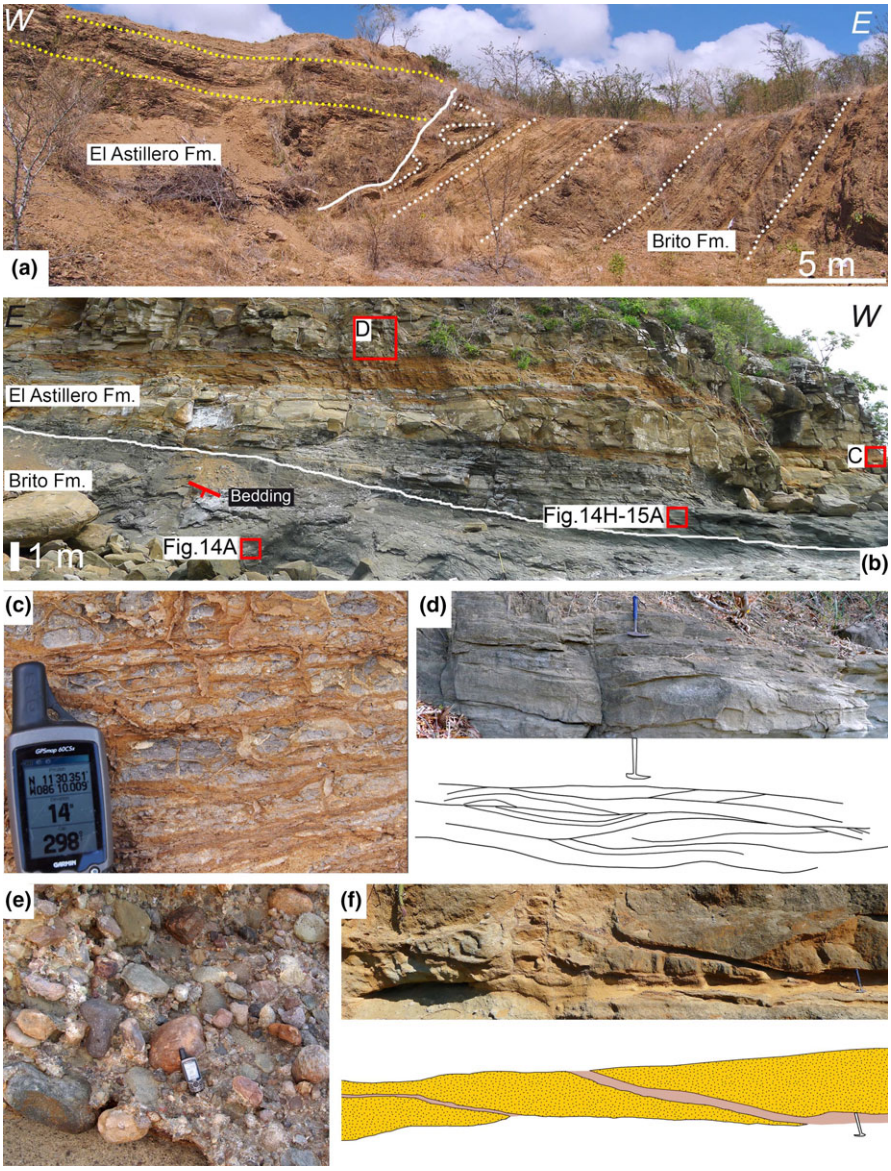

FIGURE 13 Field photographs of the lower Oligocene El Astillero Fm. (a and b) Unconformable contact between the Brito Fm. and the El Astillero Fm. (a) North-directed view of the quarry outcrop (N11°29′10.1″/W086°09′08.5″; Figure 12a). Note the opposite dip angles between the formations. The El Astillero Fm. onlaps the Brito Fm. along an irregular boundary which shows the occurrence of slumps. Dashed lines: stratification. Continuous line: formation boundary. (b) Coastal outcrop (section S1 in Figure 12). Note the contrasting dip angles between the formations. Brito Fm. dips towards the NNW. (c) Tropical palaeosol with cm-sized sandy peds outlined by a tabular network of iron-stained cutans. The cutans are associated with thin blades of silicate(?) crystals. See also the Supporting information. (d) Hummocky cross-stratifications in medium-grained sandstones. Hammer length is 31 cm. (e) Clast-supported, pebble to boulder polymict conglomerate. Height of the GPS device is 13 cm. (f) Sigmoidal cross-stratification displaying m-sized bundles separated by mud drapes

which present normal grading (Figure 13e). They rest on deeply scoured HCS-bearing lithologies. The clasts include volcanic arc rocks and shallow-water limestones rich in lepidocyclinids.

The upper part of the formation is dominated by pebble- to boulder-bearing, granule conglomerates and coarse-grained arenites. These deposits consist of metric packages separated by scour surfaces and low-angle erosional unconformities. One discontinuous stratigraphic horizon of coarse-grained arenites shows sigmoid-shaped sets of cross-strata that are separated by mud drapes (Figure 13f).

3.3.2 | Age of the El Astillero Formation

At El Astillero, dark coloured, offshore mudstones of the Brito Fm. crop out at the base of a sandy to conglomeratic unit, defined here as the El Astillero Fm. (Figures 12b, 13b and 14a). The mudstones contain planktonic Foraminifera, such as *Globigerinatheka*, *Subbotina*, *Catapsydrax*, suggesting a middle to late Eocene age (Figure 14b–g).

The unconformably overlying sandstones of the El Astillero Fm. form a steep cliff showing dm- to m- bedded laminated sandstone beds that pinch out laterally (HCS). One of the first 50 cm thick composite beds contains a 20 cm thick layer rich in LBF, up to 3 cm in size, that weather out at the surface (sample ELAS 1; Figures 12b, 14h–l, and 15a). LBF are all current oriented and set in a volcanoclastic matrix. LBF include taxa with macrospheric and microspheric broken and corroded forms of strongly pillared *Lepidocyclina* sp. comparable to *Lepidocyclina giraudi* type (sensu Cole, 1957). Tangential-equatorial sections of *Lepidocyclina* cf. *canellei* Cole show nephrolepidine embryonic and periembryonic chambers with two principal auxiliary chambers. *Nummulites* cf.

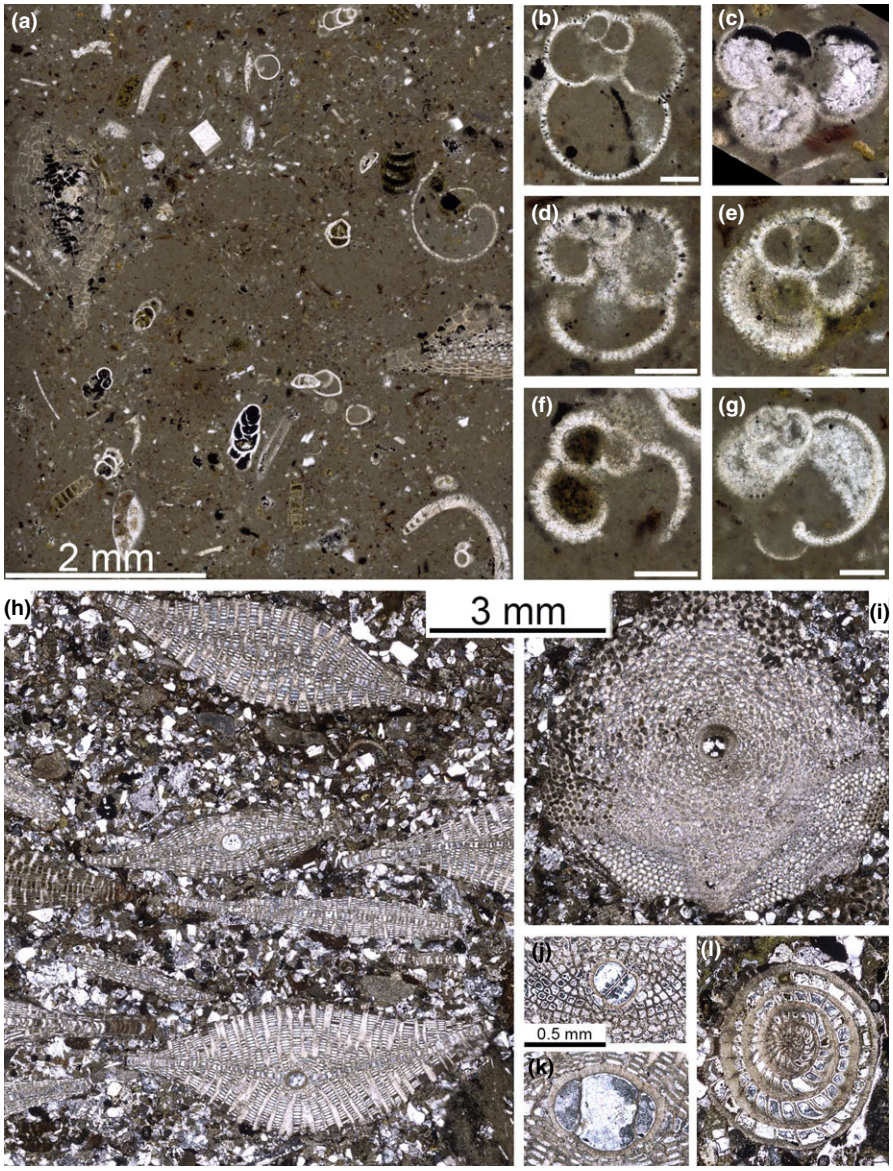

FIGURE 14 Thin section photomicrographs of the Eocene Brito Fm. (a–g) and the lower Oligocene El Astillero Fm. (h–l). Scale bars: (b–g) 0.1 mm, (j–l) 0.5 mm. The outcrop is depicted in Figure 12b (section S1) and shown in Figure 13b. (a) Silty mudstone containing smaller, larger and planktonic Foraminifera, with scarce mollusc and echinoid fragments. (b–g) Middle–late Eocene planktonic Foraminifera from the sample ELAS15-02. (b and c) *Subbotina* sp. (d and e) *Globigerinatheka* sp. (f and g) *Catapsydrax* sp. (h) Lithic-arkosic arenite, at the base of the El Astillero Fm., rich in lenticular, strongly pillared *Lepidocyclina* sp. comparable to *L. giraudi* type (sensu Cole, 1957) (sample ELAS1). (i and j) Tangential-equatorial section of *Lepidocyclina* cf. *canellei* Cole. (j) Enlargement of the embryonic and periembryonic chambers with two principal auxiliary chambers. (k) Enlargement of embryonic chambers type *Nephrolepidina*. (l) Microspheric form of probably reworked *Nummulites* cf. *striatoreticulatus* Rutten. Early Oligocene

striatoreticulatus Rutten is probably reworked from the underlying Eocene mudstone of the Brito Fm. Well preserved miliolids and rotaliids are dispersed in the matrix. This LBF association indicates an early Oligocene age.

In the upper part of the formation (Figure 12b), coarse sandy and conglomeratic lithologies contain pure limestone clast (sample ELAS14-01) and a sandy carbonate level (sample ELAS 15-03) that show a very similar LBF assemblages, but differ remarkably in lithology. The limestone clast (ELAS14-01; Figure 15d) is made of pure shallow carbonate with a very minor detrital component. LBF and oncoids sized mm- to cm are set in a microbioclastic matrix rich in corallinacean and green algae. The sandy carbonate lens (ELAS 15-03; Figure 15b,c) shows an abundant tuffaceous matrix, which is stained brown from Fe-hydroxides and possible organic matter. Opaque cubes represent oxidized pyrite. LBF are heavily corroded, intensely bioeroded and stained by oxides. Lateral chambers of LBF are filled with clays. Ill-oriented geopetal infills suggest repeated reworking and cementation. Big microspheric *Lepidocyclina* spp. reach 7 cm in size (Figure 15b). These taxa are in the *Lepidocyclina undosa-favosa* group. Small *Nummulites* with 3–4 whorls show the character of *Nummulites dia* (Cole & Ponton) and a few of *N. panamensis* gr. Gasteropod shells are abundant. The association of LBF indicates an early Oligocene age.

3.3.3 | Depositional environment

The El Astillero coastal section shows a clear shallowing which is recorded by an upward transition from the Brito Fm. distal offshore facies to the El Astillero Fm. proximal offshore facies. This transition was accompanied by the input of relatively coarser, shallow-water bioclast-rich sands preceding the onset of shallow shelf, detrital sedimentation. The transition from distal offshore to proximal

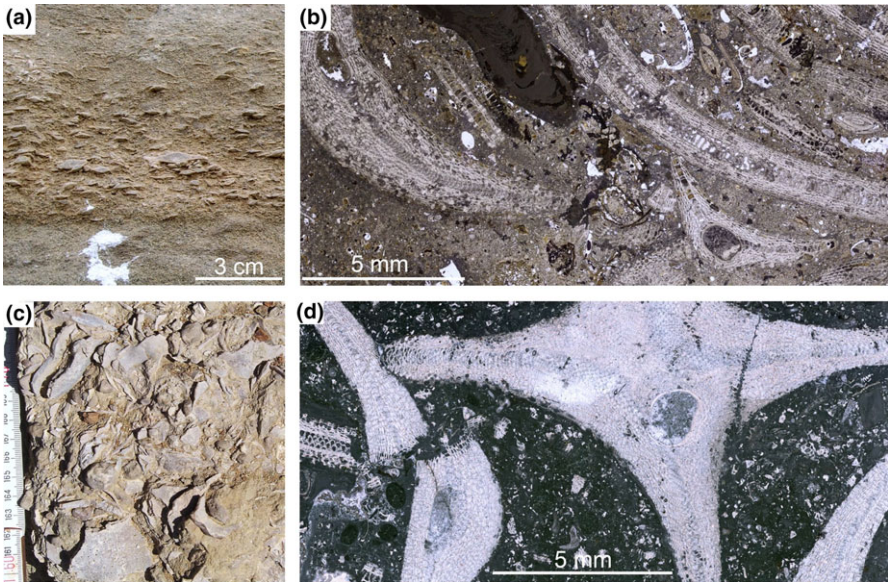

FIGURE 15 (a) Lithic-arkosic arenite rich in Larger Benthic Foraminifera (sample ELAS1 in Figure 14h–l). (b and c) *Lepidocyclina* floatstone with a tuffaceous wackestone matrix containing nummulitids and smaller benthic Foraminifera, and fragments of mollusc, echinoid and tuffaceous volcanic rock. Note the Cm-sized *Lepidocyclina* in (c) (sample ELAS15-03 in Figure 12b, lower Oligocene). (d) *Lepidocyclina* floatstone clast with a wackestone matrix composed of the *Lepidocyclina undosa-favosa* gr., red alga, green alga and echinoderm fragments (sample ELAS14-01 in Figure 12b, lower Oligocene)

offshore facies coincided also with an angular unconformity which indicates a possible tectonical, seaward tilting of the Brito Fm. The tilting is evident in the quarry section, located to the southeast (Figure 13a). There, a shallowing-upward transition is absent, as shelf deposits directly overlie tilted, deep-water turbidites. Tectonic tilting is suggested by the opposite dips between the two formations and the highly irregular formation boundary along which the El Astillero Fm. onlaps slumped turbidites of the Brito Fm.

In the coastal outcrops, the base of the formation was deposited under rather low-energy conditions, which are highlighted by silty-sandy fining-upward alternations, sandy-silty heterolithic beds, and extensive occurrence of horizontal burrows in fine-grained, thick-bedded arenites. Although a detailed geochemical analysis of the brownish sandy palaeosoil is still needed, its field characteristics seem to fit the description of soils formed under humid tropical climates (see Retallack, 2001).

These bedforms were replaced by higher energy, transgressive deposits, as the middle part of the formation is mainly characterized by storm deposits that take the form of fining-upward tempestites (Figure 13d). A further increasing in water energy was recorded upsection within progressively coarser lithologies that display large-scale, low-angle cross-stratifications in metric cosets. These deposits are encompassed between metric, matrix-supported conglomerates that transported much coarser sediments in comparison to the tempestites. Locally, clast-supported, polymict conglomerates were deposited above m-deep erosional bases and may indicate deposition close to a river mouth (Figure 13e). At the formation top, nearshore conditions were apparently recorded in sigmoidally shaped tidal bundles that are enclosed in mud drapes (Figure 15f).

In summary, the general coarsening-upward of grain size and the increasing frequency of high-energy-related, coarse deposits attest that the El Astillero Fm. was deposited under shallow shelf conditions. It experienced the constant input of coarse-grained material the source of which was an uplifted hinterland. Emergence during the deposition of the lower El Astillero Fm. may have been the result of a conjunction of eustatic sea-level drop (Eocene–Oligocene boundary; Miller et al., 2005) and uplift. Subsequent deposition and preservation of tens of meters of tempestites and stacked coarse-grained deposits was possibly the consequence of both renewed sea-level rise and subsidence of the shelf.

3.4 | Masachapa formation

3.4.1 | Facies description

During our fieldwork, we studied the Masachapa Fm. in the following sections, from the NW to the SE: Rio El Carmen, Rio Citalapa, Rio El Bongo and Rio Grande. In these river sections, the Masachapa facies consist of cm- to dm-thick, alternations of flat-bedded, silty to sandy mudstones and fine to coarse sand-sized, arkosic-lithic wackes and arenites (turbidites; Figure 16a–h). The different lithologies contain planktonic Foraminifera and show various amounts of clay- to silt-sized tuffaceous material. The mudstones display millimetric ichnofossils (Figure 16d), such as *Nereites*, *Phycosiphon*, *Chondrites*, *Planolites* and *Thalassinoides*.

The best examples of turbiditic deposits can be observed in the Rio Citalapa (north of San Cayetano; Villa El Carmen quadrangle; N11°54′07.9″/W086°30′45.8″). At the base of the section, cm-thick turbidites commonly consist of Ta–Tc, Ta–Te and Tc–Te interval couplets (Bouma, 1962; Figure 16f,g). Silty Ta intervals are generally rich in organic matter debris. The Tc intervals display climbing ripples and are often convolute laminated. Locally, a

0.7 m-thick debrite is embedded in these deposits. It overlies a massive, 0.8 m-thick sandstone bed and consists of cm- to dm- sized, disrupted sandstone beds and convoluted siltstones embedded in a scarce muddy matrix. The debrite is onlapped by turbidites.

Upsection, thin-bedded, carbonate-poor turbidites occur and consist of organic-rich, ungraded siltstones alternating with sandy mudstones (N11°54′13.2″/W086°31′17.0″; Figure 16c). These facies are overlain by metric packages of amalgamated, thin-bedded, sandy turbidites. The latter dominate in the uppermost part of the formation.

Along the Rio Grande (La Trinidad quadrangle), the Masachapa Fm. crops out over hundreds of meters; it consists of a monotonous succession of silty/sandy mudstones and fine-grained, ungraded to poorly graded sandstones (Figure 16a,b). Here, it conformably overlies the Brito Fm. and gently dips towards the SW. At the base of the formation (N11°40′26.8″/W086°18′19.3″; Figure 16b), we sampled a carbonate boulder embedded in hemipelagics. It consists of a well-washed oolitic grainstone containing LBF such as *Amphistegina*, *Lepidocyclina, Nummulites, Helicosteginoides, Caudriella, Actinocyclina, Hexagonocyclina* and fragments of mollusc and echinoderm (Figure 16i). Plagioclase crystals are the dominant nucleus type of the ooids. Upsection, scarce LBF are also present in thin-bedded, sandy turbidites.

The distinction between Masachapa and Brito facies is not always clear, especially in case of weathered exposures. However, some general differences may be stated. When compared to the Brito Fm., the Masachapa Fm. presents: (1) lighter patina and fresh surface colours (typically greyish-beige); (2) much less micro-laminated (hemi)pelagic facies (due to bioturbation ?); (3) a general lower abundance of detrital minerals, although mud-sized ash is often present; (4) no occurrences of thick channel-levee complexes; (5) much less reworked/redeposited shallow benthos; (6) higher carbonate contents in (hemi)pelagic facies, and no occurrences of cherts and radiolarian-bearing deposits.

3.4.2 | Age of the Masachapa Formation

Dorr (1933) produced a list of more than 50 smaller benthic and planktonic Foraminifera species that he recovered from soft gray-blue shales and sandstones (unknown localities). However, very few of the listed species can be restricted to the Oligocene as suggested by the author. Yet, some species are not known from earlier than the Oligocene such as *Gyroidina soldanii* d'Orbigny, *Lenticulina calcar* (Linnaeus), *Melonis pompilioides* (Fichtel & Moll), *Robulus protuberans* (Cushman) and *Uvigerina auberiana* d'Orbigny (Adegoke, Oyebamiji, Edet, Osterloff, & Ulu, 2017; Holbourn, Henderson, & Macleod, 2013; Petters & Sarmiento, 1956; Renz, 1948; Todd & Low, 1976). Dorr (1933) reported also the presence of *Planulina wuellerstorfi* (Schwager), which is generally considered to occur since the Miocene (Cassell & Sen Gupta, 1989; Holbourn et al., 2013); it implies that this species may occur in the Oligocene, as suggested by Székely and Filipescu (2015), and/or that the Masachapa Fm. reaches into the Miocene. The latter hypothesis is supported by the occurrence of palynomorphs of the Neogene genus *Tetraploa* (Rio El Carmen, Villa El Carmen quadrangle; Guy-Olson, 1998). Kumpulainen, Högdahl, Olafsson, Muñoz, and Valle (1998) found coccolithophores typical of the late early–late Oligocene interval, such as *Sphenolithus ciperoensis* Bramlette & Wilcoxon and *S. distentus* (Martini).

3.4.3 | Depositional environment

The Masachapa Fm. consists of flat-bedded deposits indicating interplay between hemipelagic and turbiditic sedimentation. A distal depositional setting is reflected by the dominance of hemipelagic muds as well as the fine-grained, thin turbidite beds suggesting a distant feeding source. Such alternations of mudstones and low-density turbidites are generally considered to be characteristic of basinal plain environments (Mutti & Ricci Lucchi, 1978; Normark, Posamentier, & Mutti, 1993), located away from large submarine channels and canyons. This is in accordance with the deposition palaeodepths (1,500–2,000 m) reported by Struss et al. (2008), based on palaeobathymetric data from offshore industry wells. These authors, as well as Struss (2008), suggest that the Masachapa Fm. formed in deep-marine, slope environments. This is in accordance with some of the smaller benthic Foraminifera reported by Dorr (1933); *G. soldanii* d'Orbigny and *P. wuellerstorfi* (Schwager) indicate bathyal palaeodepths, whereas *M. pompilioides* (Fichtel & Moll) and *Siphonina tenuicarinata* Cushman suggest lower neritic-middle bathyal depths (Hayward, Carter, Grenfell, & Hayward, 2001; Holbourn et al., 2013). Although major, mass transport deposits or erosional features are not observed in the field or in seismic profiles, the occurrence of debrites and shallow-water limestone boulders in thin-bedded hemipelagics may suggest deposition close to the base of a slope (Butler & McCaffrey, 2010). The co-occurrence of trace fossils such as *Nereites*, *Phycosiphon*, *Chondrites* and *Planolites* is common in muddy intervals associated with turbidite events (Knaust, 2009; Uchman & Wetzel, 2012; Wetzel & Uchman, 2001).

3.5 | El Fraile formation

3.5.1 | Facies description

During our fieldwork, we studied several sections of the El Fraile Formation between El Velero and Huehuete towns

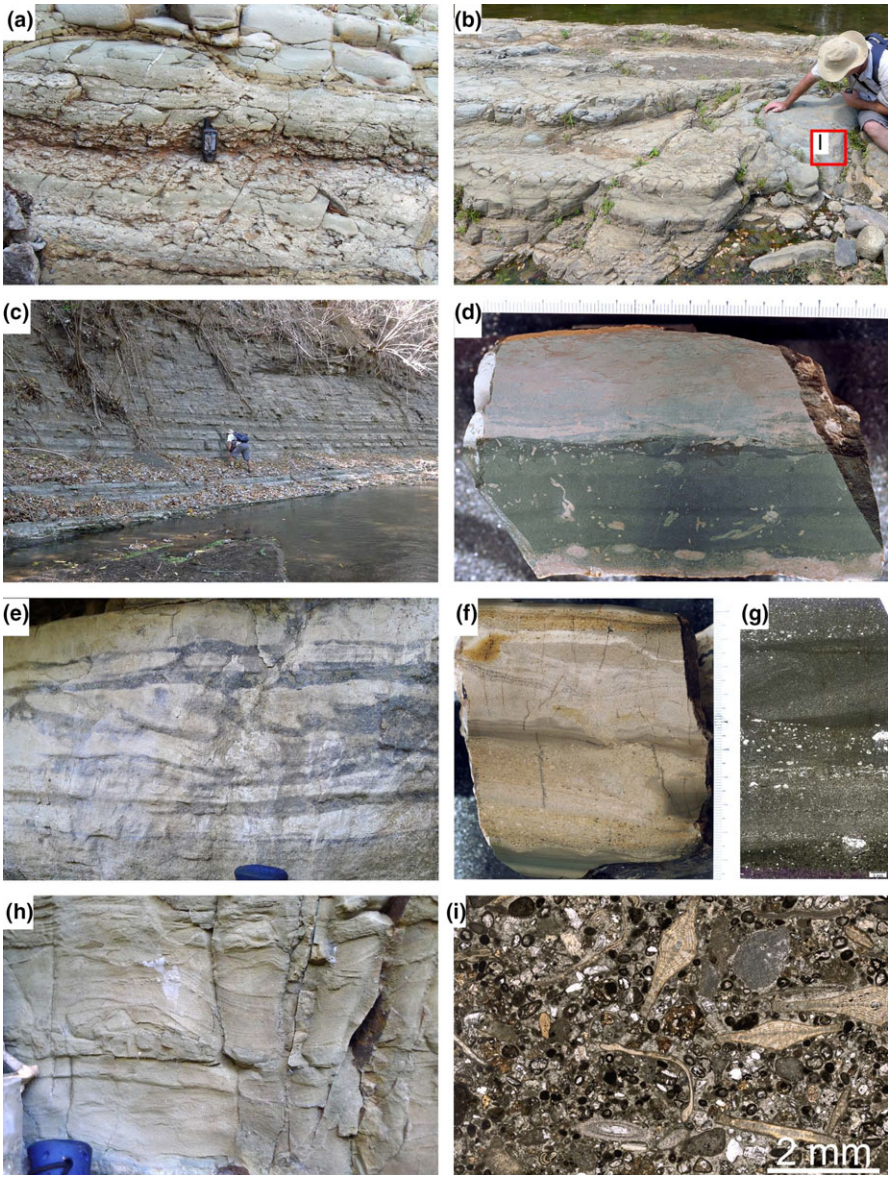

FIGURE 16 Field, fresh cut and thin section photographs of the Oligocene–lower Miocene Masachapa Fm. (a) Cm-beds of ungraded arkosic tuffaceous wackes (Rio Grande). (b) Oolitic grainstone boulder (sample BAR15-02) embedded in thin-bedded tuffaceous mudstones (Rio Grande). (c) Alternations of organic rich siltstones and sandy mudstones (Rio Citalapa). (d) Silty mudstone level overlying slightly graded arkosic wacke laminations (Rio El Carmen). Both are bioturbated. Note the centimetric scale. (e–g) Mm- to cm-thick turbidite levels in sandy tuffaceous siltstones and tuffaceous mudstones (Rio Citalapa). Scales: (e) Hammer handle is 3 cm large; (f) Centimetric scale; (g) 2 mm. (h) Climbing-ripple laminations in fine-grained sandstones (Rio Citalapa). (i) Oolitic grainstone with *Lepidocyclina* spp. (sample BAR15-02, Rio Grande). See text for the locations

(Figure 3). Here, we report the facies description of two sections (Monte Grande and Huehuete), which contain datable LBF. For a general description of the formation, the reader may refer to the detailed studies of Kolb and Schmidt (1991) and Krawinkel and Kolb (1994).

In the Monte Grande area (Figure 3), the El Fraile Fm. consists of hundreds of meters of flat-bedded, fine-grained siliciclastics alternating with minor medium-grained to coarse-grained sandstones and conglomerates, locally rich in mollusc debris. The fine-grained facies is typical of the formation: it is made of carbonate-free, cm-bedded, tuffaceous, lithic-arkosic siltstones to fine-grained wackes with light yellow to light grey fresh surfaces (Figure 17a). The microscopic observation of these sediments reveals the presence of high amounts of ash (vitric glass and glass shards), and a minor proportion of anhedral plagioclases. The high content of volcanic ash is reflected in the light colour of the rock. The remaining detrital fraction is made of pyroxenes, opaque minerals and green amphiboles.

The Monte Grande limestones are named after the neighbouring Monte Grande village (La Trinidad quadrangle; Figure 3) and comprise detrital-poor, carbonate deposits interbedded with tuffaceous volcaniclastics. The occurrence of these limestones was mentioned by Zoppis Bracci and Del Giudice (1958) and Kuang (1971) who report these lithologies as massive, lenticular, neritic limestones without describing them. The shallow-water limestones are found in two small quarries, the exploitation of which allows the observation of fresh rock exposures. These quarries correspond to isolated outcrops with a distance of 1.9 km between them. A conformable stratigraphic contact with the underlying detrital deposits is visible in the northwestern quarry.

The northwestern 5 m-thick outcrop (N11°43′22.6″/W086°24′16.5″) is made of massive-bedded, beige

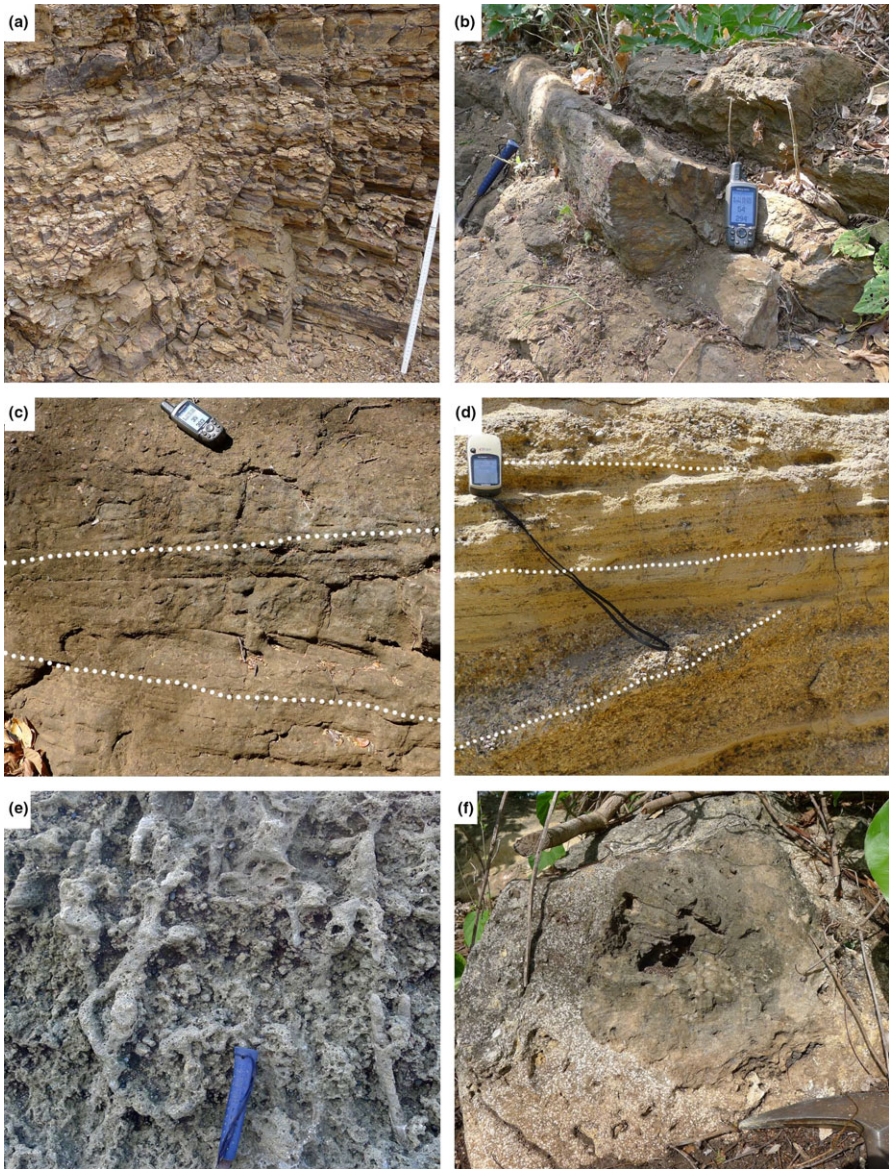

FIGURE 17 Field photographs of the Miocene El Fraile Fm. (a) Cm-bedded, tuffaceous, lithic-arkosic siltstones and fine-grained wackes (offshore facies; Monte Grande). Meter stick is 50 cm long. (b) Metric petrified wood trunk in coarse-grained deposits (base of the formation in Rio El Bongo, N11°48′17.6″/W086°28′57.9″). (c) Herringbone cross-stratification (tidal facies; Rio El Bongo). (d) Low-angle cross-stratification in coarse-grained arenites and conglomerates (shoreface facies; Huehuete beach). (e) *Thalassinoides* vertical burrows in a tempestite (Casares beach). (f) *Lepidocyclina* rudstone with a coral head (Monte Grande). See text and Figure 3 for locations

wackestones/floatstones which are essentially composed of green algae (25%–40%). The latter appear as mm- to cm-sized plate segments and stems comprised in a muddy matrix. Microscopically, the green algae present the typical tubules of udoteacean thalli. The tubular structure is still visible, although the initial aragonitic mineralogy disappeared and was replaced by drusy sparite. Other bioclasts are scarce (<8%) and correspond to lepidocyclinids, miogypsinids and clasts of coralline red alga, coral, echinoid spine and mollusc (sizes 0.15 mm–1 cm).

The southeastern outcrop (N11°42′29.9″/W086°23′47.2″) represents a 4 m-thick section of massive-bedded, beige limestones (Figure 17f). The lower part of the section is composed of floatstones mainly made of LBF, red algae and corals. The LBF are represented by mm-sized, rounded lepidocyclinids (15%) and miogypsinids (3%). Coral debris sized mm- to cm exhibits poorly preserved skeletons recrystallized in sparite. Coralline red algae appear with laminar and encrusting morphologies. Thin encrusting growth forms (0.3–1.5 mm thick) are visible on coral debris and intraclasts. Elongated, cm-sized rhodoliths are characterized by the absence of a nucleus and present mm- to cm-sized, lumpy crusts. These crusts are often made of a loose algal framework which trapped fine matrix. Other bioclasts include smaller benthic Foraminifera, gastropod shells, echinoid spines and broken bivalve tests. The muddy matrix of the wackestone was locally replaced by sparite.

The upper part of the section is marked by the absence of mud, which coincides with an increased proportion of mm-sized lepidocyclinids (50%–60%). The rock presents the characteristics of a well-sorted rudstone. Domal-shaped, dm-sized corals are present but not in growth position (Figure 19f). The proportions of the other

bioclasts remain nearly unchanged except that red algae appear only as clasts and coral debris are absent. The porosity of the rudstone was filled with at least two generations of cement. The first microcrystalline cement is slightly dominant. The remaining porosity was filled with blocky calcite.

On the Huehuete beach (Casares quadrangle; Figures 3 and 12a), 50 m of low-angle cross-stratified, coarse-grained volcaniclastic deposits overlie thin-bedded tuffaceous lithologies (N11°37′20.2″/W086°20′03.4″; Figure 17d). At the base of the coarse-grained deposits, medium-grained to coarse-grained, lithic-arkosic wackes alternate in places with granule conglomerates. A bioclastic component is only present in a 50 cm-thick floatstone/rudstone with a medium-grained wacke matrix. The bioclastic component (40%–50%) consists mainly of mm-sized, oblate lepidocyclinids, miogypsinids and of mm- to cm-sized clasts of branched coral (*Porites* sp.), bivalve, gastropod, echinoid and encrusting red alga.

3.5.2 | Age of the El Fraile Formation

Several fossil species of Miocene age were reported in the formation. Auer (1942, listed in: Hoffstetter et al., 1960; Zoppis Bracci & Del Giudice, 1958) reported bivalves, such as *Agriopoma gatunensis* (Dall) and *Trachycardium dominicense* (Gabb), gasteropods, such as *Bivetiella dariena* (Toula) and *Conus aemulator* Brown & Pilsbry, and LBF of the genera *Amphistegina* and *Miogypsina*. Kolb and Schmidt (1991) described shell lags containing *Melongena consors* (Sowerby) and *Architectonica nobilis* Röding.

Here, we present biostratigraphic information obtained from the Monte Grande area (samples MTEG5) and the Huehuete beach (sample HUE3).

The lower samples (MTEG5; N11°42′29.9″/W086° 23′47.2″; Figure 18) are relatively pure LBF-rudstones that shows well-washed grainstone and packstone portions with some yellowish-brown tuffaceous matrix. Poikilitic sparite cements perhaps indicate some freshwater influence during diagenesis. The sample contains *Amphistegina* cf. *lessonii* d'Orbigny, *Miogypsina* (*Miolepidocyclina*) aff. *staufferi* Koch with the nepionic chambers and *Amphistegina* cf. *angulata* (Cushman).

The upper sample (HUE3; N11°37′20.2″/W086° 20′03.4″; Figure 18) is a coral-LBF rudstone/floatstone with an abundant, coarse-grained volcano-detrital matrix. Oxidized pyrite is abundant and causes a yellowish-brown stain of matrix and bioclasts. Cm-sized coral fragments and rhodoids exist along with mm-sized, well-rounded clasts of volcanic rock.

The LBF assemblages are almost identical and show a *Lepidocyclina-Miogypsina* facies (Figures 18). Specimens of *Lepidocyclina yurnagunensis s.l.* Cushman, in general over 4 mm in size, are abundant (Figure 18). Some of the

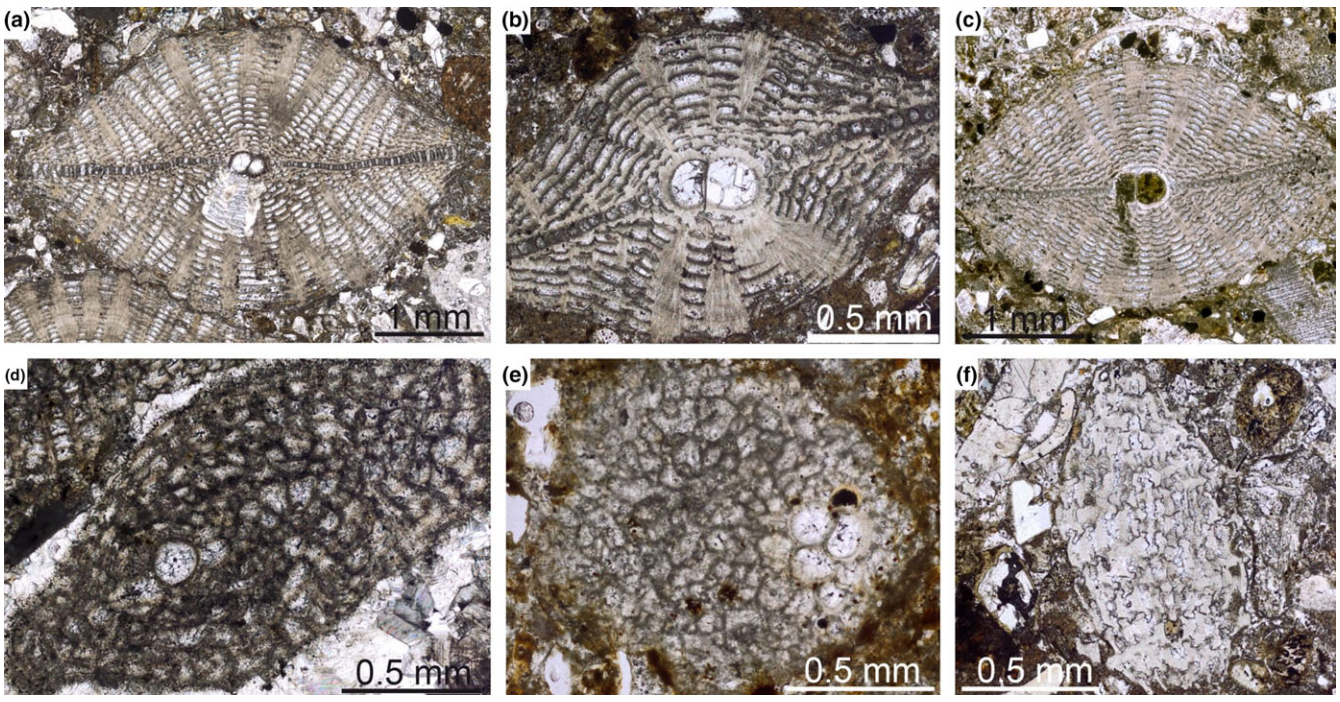

FIGURE 18 Early Miocene Larger Benthic Foraminifera form the El Fraile Formation (Monte Grande and Huehuete). (a and c) Individual variations of *Lepidocyclina yurnagunensis s.l.* Cushman. (a) Robust specimen of *L. yurnagunensis-morganopsis* type. (b) *Lepidocyclina giraudi* Douvillé. (d and e) *Miogypsina (Miolepidocyclina)* aff. *staufferi* Koch with the nepionic chambers. (f) *Miogypsina* (*Miolepidocyclina*) cf. *cushmani* Vaughan. Samples: HUE3 (a)–(c), (f); MTEG5.4 (d); MTEG5.1 (e)

specimens show the robust *L. yurnagunensis-morganopsis* type. In addition, we found *L. giraudi* Douvillé. Among the megalospheric specimens, we found forms similar to *Lepidocyclina sumatrensis* as illustred by Cushman (1920) from Cuba. The particularly inflated central body of these thickly lenticular to ufo-shaped tests is very typical. Rare *Lepidocyclina tournoueri* Lemoine & Douvillé were also found. Axial sections of *Miogypsinoides* sp. were observed (Figure 18). Several *Miogypsina* spp. show a juvenarium with two principal auxiliary chambers from which the spiral coil is developed, as described by Barker (1965). The juvenarium is in a subcentric position. At least three forms are present: *Miogypsina (Miolepidocyclina) panamensis* (Cushman) (=*Heterosteginoides panamensis*), *Miogypsina staufferi* Koch and *Miogypsina* (*Miolepidocyclina*) cf. *cushmani* Vaughan.

This assemblage has a different (younger?) phylogenetic position than the *M. gunteri-tani* assemblage described from Punta Pelada (Costa Rica; Baumgartner-Mora, Baumgartner, & Tschudin, 2008). Hence, the age can be stated as latest Oligocene to early Miocene.

The El Fraile Fm. is interbedded with the middle Miocene Tamarindo Fm. (radiometric ages: 11.7–14.7 Ma; Elming et al., 2001; Plank, Balzer, & Carr, 2002; Saginor, Gazel, Carr, Swisher, & Turrin, 2011; Weyl, 1980; Figures 3 and 4).

3.5.3 | Depositional environment

The El Fraile Fm. was deposited in a deltaic environment under the influence of tidal (Figure 17c), storm and fluvial processes (Krawinkel & Kolb, 1994). The El Fraile Fm. offshore to shoreface facies highlight a syn-sedimentary, explosive volcanic arc activity. Except for the unusual occurrence of the Monte Grande limestones, the constant input of volcaniclastic material prevented the development of carbonate-rich deposits. The co-occurrence of udoteacean wackestones and lepidocyclinid-coral grainstones confirms that parts of the formation were deposited in the photic zone, under low- to high-energy conditions. Moreover, this carbonate bank indicates that isolated, detrital-poor areas existed in the shallow shelf. This short-lived environment possibly developed on a tectonic high or an ephemerally abandoned part of the deltaic system.

4 | DISCUSSION

4.1 | Tectono-sedimentary evolution of the SFB

4.1.1 | Pre-Campanian

Due to the lack of suitable outcrops, little is known about the pre-middle Campanian evolution of the basin and the exact nature of the underlying basement. Onshore well data indicate the possible occurrence of Upper Cretaceous volcaniclastics and cherts (Loma Chumico Fm.?; Figures 3 and 4) overlying a basaltic basement (Ranero et al., 2000; Figure 19). These deep-water rocks might have been deposited on the Santa Elena tectonic pile (Figure 3) in post-Albian times, after its accretion to the MCOT (Escuder-Viruete & Baumgartner, 2014).

4.1.2 | Middle Campanian

In the southern SFB, biostromal and offshore carbonates (El Viejo Fm.; Pons et al., 2016; Figures 3 and 4) were deposited in response to basement uplift. Moreover, the southern basin basement (Santa Elena accreted arc; Escuder-Viruete et al., 2015) was partly exposed to subaerial environments (Baumgartner et al., 1984; Schmidt-Effing, 1974; Seyfried & Sprechmann, 1985). The resulting erosional processes may have removed pre-Campanian sedimentary rocks ("Loma Chumico") from the uplifted highs. The short-lived carbonate banks were rapidly overlain by pelagic limestones (Piedras Blancas Fm.), due to the subsidence of the tectonic pile to bathyal depths. Pelagic limestones were deposited until the late Maastrichtian, when arc-derived turbidites (Curú Fm.) reached these parts of the basin (Baumgartner et al., 1984). We interpret these facies changes as the consequence of the Nicoya Complex accretion to the active margin (Andjić, 2017; Figure 20). The accretion of this exotic, buoyant plateau caused the cessation of the volcanic arc activity, as well as the extensive uplift of the southern Sandino and Tempisque forearc basins. As a result, a discontinuous, 120 km-long belt of carbonate and siliciclastic, shelf sediments was deposited over inner forearc regions that were previously located in deep-water settings (Denyer & Alvarado, 2007). Post-collisional subsidence led to the deposition of pelagic limestones over the shelf facies. Volcanic arc activity restarted during the Maastrichtian, well after the accretion event.

4.1.3 | Late Maastrichtian–Eocene

During that time, the SFB experienced almost constant turbiditic accumulation, which was controlled by subsidence and volcanic arc activity. In consequence, the basin depocenter was filled with 5–7 km of turbidites (Rivas-Curú and Brito-Descartes fms.) at the end of the Eocene (McIntosh et al., 2007; Ranero et al., 2000; Struss et al., 2008). Due to differential subsidence of the depocenter, the turbidite infill pinched out trenchward, as it onlapped the outer high (Figures 5 and 21a).

4.1.4 | Late Palaeocene–early Eocene

The Sapoá and La Calera limestones (Nicaragua; Figures 6 and 10), and the Barra Honda Fm. (Costa Rica), indicated that

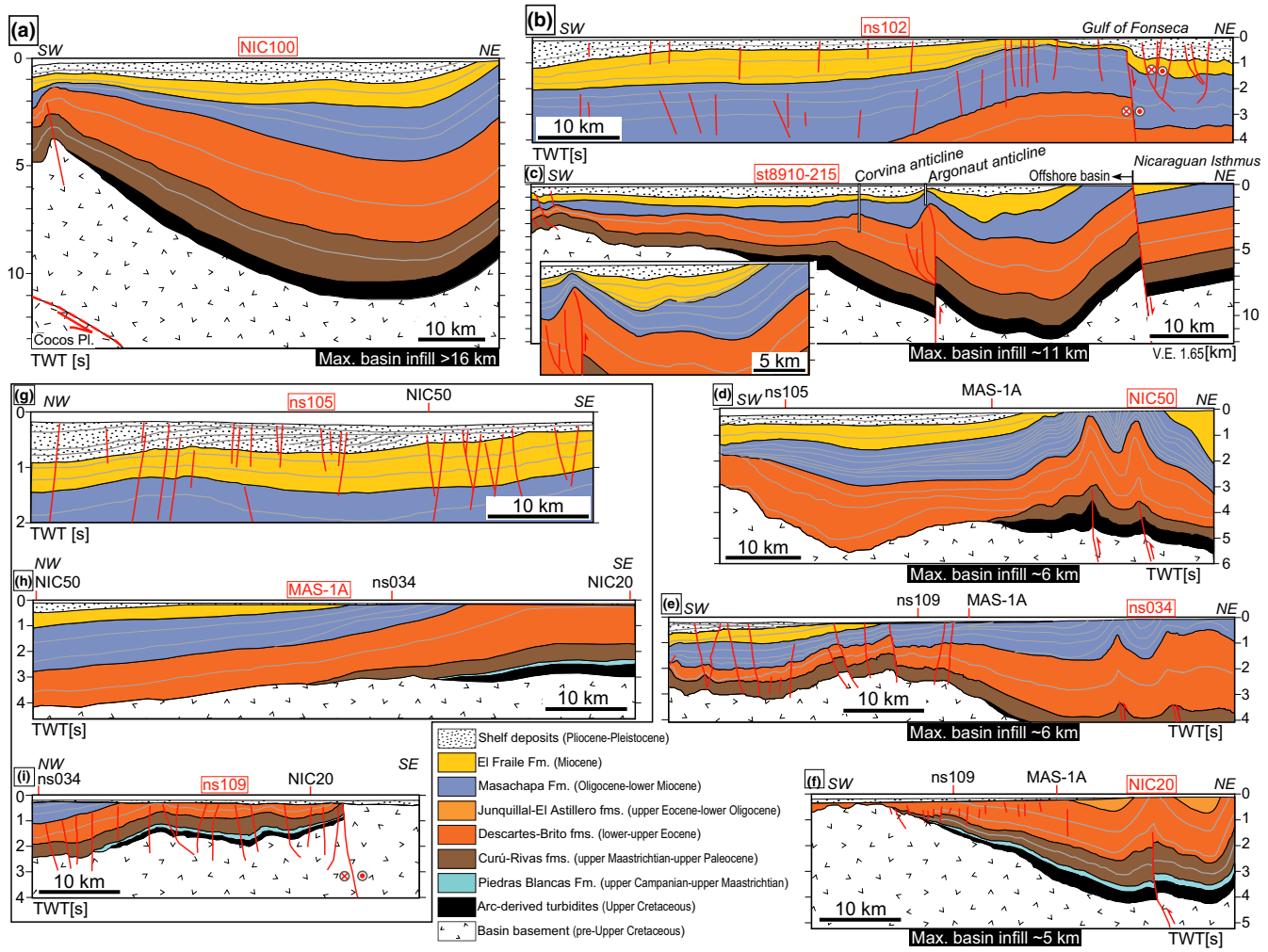

FIGURE 19 Seismic profiles of the Sandino Forearc Basin. See Figure 2b for profile locations. In (a–f): basin-normal profiles. In (g–i): basin-parallel profiles. All depths are in two-way travel time (TWT [s]), except for the profile st8910-215 in (c) [km]. (a) Profile NIC100 (after McIntosh et al., 2007). (b) Profile ns102 (after Funk et al., 2009; Stephens, 2014). (c) Profile st8910-215 (after Ranero et al., 2000; Struss et al., 2008). The onshore section is reconstructed from onland geology (after Funk et al., 2009); the vertical lines correspond to Corvina and Argonaut offshore wells (Ranero et al., 2000). (d) Profile NIC50 (after McIntosh et al., 2007). (e) Profile ns034 (after Stephens, 2014). (f) Profile NIC20 (after Berhorst, 2006). (g) Profile ns105 (after Stephens, 2014). (h) Profile MAS-1A (after Berhorst, 2006; McIntosh et al., 2007). (i) Profile ns109 (after Stephens, 2014)

shallow-water environments existed in the Sandino and Tempisque basins during the late Palaeocene–early Eocene. The fact that shallow-water carbonate banks and abundant pelagic limestones (Buenavista Fm.) coexisted in both basins suggests that a regional tectonic event may have caused uplift and shutdown of the volcanic arc (Figure 20). A hint about the origin of this tectonic event may be found in the geology of the Burica Peninsula (southern Costa Rica; Figures 1b and 20). According to Buchs et al. (2009), this area documents the Palaeocene accretion of a Coniacian–Santonian oceanic plateau (Inner Osa Igneous Complex). The accretion event was sealed by the deposition of the late Palaeocene Pavones Fm. (Di Marco, 1994; Obando Rodriguez, 1986), which reworks shallow-water facies very similar to those observed in the Barra Honda and Sapoá limestones (Baumgartner-Mora & Baumgartner, 2016). Therefore, we suspect that rough crust subduction occurred not only in the Osa-Burica area, but also operated further to the north. The impingement of another bathymetric feature along the strike of the trench may have been responsible for the uplift of the inner Tempisque basin and southern SFB.

4.1.5 | Late Eocene

During the latest Eocene–earliest Oligocene, the southern SFB experienced a different sedimentary evolution in comparison to the rest of the basin (Figure 4). The inner forearc of this basin segment reached shallow-shelf environments, contemporaneously to the Costa Rican Tempisque Forearc Basin, while the central and northern

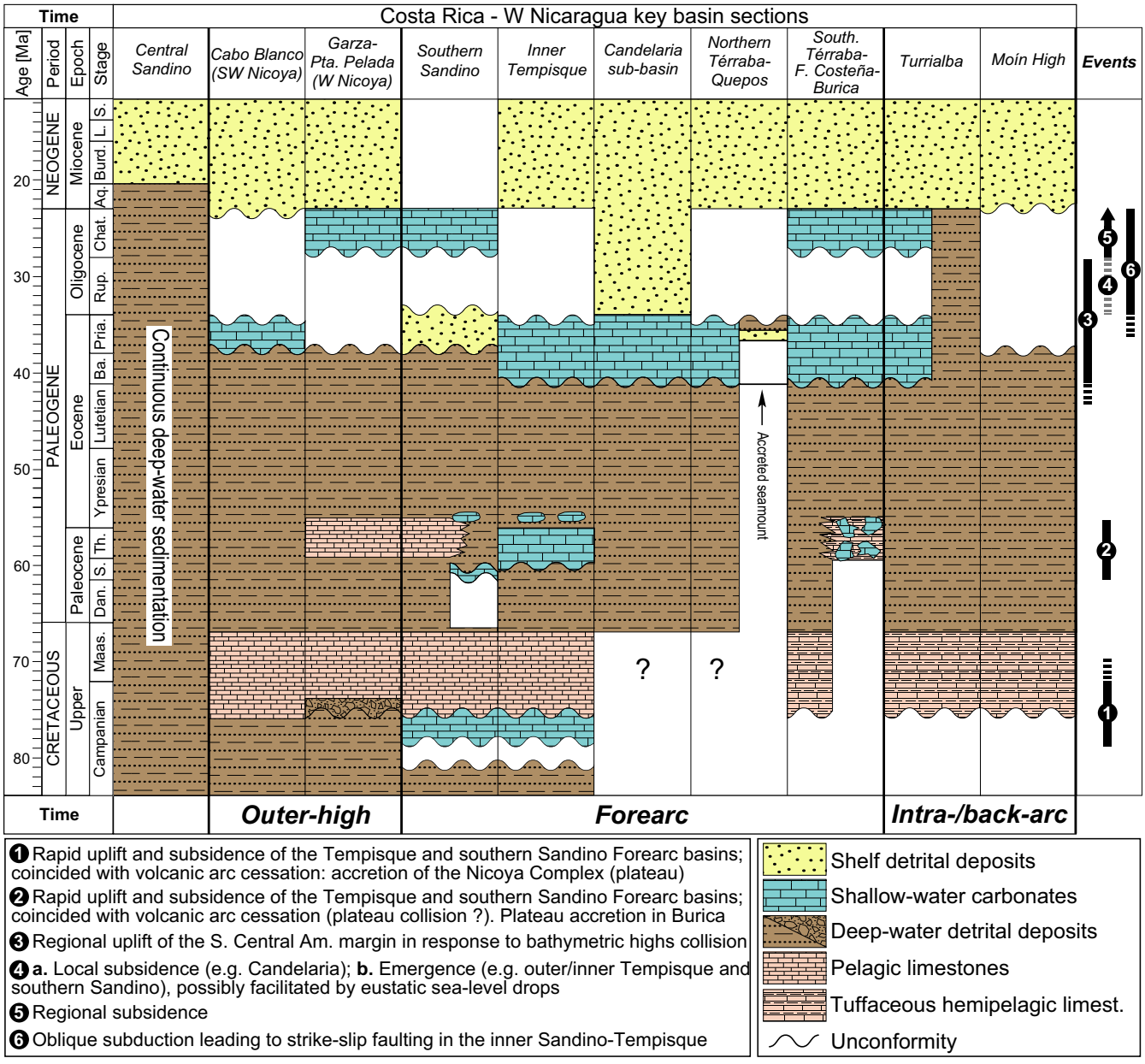

FIGURE 20 Chronostratigraphic chart of key basin sections located in outer-high, forearc and back-arc settings of Costa Rica and western Nicaragua (compiled from Amann, 1993; Aguilar & Cortés, 2001; Baumgartner-Mora & Baumgartner, 2016; Baumgartner et al., 1984; Brandes et al., 2009; Denyer & Alvarado, 2007; Hoffstetter et al., 1960; Jaccard et al., 2001; Krawinkel et al., 2000; Mende, 2001; Sprechmann, Astorga, Calvo, & Fernández, 1994; Weyl, 1980; Yuan, 1991; this study). For events 1 and 2: volcanic arc cessation seems to have occurred only inboard of the present-day Nicoya-Santa Elena and Osa-Burica Peninsulas. See Figures 1–3 for locations

segments remained in deep-water settings (Figure 21b). The southern SFB underwent a major facies change, with the replacement of deep-water turbidites (Brito-Descartes fms.) by shallow shelf tempestites (El Astillero-Junquillal fms.), with local unconformities. On the other hand, deep-basin to slope deposits (Masachapa Fm.) continued to be deposited conformably in the central SFB until the latest Oligocene (Figures 3, 4, 20, and 21). This previously unrecognized feature advocates for a differential tectonic evolution of SFB segments.

Actually, the late Eocene "shallow-marine event" was recognized in many localities of Costa Rica (Figure 20) and Panama (and also in the circum-Caribbean) and was attributed to a major uplift of the southern Central American arc (Iturralde-Vinent & MacPhee, 1999; and references therein). Recently, this uplift has been explained by different approaches: accretion of seamounts in the forearc area (Di Marco, 1994; Krawinkel et al., 2000) enhanced by a motion change in the Farallon Plate with respect to the Caribbean Plate (Buchs, Baumgartner, Baumgartner-Mora,

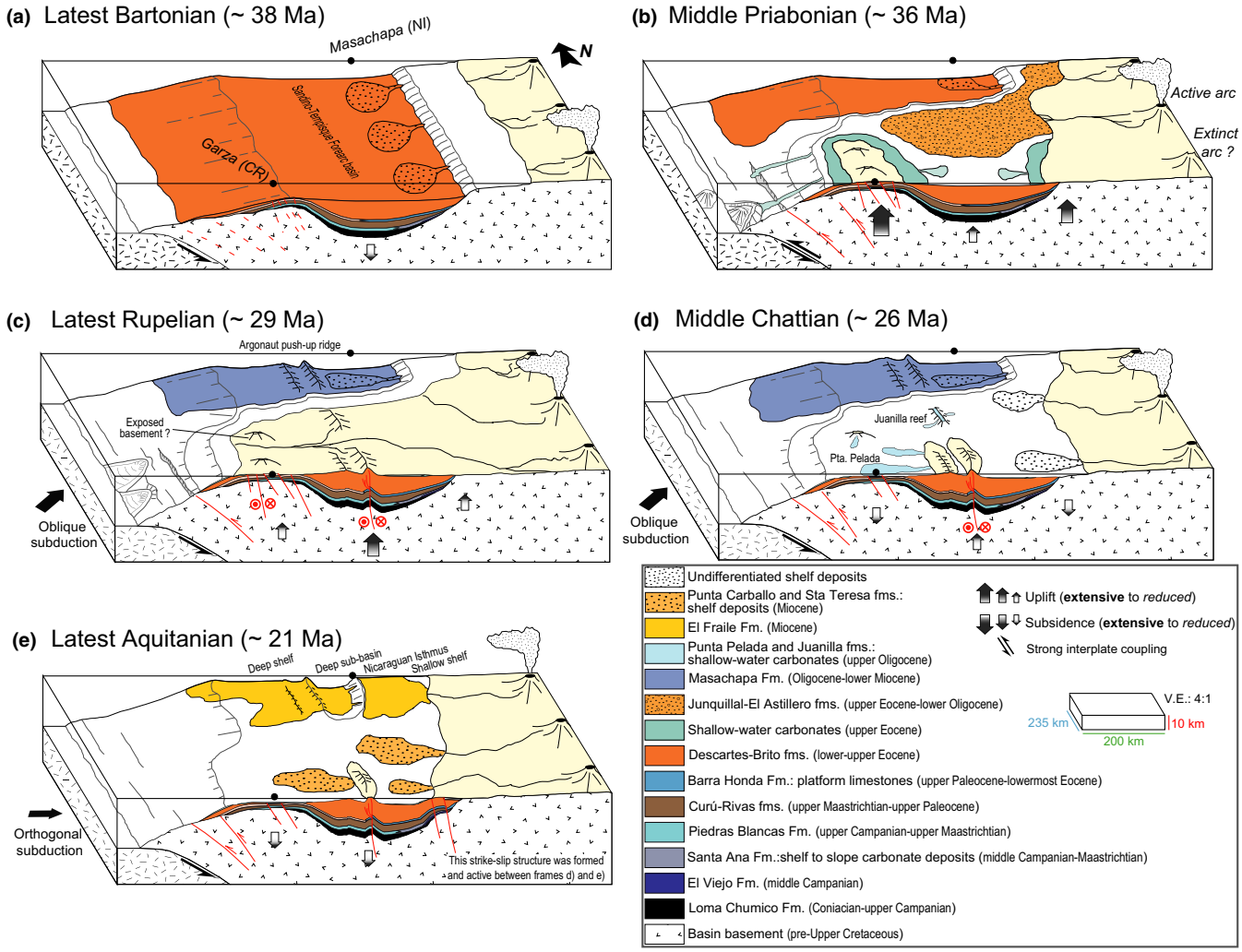

FIGURE 21 Five-step evolution of the Tempisque (TP), and southern and central Sandino (SFB) forearc basins between the late middle Eocene (~38 Ma) and the early Miocene (~21 Ma). Positions of the present-day Masachapa (Nicaragua) and Garza (Costa Rica) towns are indicated. (a) Deep-water sedimentation in subsiding TP–SFB. (b) Collision of seamounts with the Costa Rican active margin. Uplift of the TP and southern SFB. Deposition of shallow-shelf volcaniclastics and carbonates on uplifted forearc areas. Ongoing deep-water sedimentation in the central SFB, which remains unaffected by the impingement of bathymetric features. (c) Ongoing uplift and eustatic sea-level drops cause emersion episodes in the southern SFB and TP. The central SFB is still in a deep-water setting. Onset of strongly oblique subduction causes strike-slip faulting and localized uplift in the forearc (Argonaut-type structures). (d) Cessation of seamount collisions. Slight subsidence of the forearc leads to renewed shallow-shelf carbonate and volcaniclastic deposition. (e) Initiation of shallow-shelf sedimentation in the central and northern SFB, facilitated by the uplift of the Nicaraguan Isthmus. Transpressional motion and uplift along the Nicaraguan Isthmus between frames (d) and (e) was possibly caused by the Oligocene episode of oblique subduction. See text for more details

Flores, & Bandini, 2011); collision of the southern Central American arc with South America (Barat et al., 2014); rotation of far-field stresses in the Caribbean Plate due to its engulfment between Americas (Iturralde-Vinent & Gahagan, 2002). The concept proposed by Iturralde-Vinent and Gahagan (2002) appears rather seducing, however it does not account for the differential sedimentary evolution of southern Central America when compared to its northern counterpart. Although an arc-continent collision played a significant part in the tectonic evolution of Panama since the late Eocene, we favour a predominant role of subducting seamounts in the tectonic evolution of southern Central American forearc basins during the late Eocene–early Oligocene. Direct evidence of seamount accretion during the middle–late Eocene was reported from several localities (Figure 1): Herradura (Tulín Fm.), Quepos, and Osa-Burica peninsulas in Costa Rica (Arias, 2003; Baumgartner et al., 1984; Baumgartner-Mora & Baumgartner, 2016; Buchs et al., 2009), and Azuero Peninsula in Panama (Buchs, Arculus, Baumgartner, & Ulianov, 2011; Buchs, Baumgartner, et al., 2011). The accretion and/or offscrapping of seamounts caused uplift of various areas of southern Central America. It was often accompanied by deposition of shallow-water facies over tectonic highs floored by eroded,

deep-basin lithologies (Figures 20 and 21b). In Costa Rica, tectonic uplift affected outer high settings (Punta Cuevas Fm., southern Nicoya Peninsula; Baumgartner et al., 1984), forearc basins (Fila de Cal Fm.; Denyer & Alvarado, 2007), intra-arc basins (Las Animas Fm., Turrialba; Lohmann & Brinkmann, 1931) and back-arc basins (Moín High, Límon Basin; Brandes, Astorga, & Winsemann, 2009; Figures 1c and 20).

The subduction of seamounts possibly initiated the retreat of the volcanic front in Panama by subduction erosion (Lissinna, 2005; Lissinna, Hoernle, & den Bogaard, 2002). Moreover, a middle–upper Eocene collision of a buoyant indentor inducing a slab tear was invoked by Whattam et al. (2012) to explain Oligocene–lower Miocene adakitic intrusions in western Panama. However, it remains unclear whether the upper Eocene–lower Oligocene arc gap in eastern Panama is linked to the collision of an indentor with the trench (e.g. Whattam et al., 2012) or to the collision of the Central American arc with South America (e.g. Barat et al., 2014; Montes, Bayona, et al., 2012; Montes, Cardona, et al., 2012).

In summary, the Costa Rica-Panama island arc was affected by important uplift events during middle-late Eocene times. Deformation and uplift of different palaeotectonic settings strongly suggests the influence of subducting seamounts and/or ridges. Given the proximity of multiple seamounts accreted in Costa Rica during the middle-late Eocene, we consider that the upper Eocene uplift of the southern SFB was related to these collision events. Since only the southern SFB experienced uplift during the late Eocene, it implies that a bathymetric feature entered the subduction zone along this segment, or more probably further to the south. When examining upper Cenozoic examples (Gardner et al., 2001; Mann, Taylor, Lagoe, Quarles, & Burr, 1998; Meffre & Crawford, 2001; Spikings & Simpson, 2014), as well as experimental models (Geist, Fisher, & Scholl, 1993; Gerya, Fossati, Cantieni, & Seward, 2009; Martinod et al., 2013; Vogt & Gerya, 2014), it appears that subducting objects may provoke up to kilometric uplift of island arc segments not only in the vicinity of the object (outer high uplift), but also at distances reaching 200 km along strike. The deformation front may reach such distances in the case of a difference in the trend of the bathymetric feature and the subduction vector. Rapid uplift of overriding plate areas located far from the subducting object may be explained by a strong coupling of the tectonic plates at shallow depth (Taylor et al., 2005). Locking of the shallow interplate thrust zone may provoke the shortening of the upper plate due to the ongoing convergence at greater depth. Besides uplift, trans-arc strike-slip faults and back-arc folding (e.g. Moín High in Costa Rica; Figure 1c) may develop to accommodate the translation of arc blocks.

4.1.6 | Early Oligocene

Except for the very thin El Astillero Fm., lower Oligocene deposits are not known in the Tempisque and southern Sandino basins (Figures 3 and 20). It suggests that the upper Eocene shallow shelf environments did not persist during the early Oligocene and were possibly replaced by subaerial conditions (Figure 21c). The non-deposition/erosion phase can be explained by a drop of the relative sea-level, due to: (1) an important drop of the eustatic sea-level at the Eocene–Oligocene boundary (Miller et al., 2005); (2) an ongoing uplift of the basin. On the other hand, the central SFB remained in deep-water settings, as it is attested by the conformable deposition of the Masachapa Fm. (Figures 3, 20, and 21c).

During the early Oligocene, the depocenter of the southern and central SFB was folded (profiles NIC20, ns034, NIC50 and st8910; Figures 19c–f), with narrow, symmetrical, high-amplitude anticlines. The development of the Argonaut anticline and equivalent structures southward was related to vertical faults which run parallel to the depocenter. A transpressional mechanism is favoured to explain the folding (Ranero et al., 2000); (1) the vertical structures are isolated and extend along most of the offshore basin; (2) the structures lack vergence, although a fault-propagation fold cannot be excluded due to poor seismic resolution at depth. The tectonic event occurred during the deposition of the Masachapa Fm. The latter thins laterally as it onlaps the anticline; the formation remained unaffected towards the Nicaraguan Isthmus (profile st8910; Figure 19c). Also, in the profiles NIC50 and ns034 (Figure 19d,e), the Masachapa Fm. presents internal onlap surfaces, along which flat-lying reflectors are overlain by seaward-dipping, prograding successions; progradation probably occurred in response to the basin depocenter folding.

By analogy with the present-day forearc sliver tectonics, we infer that oblique subduction and bathymetric highs collision may have caused transpression and faulting of the basin depocenter.

Oblique subduction is known from well-studied active margins such as offshore Sumatra, Kurile, Tonga and Aleutian islands (Ballance et al., 1989; Mann, 2007; Nakano et al., 2010; Ryan & Scholl, 1989). In general, the stresses induced by oblique convergence are accommodated in the forearc basin which experiences strike-slip faulting (Draut & Clift, 2013; Jarrard, 1986). Consequently, forearc areas may be transported along the margin as a forearc sliver (McCaffrey, 1992).

Oblique subduction along the Central American Trench is thought to have occurred prior to the latest Oligocene breakup of the Farallon Plate (Lonsdale, 2005; Mann, Rogers, & Gahagan, 2007; Wilson, 1996). It occurs

currently along northern Central America, offshore Nicaragua, El Salvador and Guatemala, and causes the northwestward motion of a forearc sliver (DeMets, 2001; Norabuena et al., 2004).

Yet, it remains unclear what role could play the subduction of rough, hotspot-thickened crust on the development of transpressional structures. In the present-day situation, the subduction of the Cocos Ridge and related seamounts possibly triggers tectonic escape of the forearc sliver segment coinciding with the southern Nicoya Peninsula (Kobayashi et al., 2014; LaFemina et al., 2009; Montero & Denyer, 2011; Figures 1 and 2). In this case, the translation of the forearc sliver occurs in a context of orthogonal subduction. Further to the northwest, the northwestward translation of the forearc sliver is driven by the oblique convergence of the Cocos plate (Funk et al., 2009). Therefore, it appears less likely that the orthogonal subduction of rough crust influences the motion of the forearc sliver as far as Guatemala; oblique subduction represents a better candidate (Funk et al., 2009; Mann, 2007). Similarly, we suggest that the subduction of bathymetric highs beneath Costa Rica during the late Eocene–early Oligocene may have caused compression/transpression in the southern SFB. However, the Oligocene transpressional structures observed as far as the Gulf of Fonseca (northern SFB; Figures 4, 5, and 19b) are probably the result of oblique subduction alone, whereas the Tempisque Basin and the southern SFB experienced the (oblique?) subduction of bathymetric highs. As a result, the upper Eocene–lower Oligocene shallowing-upward sequence observed in the southern SFB has no equivalent in central and northern SFB. In the central SFB, localized uplift was related to vertical, strike-slip faulting ("Argonaut event") that occurred in deep-water settings during the Oligocene; shallow shelf environments were reached only during the latest Oligocene–early Miocene (see below).

4.1.7 | Late Oligocene–middle Miocene

During the late Oligocene, inner parts of the southern SFB returned locally to marine environments (Figure 21d). After a period of erosion/non-deposition, enough accommodation space was created to allow the development of an upper Oligocene coral reef (Juanilla Fm.; Figures 3, 4, 20, and 21d). The latter grew on an eroded substratum made of upper Eocene tempestites that was possibly folded during the early Oligocene (Argonaut-type anticlines; Figures 4, 19c, and 21c). Similarly, in outer-high settings of the Tempisque Basin, upper Oligocene, shallow-water calcarenites and tempestites were deposited unconformably on eroded upper Eocene turbidites (Baumgartner-Mora et al., 2008; Figures 20 and 21d). Also, in back-arc settings (Límon basin; Figure 1c), upper Oligocene–Miocene muddy shelf deposits (Uscari Fm.) succeeded to shallow-water carbonates (Aguilar, 1999; Amann, 1993; Bottazzi, Fernandez, & Barboza, 1994; Cassell & Sen Gupta, 1989; Mende, 2001; Figure 20). According to Brandes et al. (2009), deformation of the Moín High (Figure 1c) stopped during the late Oligocene; the anticline was then draped by lower Miocene sediments (Figure 20). Creation of accommodation space in these settings suggests that subsidence affected the southern SFB, the Tempisque Basin, and the Limón Basin (Figure 20). Regional subsidence was probably the result of tectonic stress relaxation after the end of seamount subduction (e.g. Krawinkel et al., 2000).

Yet, local subsidence has already affected some forearc basin segments during the early Oligocene. The Candelaria sub-basin (Figures 1c and 20) presents kilometric Oligocene shelf deposits overlying upper Eocene shallow-water limestones (Rivier & Calvo, 1988); the deposition of this thick sequence in graben structures possibly reflected the creation of extensional structures: (1) after a phase of forearc weakening/material removal due to seamount subduction: (2) due to an outward-stepping of the subduction zone after the accretion of seamounts. In the area, parts of the colliding seamounts were accreted as the Tulín Fm. and the Quepos Chaotic Complex (Figure 1b). After their accretion, these terranes may have represented high reliefs which were one of the sediment-sources which filled the Candelaria graben.

In contrast, the central and northern SFB remained in deep-water settings until the latest Oligocene–early Miocene (Figures 3, 20, and 21d). At this time, a second phase of strike-slip faulting affected the inner SFB (profile ns102; Figure 19b), which resulted in: (1) the uplift of basin parts that coincide with the present-day Nicaraguan Isthmus; (2) the arcward thinning of the uppermost Masachapa Fm. which onlaps the uplifted high in the northern SFB (profile ns102; Figure 19b); (3) the deposition of a shallowing-upward sequence in the central and northern SFB (uppermost Masachapa and El Fraile formations; Figure 21e); (4) the formation of a sub-basin in the central SFB depocenter which was filled with the El Fraile Fm. (profile st8910-215; Figures 19c and 21e). Despite the regional subsidence affecting the forearc basins, strike- slip faulting in the inner SFB produced enough uplift to allow a transition from deep-water (Masachapa) to shallow-shelf (El Fraile) environments.

During the early Miocene, the volcanic arc started to migrate seawards. At this time, the volcanoes were active east of the present-day Nicaraguan Depression (Figure 2). Yet, the upper Oligocene–lower Miocene faulting of the Nicaraguan Isthmus possibly allowed the subsequent emplacement of the middle Miocene Tamarindo Fm. volcanics (Figures 2 and 3). As it has been suggested for the

Quaternary volcanic arc (MacKenzie et al., 2008), it is possible that the faults occurring in the forearc basin may have locally acted as a preferential path for the ascent of magma. The growth of a volcanic center favoured the emergence of the central and northern SFB; in its northern exposures (north of El Transito; Figure 3), the El Fraile Fm. presents continental facies which are interstratified with the Tamarindo Fm. (McBirney & Williams, 1965; Weyl, 1980). In contrast, the southern exposures of the El Fraile Fm. (Casares-Huehuete; Figures 3 and 12) exhibit only shelf facies. These sectors were probably fed by volcaniclastics originating from volcanoes that were located on the eastern side of the present-day Nicaraguan Depression (Coyol group; Ehrenborg, 1996; Figure 2b).

During the early–middle Miocene, the Tempisque Basin remained in shelf environments, as it is attested by the Santa Teresa and Punta Carballo fms. (Amann, 1993; Baumgartner et al., 1984; Denyer, Aguilar, & Alvarado, 2003; Figures 20 and 21).

4.1.8 | Plio-Pleistocene

During that time, the southern SFB experienced a renewed episode of uplift, possibly related to rough crust subduction along the Costa Rican margin. The offshore, basin-parallel seismic profiles (ns105, MAS-1A, and ns109; McIntosh et al., 2007; Stephens, 2014; Figure 19g–i) show the differential uplift experienced by the southern SFB; in profiles MAS-1A and ns109, Pliocene–Pleistocene deposits are very thin; in profile ns109, the basement top is separated from to the sea floor surface by a very thin Pliocene–Pleistocene sedimentary veneer; in the profile ns105, Pliocene–Pleistocene deposits present a reduced thickness in the southeastern part, whereas they thicken and prograde towards the NW. Uplift is also active nowadays in the southern SFB. The Punta Descartes (Figure 3) records active coastal emergence with the occurrence of Holocene shore platforms, beach ridges and stream terraces (Marshall & Vannucchi, 2003). Uplift rates reach 3.5 mm/year and are comparable with those evidenced for the Nicoya Peninsula, which experiences active subduction of seamounts (Fisher, Gardner, Marshall, Sak, & Protti, 1998; Sak, Fisher, Gardner, Marshall, & La Femina, 2009).

In the central Nicaraguan Isthmus, the shallow-water, Pliocene El Salto Fm. unconformably overlies older sequences (Figures 3 and 4). It is not clear what event caused the tilting of the pre-Pliocene strata. The extensional structures associated with the formation of the Nicaraguan Depression (e.g. Alonso-Henar, Schreurs, Martinez-Díaz, Álvarez-Gómez, & Villamor, 2015; Canora et al., 2014) may be a candidate. Fault scarps up to 900 m high are reported along the half-graben (Alonso-Henar et al., 2015; Funk et al., 2009); these faults may have caused the tilting of the neighbouring Nicaraguan Isthmus (Figures 2 and 3). The present-day occurrence of the El Salto Fm. at more than 100 m.a.s.l. may be explained by a tectono-thermal uplift related to the emplacement of Holocene volcanic centers (Gerth et al., 1999).

4.2 | The question of tectonic erosion/accretion

During at least the last 100 million years, various subduction-related processes operated along the Middle American trench. In recent years, the Neogene–Quaternary evolution of the active margin was mainly considered in terms of tectonic accretion/erosion processes and subduction of various bathymetric highs (Mann et al., 2007; Morell, 2015). The most popular models for the recent evolution consider tectonic erosion as one of the dominant factors affecting the arc-trench system. Indeed, the present-day collision of seamounts and ridges induces erosion of upper plate material. Basal erosion leads to trench advance and forearc subsidence, although forearc regions may temporarily experience strong uplift due to the impingement of bathymetric highs. Clift and Vannucchi (2004) estimate a trench advance of 2 km/Ma for the Nicaraguan margin, as an intermediate value between those of Guatemala (0.9 km/Ma since 25 Ma) and Costa Rica (3 km/Ma since 17 Ma). If such rates operated during Neogene–Quaternary times along the Nicaraguan margin, it would imply a trench advance of ~50 km. However, such a trench advance is incompatible with the long-term, trenchward migration of the volcanic front in Nicaragua (~100 km since the early Miocene; Ehrenborg, 1996; Plank et al., 2002; Figure 2b). Other processes are to be invoked to explain the Neogene subsidence of the basin.

The geometry of the SFB changed during the Oligocene (Noda, 2016). Until the late Oligocene, the sedimentation was mainly restricted to the depocenter, resulting in a ridged basin geometry (sensu Dickinson, 1995). The outer high possibly acted as a barrier for sediment transport towards the trench slope (Figure 5). Noda (2016) explains this geometry by a compressional state of the outer wedge, which concentrated subsidence in the axis of the forearc basin. Beginning in the early Miocene, forearc sediments were more uniformly distributed on the shelf and the slope (seaward advance of the shelf edge; McIntosh et al., 2007), tending to a sloped basin configuration (sensu Dickinson, 1995; Figure 5). Indeed, the uplift of the depocenter during the Oligocene temporarily favoured the accumulation of sediments in more distal settings. Yet, a subsidence of the outer high must have occurred during the late Oligocene–early Miocene to allow sediment transport as far as the trench slope. A mechanism of basin overfilling can be excluded because the prograding Miocene–Pliocene

sequences present similar characteristics (thickness, age) among the northern, central and southern SFB, although these basin segments display very contrasting pre-Miocene subsidence histories (i.e. major thickness variations in the basin infills). In contrast, this subsidence phase may have been facilitated by two processes that possibly co-occurred: (1) relaxation of the tectonic stress that affected the basin during the late Eocene–Oligocene; (2) upper plate extension induced by slab rollback or steepening (Funk et al., 2009; Weinberg, 1992).

Process 1 relies on the following observation: in southern Nicaragua and northern Costa Rica, the late Oligocene epoch was marked by the deposition of shallow-water limestones on subaerially eroded upper Eocene lithologies, followed by the deposition of shelf siliciclastics during the Miocene. This palaeoenvironmental change suggests that the considered forearc areas subsided after an uplift phase created by seamount collisions associated with oblique subduction.

Process 2 is supported by the Neogene trenchward migration of the volcanic arc, and ultimately, by the late (?) Miocene development of an intra-arc half-graben (Nicaraguan Depression). It remains unclear if or how slab rollback/steepening may be related to the plate reorganization that occurred at ~23 Ma, following the breakup of the Farallon Plate.

Yet, a change from oblique (pre-23 Ma Farallon Plate) to faster, more orthogonal (post- 23 Ma Cocos Plate) subduction seems to have accompanied the transition from a compressional/transpressional regime to an extensional regime in the overriding plate. The mechanism behind this transition is not straightforward, challenging the common view that increased subducting plate or convergence velocities result in shortening of the overriding plate (Lallemand, Heuret, Faccenna, & Funiciello, 2008). Moreover, some natural and modelled subduction systems suggest that upper plate deformation may not be directly correlated with convergence rates, as well as subducting slab age and velocity (Baitsch-Ghirardello, Gerya, & Burg, 2014; Gerya & Meilick, 2011; Schellart, 2008). Interestingly, Jordan et al. (2001) report extension of the Southern Andes margin after the fission of the Farallon Plate. This extensional phase occurred after a change in the subduction regime, with faster, less oblique convergence in post-25 Ma times. Although seeming to involve a contradiction in plate kinematics, Cembrano et al. (2007) consider that the extension could be related to a reduction in plate coupling. They consider that increased convergence velocities reduced the effective viscosity at the trench. Also, decoupling may have been facilitated by an increasing dehydration of the slab (Baitsch-Ghirardello et al., 2014), which was possibly reduced during the episode of oblique subduction and seamount collisions (Seno, 2007).

In addition, the extension of the forearc area could have been enhanced by an eastward motion of the overriding plate segment (Chortis Block *s.l.*; Figure 1). During the Cenozoic, the northwestern and the southwestern edges of the Caribbean Plate experienced very different tectonic evolutions. Since the middle Palaeogene, the northwestern corner of the Caribbean Plate has been marked by left-lateral, strike-slip movements which accompanied the eastward migration and counter-clockwise rotation of the Chortis Block with respect to North America (Rogers, Mann, & Emmet, 2007; Rosencrantz, Ross, & Sclater, 1988; Pindell, Kennan, Stanek, Maresch, & Draper, 2006; Figure 1). These movements induced an extensional regime in the Chortis Block, with the opening of N–S-directed rifts at least since the Miocene (Mann & Burke, 1984; Morán-Zenteno, Keppie, Martiny, & González-Torres, 2009; Rogers & Mann, 2007; Sanchez, Mann, & Emmet, 2015; Figure 1). On the other hand, the southwestern corner of the Caribbean Plate has been characterized by a compressional regime, mainly related to the collision of the South Central American arc with South America, possibly since the latest Eocene (Barat et al., 2014; Montes, Bayona, et al., 2012). Since the Eocene, this segment of the Middle American trench has also endured periodic collisions of bathymetric highs, augmenting the compression in the upper plate. It is noteworthy to point out that the SFB recorded the influence of both tectonic regimes. The southern SFB has experienced uplift/subaerial exposure phases due to bathymetric highs indentation, resulting in a basin thickness of ~5 km (Figures 5c and 19f). On the contrary, the northern SFB did not experience such compressional tectonics. During the late Oligocene and the Pliocene–Pleistocene, it was only affected by localized strike-slip faulting that induced slight uplift of its inner part (profiles NIC100 and ns102; Figure 19a,b). Since the Late Cretaceous, almost continuous subsidence of the depocenter has allowed the accumulation of a 16-km-thick sedimentary pile (Figure 5a), which precludes the possibility that an efficient, long-term process of subduction erosion affected the northern SFB (Mann et al., 2007). Nevertheless, there is no evidence of accretion processes at the trench or underplating beneath the wedge, since the later seems to be only composed of igneous basement rocks emplaced prior to the basin inception (McIntosh et al., 2007).

4.3 | Origin of the Nicaraguan Depression and its relation to vertical motions in onshore Central America

4.3.1 | State of the art

The timing and the cause of the Nicaraguan Depression (Figures 1 and 2) opening remain an enigmatic issue.

Several studies have tentatively described the tectonic structure of the today Nicaraguan Isthmus and the neighbouring Nicaraguan Depression, which represent the emerged parts of the SFB. Different structural models have been proposed and are gathered in essentially two groups (Funk et al., 2009). The first group is composed of models which suggest that the Nicaraguan Depression developed either as an asymmetrical graben (Carr, 1976; McBirney & Williams, 1965; Weinberg, 1992), in relation to slab rollback-induced extension or changes in the subducting slab dip angle (volcanic front migration; Figure 2b), or as a symmetrical graben formed by strike-slip faulting (Cruden, 1989). Mann et al. (2007) proposed that the depression formed either in relation to slab rollback, possibly triggered by a slab break-off during the late Miocene (Rogers, Karason, & van der Hilst, 2002), or by right-lateral, strike-slip faulting (forearc sliver) due to the oblique subduction of the Cocos Plate. On the contrary, the second group proposes that the depression represents a piggyback syncline which was produced by a shortening event during the Pliocene (Borgia & van Wyk Vries, 2003; Van Wyk Vries, 1993). In these models, the neighbouring Rivas anticline is related to a thrust-fault.

However, recent offshore and onshore seismic-reflection studies of Stephens, Fulthorpe, and McIntosh (2007), Funk et al. (2009), and Stephens (2014) have shed a new light on the structure of the Pacific coast of Nicaragua. It appears that the slightly-folded Nicaraguan Isthmus represents an uplifted rift shoulder bordered to the east by the Nicaraguan Depression. The latter corresponds to a highly asymmetrical half-graben separated from the uplifted isthmus by northeast-dipping, oblique-slip normal faults (Funk et al., 2009). These geophysical studies point out significant variations in the uplift pattern along the 300-km-long Nicaraguan Isthmus. The southeastern isthmus, close to the border with Costa Rica, shows the most extensive footwall uplift with a supposed offset of more than 4 km along the master fault which separates it from the Nicaraguan Depression (mature footwall uplift). Also, the oldest outcropping rocks of the isthmus (Uppermost Cretaceous) are exposed in this area. Offshore structures such as the Argonaut and Corvina anticlines (profile st8910-215; Figure 19c) are explained by an out-of-syncline compression due to the extension-related uplift of the Nicaraguan Isthmus. In contrast, the northwestern isthmus, close to the Gulf of Fonseca, displays juvenile footwall uplift, with an offset of only a few hundreds of meters along the normal faults that delimit the border with the depression (profile ns102; Figure 19b). Funk et al. (2009) explain these along-isthmus uplift variations by a time-transgressive migration of the extensional event. According to these authors, the rifting event initiated in the southeast, during the late Oligocene–early Miocene, and propagated to the northwest during the Miocene–Pliocene. Masachapa, El Fraile and El Salto formations are considered as syn-rift deposits.

4.3.2 | The Nicaraguan Depression: mode and timing of initiation

In the most recent model of development of the Nicaraguan Depression, Funk et al. (2009) suggested that the SFB offshore anticlines (e.g. Argonaut, Corvina) formed in response to the time-trangressive uplift of the Nicaraguan Isthmus ("out-of-syncline folding"; see examples in Mitra, 2002). This solution is not feasible for the following reasons: (1) the anticlines are separated from the uplifted Nicaraguan Isthmus ("rift shoulder or footwall") by a 10-km-long, undeformed, flat-lying section of the basin which shows no connection between the two structures (profile st8910-215; Figure 19c); (2) the anticlines formed prior to the uplift of the Nicaraguan Isthmus, as discussed previously; (3) these narrow, high-amplitude, folded structures appear as push-up ridges clearly related to vertical faults, suggesting a strike-slip mechanism of formation (e.g. Ranero et al., 2000); (4) the folding of the depocenter in the offshore was not time transgressive, as it occurred in southern (Andjić et al., 2016) and central SFB (profile st8910-215; Figure 19c) during the Oligocene.

During the Oligocene, the southern SFB experienced a transpressional regime which produced strike-slip faulting in the entire SFB, with a decreasing intensity of deformation towards the north (i.e. only one low-amplitude anticline formed in the northern SFB). The transpressive structures formed during the deposition of the Oligocene Masachapa Fm., which shows syn-sedimentary folding (profiles st8910-215, NIC50, ns034, NIC20; Ranero et al., 2000; Stephens, 2014; Figure 19c–f) and lateral thinning towards the uplifted Nicaraguan Isthmus (profile ns102; Funk et al., 2009; Stephens, 2014; Figure 19b). Therefore, we are doubtful that the Masachapa Fm. recorded the initiation of the Nicaraguan Depression as the consequence of an Oligocene extensional regime (rifting), as stated by Funk et al. (2009). An extensional regime intervened only after the transpressional events and affected the whole basin, possibly starting during the latest Oligocene–early Miocene (see above). Subsidence of the outer high led to progradation of Miocene–Pliocene strata as far as the lower trench slope (Figure 5).

Funk et al. (2009) also stated that a rifting event initiated in the south during the late Oligocene–early Miocene and reached the Gulf of Fonseca during the Miocene–Pliocene. Several observations may be opposed to their view of a time-transgressive rifting in the Nicaragua Depression:

1. Earliest evidence for the uplift of the Nicaraguan Isthmus correspond to; (1) the eastward, lateral thinning of

the Masachapa in the northern SFB (offshore profile ns102); (2) the eastward, lateral thinning of the El Fraile Fm. on uplifted Masachapa lithologies in the central SFB (offshore profile st8910-215). In both areas, the uplift event occurred during the same time period, i.e. the late Oligocene–earliest Miocene. Similar uplift timings for both basin segments preclude a time-transgressive rifting event. Moreover, the uplift of the Nicaraguan Isthmus in the Gulf of Fonseca may not have occurred later than the early Miocene, contradicting the Miocene–Pliocene timing proposed by Funk et al. (2009).

2. If a rifting event initiated in the southern SFB during the Oligocene and reached the northern SFB during the Miocene–Pliocene, one should expect: (1) a northward younging of the volcanic activity along the volcanic front located in the Nicaraguan Depression; (2) a relatively short period of time (a few m.y.) between the initiation of forearc rifting and onset of arc volcanism in the forearc rift (see for example Martinez & Taylor, 2006); (3) a northward younging of the syn-rift deposits formed in the Nicaraguan Depression and in the offshore SFB. Phenomenon (a) is not observed, since no volcanic center older than 3.6 Ma is observed in the Nicaraguan Depression (Saginor et al., 2011). Phenomenon (b) is not observed, since no volcanic centers formed in the vicinity of the Nicaraguan Isthmus following its late Oligocene–early Miocene uplift. In other words, it is not possible to reconcile a late Oligocene–early Miocene rifting event with an onset of arc volcanism 20 m.y. later, i.e. during the Quaternary. Phenomenon (c) is not observed, since the oldest "syn-rift deposits" systematically correspond to Oligocene–early Miocene Masachapa Fm. in all the basin segments (see above and Funk et al., 2009).
3. There is no sedimentary evidence in the onshore and offshore SFB for significant footwall uplift during the Miocene. The earliest uplift event occurred in the southern SFB during the late Eocene–early Oligocene, followed by a period of subsidence during the late Oligocene (Andjić et al., 2016). Then, all the basin segments were affected by strike-slip faulting during the Oligocene, first along the depocenter (lower Oligocene) and then along the Nicaraguan Isthmus (late Oligocene–early Miocene). Finally, Miocene–Pliocene shallow-shelf drape sequences were deposited above these anticlines. In summary, the Nicaraguan Isthmus reached shallow-shelf environments until the early Miocene, discarding a northward uplift propagation from the Oligocene to the Pliocene.

In contrast, several arguments are in favour of a Pliocene development of the Nicaraguan Depression:

1. The seaward-tilting of pre-Pliocene strata and the unconformable deposition of the Pliocene El Salto Fm. occurred in the vicinity of the most prominent fault bounding the depression, the Mateare Fault, which presents a relief of 900 m (Funk et al., 2009).
2. The oldest volcanic rocks recovered from the Nicaragua Depression so far are dated at ~3.6 Ma (middle Pliocene, Encanto; Saginor et al., 2011). If we assume that the faults underlying the Nicaraguan Depression represent a preferential path for magma emplacement, then these structures may have been formed during the Pliocene.
3. The most recent structural studies of the El Salvador Fault Zone (or Median Trough) show that the graben structures are the result of a two-phase evolution (Alonso-Henar et al., 2015; Canora et al., 2014). An initial, extensional phase occurred between 7.2–6.1 Ma (latest Miocene) and 1.9–0.8 Ma (early Pleistocene) and may be related to the slab rollback of the Cocos Plate. It produced 300-m-high fault scarps. A second, transtensional phase has occurred since 1.9–0.8 Ma and reactivated the extensional structures as strike-slip faults. Oblique subduction is considered to drive the margin-parallel movement of the forearc sliver.
4. Slab breakoff beneath northern Central America is thought to have occurred between 10 Ma (middle Miocene) and 4 Ma (early Pliocene) and triggered epeiorogenic uplift of the Central American plateau (Rogers et al., 2002). Formation of the Nicaraguan Depression may represent an additional effect of this event (Mann et al., 2007), since extensional tectonics generally accompany or follow episodes of slab breakoff in forearc and back-arc settings (Boutelier & Cruden, 2017; Garzanti, Radeff, & Malusà, 2018; Guillaume, Funiciello, Faccenna, Martinod, & Olivetti, 2010).

Finally, it is possible that some of the Oligocene strike-slip faults have been reactivated during a subsequent extensional tectonic regime, facilitating the development of the Nicaraguan Depression. The apparent rift shoulder geometry of the Nicaraguan Isthmus (Figure 19b,c,f) may be a push-up structure inherited from the Oligocene transpressional phase. Examples of such transpressional structures were imaged offshore California (Legg, Kohler, Shintaku, & Weeraratne, 2015) and Sumatra (Berglar et al., 2010; Ghosal, Singh, Chauhan, & Hananto, 2012; Mosher, Austin, Fisher, & Gulick, 2008).

In summary, the extensional structures of the Nicaraguan Depression must have formed after the upper Eocene–upper Oligocene compressional/transpressional phase and prior to the Pleistocene–Holocene transtensional phase (e.g. Alonso-Henar et al., 2015; Canora et al., 2014). These extensional structures possibly reactivated some of

the Oligocene strike-slip faults of the inner SFB that are observed along the Nicaraguan Isthmus (Figure 19b). Extensional faulting along the Nicaraguan Depression possibly occurred during the Pliocene and caused seaward-tilting of the Nicaraguan Isthmus with the unconformable deposition of the El Salto Fm. Although it appears as the apparent footwall of the Nicaraguan Depression, the folded Nicaraguan Isthmus represents an inherited structure from an earlier tectonic phase, as suggested by Weinberg (1992). Faults of the depression acted as magma conduits for the emplacement of the Pliocene–Recent volcanic front. The latter migrated westward to its present position over a distance of 100 km during the Miocene–Pliocene (Figure 2b).

4.3.3 | Thickness variation in the SFB

The drastic thickness variation between the southern SFB (5 km; Figure 5c) and the northern SFB (16 km; Figure 5a) has probably not been produced by the uplift of Nicaraguan Isthmus (footwall of the Nicaraguan Depression). If a rifting process was responsible for the post-Oligocene geometry of the basin (e.g. Funk et al., 2009), the southern SFB, which inner part presents the most uplifted footwall, should have presented the thickest "syn-rift" deposits of the entire basin (see e.g. Sharp, Gawthorpe, Underhill, & Gupta, 2000). In other words, the greater rift shoulder uplift the greater subsidence should be produced seaward of this shoulder. Actually, the opposite is true for the different segments of the SFB. In our view, the reduced thickness and the almost complete absence of post-Eocene lithologies in the southern SFB may be explained by the proximity of this basin segment with a domain periodically affected by uplift and possibly strike-slip in relation to the collision of bathymetric features. The resulting erosion and lack of accommodation space allowed the preservation of an only 5-km-thick depocenter (Figure 5c). The strong uplift of the Nicaraguan Isthmus in this area ("mature footwall uplift" of Funk et al., 2009) is actually the result of high compression/transpression. Inversely, the much thicker northern SFB (16 km; Figure 5a) seems to have experienced only one uplift phase of much lower amplitude, which excludes an influence of rough crust subduction on this basin segment during the Cretaceous–Cenozoic.

Finally, the northward thickening of the SFB may be additionally explained by contrasting, along-basin sediment supplies. The Central American Isthmus is wide and mountainous inboard of the northern SFB, whereas it is characterized by narrow lowlands further to the south; this morphology difference has probably persisted since Cretaceous times, given the basement difference between northern Nicaragua-Honduras (continental crust, Chortis Block) and southern Nicaragua (oceanic ultramafics-mafics, MCOT; Figure 1b). The Gulf of Fonseca area has drained a large area with longer river systems than those of the narrow isthmus. Therefore, the northern SFB has received a much higher sedimentary supply when compared to its southern counterparts.

Interestingly, back-arc basins located along southern Central America (Providencia, Limón; Brandes et al., 2009; Muñoz, Artiles, Duarte, & Barboza, 1997) present a thickness of 8–10 km, which is twice as much as the southern SFB. This fact suggests a predominance of tectonic factors in the subsidence history of the southern SFB.

5 | CONCLUSIONS

Despite its long geological history, the SFB revealed the existence of new geological features which are meaningful for the understanding of the southern Central American margin evolution. New bio-lithostratigraphic data allowed us to update the chronostratigraphic chart of the basin and to propose a tectono-stratigraphic evolution of the basin.

Three new, shallow-shelf formations were recognized in the basin stratigraphy; the upper Eocene Junquillal and the upper Oligocene Juanilla formations in Costa Rica (Andjić et al., 2016), and the lower Oligocene El Astillero Fm. in Nicaragua (Figure 3). During the late Eocene, a shallowing-upward of the southern SFB is evidenced by a transition from turbidites of the Descartes-Brito formations to shelf deposits of the Junquillal-El Astillero formations. A similar sedimentary evolution is recorded in the forearc basins located further to the south (Figure 20). A regional uplift caused the shallowing and is regarded as the response of the forearc basins to the collision of bathymetric highs. In the southern Sandino and Tempisque basins, erosion/non-deposition encompassed the latest Eocene–lower Oligocene as a possible result of eustatic sea-level drops and active tectonic uplift; subsidence occurred during the late Oligocene–early Miocene, leading to the deposition of shelf volcaniclastics and scarce carbonates.

In contrast, the central and northern SFB hosted deep-water sediments until the latest Oligocene-earliest Miocene. There, the basin depocenter experienced two phases of transpressional, strike-slip faulting: (1) a lower Oligocene phase caused localized uplift of the basin depocenter (Argonaut-type anticlines); (2) an uppermost Oligocene phase uplifted the inner SFB (Nicaraguan Isthmus) and possibly favoured the seaward progradation of shelf volcaniclastics (El Fraile Fm.; Figure 21). We propose that the transpressional events were the result of oblique subduction, which occurred along the Central American trench prior to the breakup of the Farallon Plate during the latest Oligocene (Lonsdale, 2005).

The Nicaraguan Depression probably developed after the Oligocene transpressional events, as its formation

implies an initial phase of extension (Alonso-Henar et al., 2015; Canora et al., 2014). Yet, the extensional structures of the depression formed prior to the renewed Quaternary strike-slip faulting and forearc sliver development along western Nicaragua. During the Neogene, trenchward arc migration and outer-high subsidence were the result of slab-roll back; these conditions were favourable to the development of the Nicaraguan Depression, possibly during the Pliocene.

Although the Nicaraguan Isthmus appears as the present-day footwall of the Nicaraguan Depression, its uplift/folding has already occurred during the Oligocene transpressional faulting of the SFB. Structural measurements of Weinberg (1992) also imply that folding of the Nicaraguan Isthmus occurred prior to the extensional episode which formed the Nicaraguan Depression.

The depositional record of the SFB represents a unique example of sedimentary response to tectonic events and subduction zone processes. This record may serve as a precious guide for the recognition of past tectonic events in forearc basins exposed around the world.

ACKNOWLEDGMENTS

The field work in Nicaragua would not have been possible without the support of the Instituto de Geología y Geofísica (IGG-CIGEO, UNAN, Managua), and especially without the help of Dionisio Rodríguez Altamirano. In the field, we received the help of Elliet Romero, Mélida Schliz and Mayela. Many thanks to Don Santiago who drove us safely through beautiful Nicaragua. We are grateful to Norman Henriquez Blandón (Ministerio de Energía y Minas, MEM) for providing us the documentation for sample exportation and giving us the access to some unpublished literature. Many thanks to Reyna Dania Baca R. from the MEM Hydrocarbon Division for providing us copies of the report and map of Darce and Duarte (2002). Many thanks go to André Strasser, Romain Vaucher and Eric Verrecchia for their help with some sedimentary structures of the El Astillero–Junquillal formations. We are thankful to Paul Mann and an anonymous reviewer for their thoughtful reviews, which greatly improved our manuscript. We thank the editors Peter Swart and Matthieu Cartigny for their dedicated editorial handling. Thanks to Alfred Uchman for checking some ichnofossils of the El Astillero formation. This research was supported by funds of the Swiss National Science Foundation (projects 200021-134873 and 200020-143894) and the Herbette Foundation at the University of Lausanne, granted to P.O. Baumgartner.

CONFLICT OF INTEREST

No conflict of interest declared.

ORCID

Maria Rose Petrizzo http://orcid.org/0000-0002-9584-8471

REFERENCES

Adegoke, O. S., Oyebamiji, A. S., Edet, J. J., Osterloff, P. L., & Ulu, O. K. (Eds) (2017). *Cenozoic foraminifera and calcareous nannofossil biostratigraphy of the Niger delta*. Amsterdam, Netherlands, Elsevier, 592 pp.

Aguilar, T. (1999). Organismos de un arrecife fósil (Oligoceno Superior-Mioceno Inferior), del Caribe de Costa Rica. *Revista de Biologia Tropical*, *47*, 453–474.

Aguilar, T., & Cortés, J. (2001). Arrecifes coralinos del Oligoceno Superior-Mioceno Inferior, de Turrialba, Costa Rica. *Revista de Biologia Tropical*, *49*, 203–213.

Alonso-Henar, J., Schreurs, G., Martinez-Díaz, J. J., Álvarez-Gómez, J. A., & Villamor, P. (2015). Neotectonic development of the El Salvador Fault Zone and implications for deformation in the Central America Volcanic Arc: Insights from 4-D analog modeling experiments. *Tectonics*, *34*, 133–151. https://doi.org/10.1002/2014TC003723

Alvarado, G. E., Dengo, C., Martens, U., Bundschuh, J., Aguilar, T., & Bonis, S. B. (2007). Stratigraphy and geologic history. In J. Bundschuh & G. E. Alvarado (Eds.), *Central America: Geology, resources, hazards* (Vol. 1, pp. 345–394). London: Taylor & Francis. https://doi.org/10.1201/9780203947043

Amann, H. (1993). Randmarine und terrestrische Ablagerungsräume des neogenen Inselbogensystems in Costa Rica (Mittelamerika). *Profil (Stuttgart)*, *4*, 161 pp.

Andjić, G. (2017). Late Mesozoic–Cenozoic sedimentary and tectonic evolution of Middle American plateau and forearc terranes (Nicaragua, Costa Rica). PhD thesis, University of Lausanne, 203 pp.

Andjić, G., Baumgartner-Mora, C., & Baumgartner, P. O. (2016). An upper Paleogene shallowing-upward sequence in the southern Sandino Forearc Basin (NW Costa Rica): Response to tectonic uplift. *Facies*, *62*, 1–35. https://doi.org/10.1007/s10347-016-0463-y

Arias, O. (2003). Redefinición de la Formación Tulín (Maastrichtiano–Eoceno) del Pacifico Central de Costa Rica. *Revista Geologica de America Central*, *28*, 47–68.

Astorga, A. (1987). El Cretácico Superior y el Paleógeno de la vertiente pacífica de Nicaragua meridional y Costa Rica septentrional: Origen, evolución y dinámica de las cuencas profundas relacionadas al margen convergente de Centroamérica. Licensed Thesis, University of Costa Rica, 250pp.

Auer, W. F. (1942). Summary report of paleontology of Pacific coast area, Nicaragua. Catastro-Managua, 18 pp.

Baitsch-Ghirardello, B., Gerya, T. V., & Burg, J.-P. (2014). Geodynamic regimes of intra-oceanic subduction: Implications for arc extension vs. shortening processes. *Gondwana Research*, *25*, 546–560. https://doi.org/10.1016/j.gr.2012.11.003

Ballance, P. F., Scholl, D. W., Vallier, T. L., Stevenson, A. J., Ryan, H., & Herzer, R. H. (1989). Subduction of a Late Cretaceous Seamount of the Louisville Ridge at the Tonga Trench: A model of normal and accelerated tectonic erosion. *Tectonics*, *8*, 953–962. https://doi.org/10.1029/TC008i005p00953

Bandini, A. N., Baumgartner, P. O., Flores, K., Dumitrica, P., & Jackett, S.-J. (2011). Early Jurassic to early Late Cretaceous

radiolarians from the Santa Rosa accretionary complex (northwestern Costa Rica). *Ofioliti*, *36*, 1–35.

Barat, F., Mercier de Lépinay, B., Sosson, M., Müller, C., Baumgartner, P. O., & Baumgartner-Mora, C. (2014). Transition from the Farallon Plate subduction to the collision between South and Central America: Geological evolution of the Panama Isthmus. *Tectonophysics*, *622*, 145–167. https://doi.org/10.1016/j.tecto.2014.03.008

Barbosa, G., Astorga, A., Bottazzi, G., Barrientos, J., Muñoz, A., Darce, M., … Espinoza, M. (1993). Integrated petroleum evaluation report, Pacific margin, Sandino basin, Nicaragua. Inst. Nic. Energia-Refinadora Costarricense de Petroleo, Managua.

Barker, R. W. (1965). Notes on Miogypsinidae in the Gulf of Mexico region. In *D.N. Wadia commemorative volume*. Calcutta: Mining, Geological and Metallurgical Institute of India, pp. 306–342.

Baumgartner, P. O., Baumgartner-Mora, C., & Andjić, G. (2016). Late Cretaceous–Paleogene forearc sedimentation and accretion of oceanic plateaus and seamounts along the Middle American convergent margin (Costa Rica). EGU General Assembly, Vienna, vol. 18, EGU2016-7226.

Baumgartner, P. O., Baumgartner-Mora, C., Andjić, G., Salazar Ortiz, E. A., & Rincon Martinez, D. (2015). The role of short-lived Late Mesozoic–Tertiary Carbonate banks along convergent margins, Nicaragua-Costa Rica-Panama-Colombia. 20th Caribbean Geological Conference, Trinidad and Tobago, abstracts.

Baumgartner, P. O., & Denyer, P. (2006). Evidence for middle Cretaceous accretion at Santa Elena Peninsula (Santa Rosa Accretionary Complex), Costa Rica. *Geological Acta*, *4*, 179–191.

Baumgartner, P. O., Flores, K., Bandini, A. N., Girault, F., & Cruz, D. (2008). Upper Triassic to Cretaceous radiolaria from Nicaragua and northern Costa Rica – The Mesquito composite oceanic terrane. *Ofioliti*, *33*, 1–19.

Baumgartner, P. O., Mora, C. R., Butterlin, J., Sigal, J., Glacon, G., Azéma, J., & Bourgois, J. (1984). Sedimentación y paleogeografía del Cretácico y Cenozoico del litoral pacífico de Costa Rica. *Revista Geologica de America Central*, *1*, 57–136.

Baumgartner-Mora, C., & Baumgartner, P. O. (2016). Paleocene-earliest Eocene larger benthic foraminifera and Ranikothalia-bearing carbonate paleo-environments of Costa Rica (South Central America). *Micropaleontology*, *62*, 453–508.

Baumgartner-Mora, C., Baumgartner, P. O., & Tschudin, P. (2008). Late Oligocene Larger Foraminifera from Nosara, Nicoya Península (Costa Rica) and Windward, Carriacou (Lesser Antilles), calibrated by 87Sr/86Sr isotope stratigraphy. *Revista Geologica de America Central*, *38*, 33–52.

Berglar, K., Gaedicke, K., Franke, D., Ladage, S., Klingelhoefer, F., & Djajadihardja, Y. S. (2010). Structural evolution and strike-slip tectonics off north-western Sumatra. *Tectonophysics*, *480*, 119–132. https://doi.org/10.1016/j.tecto.2009.10.003

Berhorst, A. (2006). Die Struktur des aktiven Kontinentalhangs vor Nicaragua und Costa Rica: Marin-seismische Steil- und Weitwinkelmessungen. PhD thesis, Christian Albrechts Universität, Kiel, 153 pp.

Borgia, A., & devan Wyk Vries, B. (2003). The volcano-tectonic evolution of Concepción, Nicaragua. *Bulletin of Volcanology*, *65*, 248–266. https://doi.org/10.1007/s00445-002-0256-8

Bottazzi, G., Fernandez, A., & Barboza, G. (1994). Sedimentologia e historia tectono-sedimentaria de la cuenca Limón Sur. In H. Seyfried & W. Hellmann (Eds.), *Geology of an evolving Island arc: The isthmus of Southern Nicaragua, Costa Rica and Western Panamá. Profil (Stuttgart)*, *7*, 351–391.

Bouma, A. H. (1962). *Sedimentology of some flysch deposits: A graphic approach to facies interpretation*. Amsterdam: Elsevier, 168 pp.

Boutelier, D., & Cruden, A. R. (2017). Slab breakoff: Insights from 3D thermo-mechanical analogue modelling experiments. *Tectonophysics*, *694*, 197–213. https://doi.org/10.1016/j.tecto.2016.10.020

Brandes, C., Astorga, A., Littke, R., & Winsemann, J. (2008). Basin modelling of the Limón back-arc basin (Costa Rica): Burial history and temperature evolution of an island arc-related basin system. *Basin Research*, *20*, 119–142. https://doi.org/10.1111/j.1365-2117.2007.00345.x

Brandes, C., Astorga, A., & Winsemann, J. (2009). The Moín High, East Costa Rica: Seamount, laccolith or contractional structure? *Journal of South American Earth Sciences*, *28*, 1–13. https://doi.org/10.1016/j.jsames.2009.02.005

Buchs, D.M., Arculus, R.J., Baumgartner, P.O., Baumgartner-Mora, C., & Ulianov, A. (2010). Late Cretaceous arc development on the SW margin of the Caribbean Plate: Insights from the Golfito, Costa Rica, and Azuero, Panama, complexes. *Geochemistry, Geophysics, Geosystems*, *11*, Q07S24. https://doi.org/10.1029/2009gc002901

Buchs, D. M., Arculus, R. J., Baumgartner, P. O., & Ulianov, A. (2011). Oceanic intraplate volcanoes exposed: Example from seamounts accreted in Panama. *Geology*, *39*, 335–338. https://doi.org/10.1130/G31703.1

Buchs, D. M., Baumgartner, P. O., Baumgartner-Mora, C., Bandini, A. N., Jackett, S.-J., Diserens, M.-O., & Stucki, J. (2009). Late Cretaceous to Miocene seamount accretion and mélange formation in the Osa and Burica peninsulas (southern Costa Rica): Episodic growth of a convergent margin. In K. H. James, M. A. Lorente & J. Pindell (Eds.), *The origin and evolution of the caribbean plate*. *Geological Society of London, Special Publication*, *328*, 411–456. https://doi.org/10.1144/sp328.17

Buchs, D. M., Baumgartner, P. O., Baumgartner-Mora, C., Flores, K., & Bandini, A. N. (2011). Late Cretaceous to Miocene tectonostratigraphy of the Azuero area (west Panama) and the discontinuous accretion and subduction erosion along the Middle American margin. *Tectonophysics*, *512*, 31–46. https://doi.org/10.1016/j.tecto.2011.09.010

Buchs, D. M., Pilet, S., Baumgartner, P. O., Cosca, M., Flores, K. E., & Bandini, A. N. (2013). Low-volume intraplate volcanism in the Early/Middle Jurassic Pacific basin documented by accreted sequences in Costa Rica. *Geochemistry, Geophysics, Geosystems*, *14*, 1552–1568. https://doi.org/10.1002/ggge.20084

Bundschuh, J., & Alvarado, G. E. (Eds) (2007). *Central America: Geology, resources, hazards*. London: Taylor & Francis, vol. 1, 663 pp. https://doi.org/10.1201/9780203947043

Butler, R. W. H., & McCaffrey, W. D. (2010). Structural evolution and sediment entrainment in mass-transport complexes: Outcrop studies from Italy. *Journal of the Geological Society*, *167*, 617–631. https://doi.org/10.1144/0016-76492009-041

Cailleau, B., & Oncken, O. (2008). Past forearc deformation in Nicaragua and coupling at the megathrust interface: Evidence for subduction retreat? *Geochemistry, Geophysics, Geosystems*, *9*, Q03016. https://doi.org/10.1029/2007GC001754

Canora, C., Martínez-Díaz, J. J., Villamor, P., Berryman, K., Álvarez-Gómez, J. A., Capote, R., & Díaz, M. (2014). Structural

development of El Salvador fault zone. *Journal of Iberian Geology*, *40*, 471–488.

Carr, M. (1976). Underthrusting and quaternary faulting in Central America. *Geological Society of America Bulletin*, *87*, 825–829. https://doi.org/10.1130/0016-7606(1976) 87<825:UAQFIN>2.0.CO;2

Cassell, D. T., & Sen Gupta, B. K. (1989). Foraminiferal stratigraphy and paleoenvironments of the Tertiary Uscari Formation, Limon Basin, Costa Rica. *Journal of Foraminiferal Research*, *19*, 52–71. https://doi.org/10.2113/gsjfr.19.1.52

Cembrano, J., Lavenu, A., Yañez, G., Riquelme, R., Garcia, M., Gonzalez, G., & Hérail, G. (2007). Neotectonics. In T. Moreno, & W. Gibbons (Eds.), *The geology of Chile* (pp. 231–261). London: London Geological Society Press.

Clerc, C. (1998). *Foraminifères planctoniques en sections de la couverture du terrain de Nicoya (Costa Rica)*. Crétacé supérieur-Paléogène: Travail de diplôme, Université de Genève, 121 pp.

Clift, P., & Vannucchi, P. (2004). Controls on tectonic accretion versus erosion in subduction zones: Implications for the origin and recycling of the continental crust. *Reviews of Geophysics*, *42*, RG2001. https://doi.org/10.1029/2003rg000127

Clowser, D. R., Cutler, I., Girges, M.H., Laing, J.F., & Wall, D. (1993). Nicaragua (Project CAM-009): Biostratigraphic and geochemical studies of outcrop samples, Report No. 4782/IB, Project No. Ib/15429. Simon Petroleum Technology Limited, Llandudno, Gwynedd,.

Cole, W. S. (1957). Variation in American Oligocene species of Lepidocyclina. *Bulletins of American Paleontology*, *38*, 31–51.

Cruden, A. R. (1989). The structure of south-western Nicaragua: A preliminary assessment. Swedish Geological Company-SGAB/ Corporacion Nicaraguense de Minas-INMINE/Swedish Agency for Research Cooperation with Developing Countries-SAREC report, URAP 89001, 26 pp.

Cushman, J. A. (1920). The American species of Orthophragmina and Lepidocyclina. *U.S. Geological Survey Professional Paper*, *125D*, 39–105.

Darce, M., & Duarte, M. (2002). *Geologia de la Cuenca Sandino en costadentro, Nicaragua, Centro America*. Managua: Instituto Nicaragüense de Energia, 23 pp.

DeMets, C. (2001). A new estimate for present-day Cocos-Caribbean Plate motion: Implications for slip along the Central American volcanic arc. *Geophysical Research Letters*, *28*, 4043–4046. https://doi.org/10.1029/2001GL013518

Dengo, G. (1962). *Estudio Geológico de la Región de Guanacaste*. Instituto Geografico Nacional: Costa Rica. San José-Costa Rica, 112, pp.

Dengo, C. A. (2007). Petroleum geology. In J. Bundschuh & G. E. Alvarado (Eds.), *Central America: Geology, resources, hazards* (vol. 1, pp. 895–916). London: Taylor & Francis.

Dengo, G., & Case, J. E. (Eds) (1990). The geology of North America: The Caribbean region. *Geological Society of America*, *H*, 528.

Denyer, P., Aguilar, T., & Alvarado, G. E. (2003). Geologia y estratigrafia de la hoja Barranca, Costa Rica. *Revista Geológica de América Central*, *29*, 105–125.

Denyer, P., Aguilar, T., & Montero, W. (2014). *Cartografia geológica de la Peninsula de Nicoya*. Costa Rica: Estratigrafia y tectónica. Editorial Universidad de Costa Rica, 207 pp.

Denyer, P., & Alvarado, G. E. (2007). Mapa Geológico de Costa Rica 1: 400'000. Librería Francesa S.A

Denyer, P., & Gazel, E. (2009). The Costa Rican Jurassic to Miocene oceanic complexes: Origin, tectonics and relations. *Journal of South American Earth Sciences*, *28*, 429–442. https://doi.org/10.1016/j.jsames.2009.04.010

Di Marco, G. (1994). Les terrains accrétés du Costa Rica: Évolution tectonostratigraphique de la marge occidentale de la Plaque Caraïbe. *Mémoires de Géologie (Lausanne)*, *20*, 166.

Di Marco, G., Baumgartner, P. O., & Chanell, J. E. T. (1995). Late Cretaceous-Early Tertiary paleomagnetic data and a revised tectonostratigraphic subdivision of Costa Rica and western Panama. In P. Mann (Eds.), *Geologic and tectonic development of the Caribbean plate boundary in Southern Central America*. *Geological Society of America Special Paper*, *295*, 1–27.

Dickinson, W. R. (1995). Forearc basins. In C. J. Busby & R. V. Ingersoll (Eds.), *Tectonics of sedimentary basins* (pp. 221–261). Oxford: Blackwell Science.

Dorr, J. B. (1933). New data on the correlation of the Lower Oligocene of South and Central America with that of southern Mexico. *Journal of Paleontology*, *7*, 432–438.

Draut, A. E., & Clift, P. D. (2013). Differential preservation in the geologic record of intraoceanic arc sedimentary and tectonic processes. *Earth Science Reviews*, *116*, 57–84. https://doi.org/10.1016/j.earscirev.2012.11.003

Ehrenborg, J. (1996). A new stratigraphy for the Tertiary volcanic rocks of the Nicaraguan highland. *Geological Society of America Bulletin*, *108*, 830–842. https://doi.org/10.1130/0016-7606(1996)108<0830:ANSFTT>2.3.CO;2

Elming, S.-A., Layer, P., & Ubieta, K. (2001). A paleomagnetic study and age determinations of Tertiary rocks in Nicaragua, Central America. *Geophysical Journal International*, *147*, 294–309. https://doi.org/10.1046/j.0956-540x.2001.01526.x

Elming, S.-A., & Rasmussen, T. (1997). Results of magnetotelluric and gravimetric measurements in western Nicaragua, central America. *Geophysical Journal International*, *128*, 647–658. https://doi.org/10.1111/j.1365-246X.1997.tb05326.x

Elming, S.-A., Widenfalk, L., & Rodriguez, D. (Eds.) (1998). *Investigación geocientifica en Nicaragua 1981–1991* (p. 340). Suecia: Universidad Tecnologica de Lulea.

Escalante, G. (1990). The geology of southern Central America and western Colombia. In G. Dengo & J. E. Case (Eds.), *The geology of North America: The Caribbean region, The Decade of North American Geology*. *Geological Society of America*, *H*, 201–230.

Escuder-Viruete, J., & Baumgartner, P. O. (2014). Structural evolution and deformation kinematics of a subduction-related serpentinite-matrix mélange, Santa Elena Peninsula, northwest Costa Rica. *Journal of Structural Geology*, *66*, 356–381. https://doi.org/10.1016/j.jsg.2014.06.003

Escuder-Viruete, J., Baumgartner, P. O., & Castillo-Carrión, M. (2015). Compositional diversity in ophiolitic peridotites as result of a multi-process history: The Santa Elena ophiolite, northwest Costa Rica. *Lithos*, *231*, 16–34. https://doi.org/10.1016/j.lithos.2015.05.019

Fisher, D. M., Gardner, T. W., Marshall, J. S., Sak, P. B., & Protti, M. (1998). Effect of subducting sea-floor roughness on fore-arc kinematics, Pacific coast, Costa Rica. *Geology*, *26*, 467–470. https://doi.org/10.1130/0091-7613(1998)026<0467:EOSSFR>2.3.CO;2

Flores, K. (2003). Propuesta tectonoestratigráfica de la región septentrional del Golfo de Nicoya, Costa Rica. Licenciatura thesis, University of Costa Rica, 176 pp.

Flores, K. (2009). Mesozoic oceanic terranes of Southern Central America: Geology, geochemistry and geodynamics. PhD thesis, University of Lausanne, 290 pp.

Flores, K., Skora, S., Martin, C., Harlow, G. E., Rodríguez, D., & Baumgartner, P. O. (2015). Metamorphic history of riebeckite- and aegirine-augite-bearing high-pressure–low-temperature blocks within the Siuna Serpentinite Mélange, northeastern Nicaragua. *International Geology Review*, *57*, 943–977. https://doi.org/10.1080/00206814.2015.1027747

Flügel, E. (2010). *Microfacies of carbonate rocks* (2nd ed.). Berlin: Springer Verlag, pp. 657–724. https://doi.org/10.1007/978-3-642-03796-2

Funk, J., Mann, P., McIntosh, K., & Stephens, J. (2009). Cenozoic tectonics of the Nicaraguan depression, Nicaragua, and Median Trough, El Salvador, based on seismic-reflection profiling and remote-sensing data. *Geological Society of America Bulletin*, *121*, 1491–1521. https://doi.org/10.1130/B26428.1

Gammon, P. R., & James, N. P. (2001). Palaeogeographical influence on Late Eocene biosiliceous sponge-rich sedimentation, southern Western Australia. *Sedimentology*, *48*, 559–584. https://doi.org/10.1046/j.1365-3091.2001.00379.x

Gardner, T. W., Marshall, J., Merrits, D., Bee, B., Burgette, R., Burton, B., … Sak, P. (2001). Holocene forearc block rotation in response to seamount subduction, southeastern Peninsula de Nicoya, Costa Rica. *Geology*, *29*, 151–154. https://doi.org/10.1130/0091-7613(2001)029<0151:HFBRIR>2.0.CO;2

Garzanti, E., Radeff, G., & Malusà, M. G. (2018). Slab breakoff: A critical appraisal of a geological theory as applied in space and time. *Earth Science Reviews*, *177*, 303–319. https://doi.org/10.1016/j.earscirev.2017.11.012

Geist, E. L., Fisher, M. A., & Scholl, D. W. (1993). Large-scale deformation associated with ridge subduction. *Geophysical Journal International*, *115*, 344–366. https://doi.org/10.1111/j.1365-246X.1993.tb01191.x

Geldmacher, J., Hoernle, K., van den Bogaard, P., Hauff, F., & Klügel, A. (2008). Age and geochemistry of the Central American forearc basement (DSDP Leg 67 and 84): Insights into Mesozoic arc volcanism and seamount accretion on the fringe of the Caribbean LIP. *Journal of Petrology*, *49*, 1781–1815. https://doi.org/10.1093/petrology/egn046

Gerth, R., Silver, E., Marshall, J., Duarte, M., Carr, M., McIntosh, K., … Protti, M. (1999). La Boquita Terrace, Nicaragua: Evidence for uplift of the Central Pacific Coastal Zone. *Eos, Transactions of the American Geophysical Union*, *80*, F1033.

Gerya, T. V., Fossati, D., Cantieni, C., & Seward, D. (2009). Dynamic effects of aseismic ridge subduction: Numerical modelling. *European Journal of Minerology*, *21*, 649–661. https://doi.org/10.1127/0935-1221/2009/0021-1931

Gerya, T. V., & Meilick, F. I. (2011). Geodynamic regimes of subduction under an active margin: Effects of rheological weakening by fluids and melts. *Journal of Metamorphic Geology*, *29*, 7–31. https://doi.org/10.1111/j.1525-1314.2010.00904.x

Ghosal, D., Singh, S. C., Chauhan, A. P. S., & Hananto, N. D. (2012). New insights on the offshore extension of the Great Sumatran fault, NW Sumatra, from marine geophysical studies. *Geochemistry, Geophysics, Geosystems*, *13*, Q0AF06. https://doi.org/10.1029/2012gc004122

Green, G. L. (1930). Detailed reconnaissance geological report of the southwestern portion of Nicaragua, Central America. Catastro-Managua.

Guillaume, B., Funiciello, F., Faccenna, C., Martinod, J., & Olivetti, V. (2010). Spreading pulses of the Tyrrhenian Sea during the narrowing of the Calabrian slab. *Geology*, *38*, 819–822. https://doi.org/10.1130/G31038.1

Guy-Olson, D. (1998). Palinomorfos de la cuenca Terciaria ante arco en el SW de Nicaragua. In S. A. Elming, L. Widenfalk, & D. Rodriguez (Eds.), *Investigación geocientifica en Nicaragua 1981–1991* (pp. 117–128). Suecia: Universidad Tecnologica de Lulea.

Hauff, F., Hoernle, K., van den Bogaard, P., Alvarado, G., & Garbe-Schönberg, D. (2000). Age and geochemistry of basaltic complexes in western Costa Rica: Contributions to the geotectonic evolution of Central America. *Geochemistry, Geophysics, Geosystems*, *1*, 1009. https://doi.org/10.1029/1999GC000020

Hayes, C. W. (1899). Physiography and geology of region adjacent to the Nicaragua canal route. *Geological Society of America Bulletin*, *10*, 285–448. https://doi.org/10.1130/GSAB-10-285

Hayward, B. W., Carter, R., Grenfell, H. R., & Hayward, J. J. (2001). Depth distribution of recent deep-sea benthic foraminifera east of New Zealand, and their potential for improving paleobathymetric assessments of Neogene microfaunas. *New Zealand Journal of Geology and Geophysics*, *44*, 555–587. https://doi.org/10.1080/00288306.2001.9514955

Hoffstetter, R., Dengo, G., Dixon, C. G., Meyer-Abich, H., Weyl, R., Woodring, W. P., & Zoppis Bracci, L. (1960). Nicaragua. In R. Hoffstetter) (Ed.), *Lexique stratigraphique international* (V2a, pp. 171–224). Paris: CNRS.

Holbourn, A., Henderson, A. S., & Macleod, N. (2013). *Atlas of benthic foraminifera*. Oxford: Wiley-Blackwell, 654 pp. https://doi.org/10.1002/9781118452493

Iturralde-Vinent, M., & Gahagan, L. (2002). Latest Eocene to Middle Miocene tectonic evolution of the Caribbean: Some principles and their implications for plate tectonic modeling. In T. A. Jackson (Ed.), *Caribbean geology into the third millennium* (pp. 47–62). Transactions of the Fifteenth Caribbean Geological Conference, Kingston.

Iturralde-Vinent, M., & MacPhee, R. (1999). Paleogeography of the Caribbean region, implications for Cenozoic biogeography. *Bulletin of the American Museum of Natural History*, *238*, 1–95.

Jaccard, S., Münster, M., Baumgartner, P. O., Baumgartner-Mora, C., & Denyer, P. (2001). Barra Honda (Upper Paleocene – Lower Eocene) and El Viejo (Campanian - Maastrichtian) carbonate platforms in the Tempisque area (Guanacaste, Costa Rica). *Revista Geologica de America Central*, *24*, 9–28.

Jarrard, R. D. (1986). Relations among subduction parameters. *Reviews of Geophysics*, *24*, 217–284. https://doi.org/10.1029/RG024i002p00217

Jordan, T. E., Burns, W. M., Veiga, R., Pangaro, F., Copeland, P., Kelley, S., & Mpodozis, C. (2001). Mid-Cenozoic intra-arc basins in the southern Andes. *Tectonics*, *20*, 308–324. https://doi.org/10.1029/1999TC001181

Joy, O. T. (1941). Structure and stratigraphy of the Rivas area, Department of Rivas, Nicaragua. Unpublished.

Kirby, M. X., & Jackson, J. B. C. (2004). Extinction of a fast-growing oyster and changing ocean circulation in Pliocene tropical America. *Geology*, *32*, 1025–1028. https://doi.org/10.1130/G21039.1

Knaust, D. (2009). Characterisation of a Campanian deep-sea fan system in the Norwegian Sea by means of ichnofabrics. *Marine and Petroleum Geology*, *26*, 1199–1211. https://doi.org/10.1016/j.marpetgeo.2008.09.009

Kobayashi, D., LaFemina, P., Geirsson, H., Chichaco, E., Abrego, A. A., Mora, H., & Camacho, E. (2014). Kinematics of the western Caribbean: Collision of the Cocos Ridge and upper plate deformation. *Geochemistry, Geophysics, Geosystems*, *15*, 1671–1683. https://doi.org/10.1002/2014GC005234

Kolarsky, R. A., Mann, P., Monechi, S., Meyerhoff, H. D., & PessagnoJr, E. A. (1995). Stratigraphic development of southwestern Panama as determined from integration of marine seismic data and onshore geology. In P. Mann (Ed.), *Geologic and tectonic development of the Caribbean plate boundary in southern Central America*. *Geological Society of America Special Paper*, *295*, 159–200. https://doi.org/10.1130/SPE295

Kolb, W., & Schmidt, H. (1991). Depositional sequences associated with equilibrium coastlines in the Neogene of South-Western Nicaragua. In D. I. M. Macdonald (Ed.), *Sedimentation, tectonics and eustasy: Sea-level changes at active margins*. *SEPM Special Publications*, *12*, 259–272.

Krawinkel, H., & Kolb, W. (1994). Sequential aspects of the El Fraile Formation (Nicaragua Through, SW Nicaragua). In H. Seyfried & W. Hellmann (Eds.), *Geology of an evolving Island arc: The isthmus of Southern Nicaragua, Costa Rica and Western Panamá*. *Profil (Stuttgart)*, *7*, 325–333.

Krawinkel, H., Seyfried, H., Calvo, C., & Astorga, A. (2000). Origin and inversion of sedimentary basins in southern Central America. *Zeitschrift für Angewandte Geologie, Sonderheft SH*, *1*, 71–77.

Kuang, S. J. (1971). Estudio geologico del Pacifico de Nicaragua. Catastro de Inventario de Recursos naturales, Division de Geologia, 10, 101.

Kumpulainen, R. A., Högdahl, K., Olafsson, G., Muñoz, A., & Valle, M. (1998). Sedimentologia y sstratigrafia de la cueanca ant arco en el suroeste de Nicaragua. In S. A. Elming, L. Widenfalk, & D. Rodriguez (Eds.), *Investigación geocientifica en Nicaragua 1981–1991* (pp. 107–116). Suecia: Universidad Tecnologica de Lulea.

LaFemina, P., Dixon, T.H., Govers, R., Norabuena, E., Turner, H., Saballos, A., … Strauch, W. (2009). Fore-arc motion and Cocos Ridge collision in Central America. *Geochemistry, Geophysics, Geosystems*, *10*, Q05S14. https://doi.org/10.1029/2008gc002181

Lallemand, S., Heuret, A., Faccenna, C., & Funiciello, F. (2008). Subduction dynamics as revealed by trench migration. *Tectonics*, *27*, TC3014. https://doi.org/10.1029/2007tc002212

Lang, J., Brandes, C., & Winsemann, J. (2017). Erosion and deposition by supercritical density flows during channel avulsion and backfilling: Field examples from coarse-grained deepwater channel-levée complexes (Sandino Forearc Basin, southern Central America). *Sedimentary Geology*, *349*, 79–102. https://doi.org/10.1016/j.sedgeo.2017.01.002

Legg, M. R., Kohler, M. D., Shintaku, N., & Weeraratne, D. S. (2015). High resolution mapping of two large-scale transpressional fault zones in the California Continental Borderland: Santa Cruz-Catalina Ridge and Ferrelo faults. *Journal of Geophysical Research: Earth Surface*, *120*, 915–942. https://doi.org/10.1002/2014JF003322

Lissinna, B. (2005). A profile through the Central American Landbridge in western Panama: 115 Ma interplay between the Galápagos Hotspot and the Central American Subduction Zone, PhD thesis, Christian Albrechts University, Kiel, Germany, 102 pp.

Lissinna, B., Hoernle, K., & vanden Bogaard, P. (2002). Northern migration of arc volcanism in western Panama: Evidence for subduction erosion? AGU Fall Meeting, abstract #V11A-1368.

Lohmann, W., & Brinkmann, M. (1931). Uber obereocäne Kalke, Gabbros, und Andesite von Costa Rica. *Zentralblatt für Mineralogie, Geologie und Paläontologie Abt.*, *10*, 553–559.

Lonsdale, P. (2005). Creation of the Cocos and Nazca plates by fission of the Farallon plate. *Tectonophysics*, *404*, 237–264. https://doi.org/10.1016/j.tecto.2005.05.011

MacKenzie, L., Abers, G.A., Fischer, K.M., Syracuse, E.M., Protti, J.M., Gonzalez, V., & Strauch, W. (2008). Crustal structure along the southern Central American volcanic front. *Geochemistry, Geophysics, Geosystems*, *9*, Q08S09. https://doi.org/10.1029/2008gc001991

Madrigal, P., Gazel, E., Denyer, P., Smith, I., Jicha, B., Flores, K. E., … Snow, J. (2015). A melt-focusing zone in the lithospheric mantle preserved in the Santa Elena ophiolite, Costa Rica. *Lithos*, *230*, 189–205. https://doi.org/10.1016/j.lithos.2015.04.015

Mann, P. (Ed.) (1995). Geologic and tectonic development of the Caribbean plate boundary in Southern Central America. *Geological Society of America, Special Paper*, *295*, 349 pp.

Mann, P. (2007). Overview of the tectonic history of northern Central America. In P. Mann (Ed.), *Geologic and tectonic development of the Caribbean plate boundary in northern Central America*. *Geological Society of America, Special Paper*, *428*, 1–19.

Mann, P., & Burke, K. (1984). Cenozoic rift formation in the northern Caribbean. *Geology*, *12*, 732–736. https://doi.org/10.1130/0091-7613(1984) 12<732:CRFITN>2.0.CO;2

Mann, P., & Kolarsky, R. A. (1995). East Panama deformed belt; structure, age, and neotectonic significance. In P. Mann (Ed.), *Geologic and tectonic development of the Caribbean plate boundary in southern Central America*. *Geological Society of America Special Paper*, *295*, 111–130. https://doi.org/10.1130/SPE295

Mann, P., Rogers, R.D., & Gahagan, L. (2007). Overview of plate tectonic history and its unresolved tectonic problems. In J. Bundschuh & G.E. Alvarado (Eds.), *Central America: Geology, resources, hazards* (Vol. 1, pp. 201–241). London: Taylor and Francis.

Mann, P., Taylor, F. W., Lagoe, M. B., Quarles, A., & Burr, G. (1998). Accelerating late Quaternary uplift of the New Georgia Island Group (Solomon island arc) in response to subduction of the recently active Woodlark spreading center and Coleman seamount. *Tectonophysics*, *295*, 259–306. https://doi.org/10.1016/S0040-1951(98)00129-2

Marshall, J. S., & Vannucchi, P. (2003). Forearc deformation influenced by subducting plate morphology and upper plate discontinuity, Pacific Coast, Costa Rica. GSA 99th Annual Meeting, Cordilleran section, 33-3.

Martinez, F., & Taylor, B. (2006). Modes of crustal accretion in back-arc basins: Inferences from the Lau Basin. In D. M. Christie, C. R. Fisher, S. M. Lee & S. Givens (Eds.), *Back-arc spreading systems: Geological, biological, chemical, and physical interactions*. Washington, DC: American Geophysical Union. https://doi.org/10.1029/166gm03

Martinod, J., Guillaume, B., Espurt, N., Faccenna, C., Funiciello, F., & Regard, V. (2013). Effect of aseismic ridge subduction on slab geometry and overriding plate deformation: Insights from analogue modeling. *Tectonophysics*, *588*, 39–55. https://doi.org/10.1016/j.tecto.2012.12.010

McBirney, A., & Williams, H. (1965). Volcanic history of Nicaragua. *University of California Publications in Geological Science*, *55*, 1–73.

McCaffrey, R. (1992). Oblique plate convergence, slip vectors, and forearc deformation. *Journal of Geophysical Research*, *97*, 8905–8915. https://doi.org/10.1029/92JB00483

McIntosh, K. D., Silver, E. A., Ahmed, I., Berhorst, A., Ranero, C. R., Kelly, R. K., & Flueh, E. R. (2007). The Nicaragua convergent margin. In T. H. Dixon & J. C. Moore (Eds.), *The seismogenic zone of subduction thrust faults, Part III* (pp. 257–287). New York, NY: Columbia University of Press.

Meffre, S., & Crawford, A. J. (2001). Collision tectonics in the New Hebrides arc (Vanuatu). *Island Arc*, *10*, 33–50. https://doi.org/10.1046/j.1440-1738.2001.00292.x

Mende, A. (2001). Sedimente und Architektur der Forearc- und Back-arc-Becken von Südost-Costa Rica und Nordwest-Panamá. *Profil (Stuttgart)*, *19*, 130.

Miller, K. G., Kominz, M. A., Browning, J. V., Wright, J. D., Mountain, G. S., Katz, M. E., … Pekar, S. F. (2005). The Phanerozoic record of global sea-level change. *Science*, *310*, 1293–1298. https://doi.org/10.1126/science.1116412

Mitra, S. (2002). Fold-accomodation faults. *AAPG Bulletin*, *86*, 671–693.

Montero, P. W., & Denyer, P. (2011). Fallamiento neotectónico de la Península de Nicoya y su relación con el escape tectónico delantearco Centroamericano. *Revista Geologica de America Central*, *45*, 9–52.

Montes, C., Bayona, G., Cardona, A., Buchs, D. M., Silva, C. A., Morón, S., … Valencia, V. (2012). Arc-continent collision and orocline formation: Closing of the Central American seaway. *Journal of Geophysical Research*, *117*, B04105. https://doi.org/10.1029/2011JB008959

Montes, C., Cardona, A., McFadden, R., Moron, S. E., Silva, C. A., Restrepo-Moreno, S. A, … Bayona, G. A. (2012). Evidence for middle Eocene and younger emergence in Central Panama: Implications for Isthmus closure. *Geological Society of American Bulletin*, *124*, 780–799. https://doi.org/10.1130/b30528.1

Morán-Zenteno, D. J., Keppie, J. D., Martiny, B., & González-Torres, E. (2009). Reassessment of the Paleogene position of the Chortis block relative to southern Mexico: Hierarchical ranking of data and features. *Revista Mexicana de Ciencias Geológicas*, *26*, 77–188.

Morell, K. D. (2015). Late Miocene to recent plate tectonic history of the southern central America convergent margin. *Geochemistry, Geophysics, Geosystems*, *16*, 3362–3382. https://doi.org/10.1002/2015GC005971

Mosher, D. C., Austin, J. A. Jr, Fisher, D., & Gulick, S. P. S. (2008). Deformation of the northern Sumatra accretionary prism from high-resolution seismic reflection profiles and ROV observations. *Marine Geology*, *252*, 89–99. https://doi.org/10.1016/j.margeo.2008.03.014

Muñoz, A., Artiles, U., Duarte, M., & Barboza, G. (1997). Nicaragua: Petroleum geology of the Caribbean margin. *The Leading Edge*, *16*, 1799–1805.

Mutti, E., & Ricci Lucchi, F. (1978). Turbidites of the northern Apennines: Introduction to facies analysis. *American Geological Institute, Reprint Series*, *3*, 127–166.

Nakano, M., Kumagai, H., Toda, S., Ando, R., Yamashina, T., Inoue, H., & Sunarjo. (2010). Source model of an earthquake doublet that occurred in a pull-apart basin along the Sumatran fault, Indonesia. *Geophysical Journal International*, *181*, 141–153. https://doi.org/10.1111/j.1365-246x.2010.04511.x

Noda, A. (2016). Forearc basins: Types, geometries, and relationships to subduction zone dynamics. *Geological Society of America Bulletin*, *B31345*, 1. https://doi.org/10.1130/B31345.1

Norabuena, E., Dixon, T., Schwartz, S., DeShon, H., Newman, A., Protti, M., … Sampson, D. (2004). Geodetic and seismic constraints on some seismogenic zone processes in Costa Rica. *Journal of Geophysical Research*, *109*, B11403. https://doi.org/10.1029/2003JB002931

Normark, W. R., Posamentier, H., & Mutti, E. (1993). Turbidite systems: State of the art and future directions. *Reviews of Geophysics*, *31*, 91–116. https://doi.org/10.1029/93RG02832

Obando Rodriguez, J. A. (1986). Sedimentología y tectónica del Cretacico y Paleógeno de la región de Golfito, Península de Burica y Península de Osa, Provincia de Puntarenas, Costa Rica. Tesis de Licenciatura. Escuela Centroamericana de Geología, Universidad de Costa Rica (unpubl).

Petters, V., & Sarmiento, R. (1956). Oligocene and lower Miocene biostratigraphy of the Carmen-Zambraon Area, Colombia. *Micropaleontology*, *2*, 7–35. https://doi.org/10.2307/1484490

Pindell, J. L., & Kennan, L. (2009). Tectonic evolution of the Gulf of Mexico, Caribbean and northern South America in the mantle reference frame: An update. In: *The Origin and evolution of the Caribbean plate* (Eds K. James, M. A. Lorente & J.L. Pindell), *Geological Society of London Special Publications*, *328*, 1–55.

Pindell, J., Kennan, L., Stanek, K., Maresch, W., & Draper, G. (2006). Foundations of Gulf of Mexico and Caribbean evolution: Eight controversies resolved. *Geologica Acta*, *4*, 303–341.

Plank, T., Balzer, V., & Carr, M. J. (2002). Nicaraguan volcanoes record paleoceanographic changes accompanying closure of the Panama Gateway. *Geology*, *30*, 1087–1090. https://doi.org/10.1130/0091-7613(2002)030<1087:NVRPCA>2.0.CO;2

Pons, J. M., Vicens, E., & Schmidt-Effing, R. (2016). Campanian rudists (Hippuritida, Bivalvia) from Costa Rica (Central America). *Journal of Paleontology*, *90*, 211–238. https://doi.org/10.1017/jpa.2016.27

Ranero, C., von Huene, R., Flueh, E., Duarte, M., Baca, D., & McIntosh, K. (2000). A cross section of the convergent Pacific margin of Nicaragua. *Tectonics*, *19*, 335–357. https://doi.org/10.1029/1999TC900045

Rasser, M. W. (2001). Influence of bottom stability and sediment input on growth forms of Polystrata alba (red algae) from the Late Eocene Alpine Foreland: A new tool for the reconstruction of sedimentary environments. *Palaios*, *16*, 532–538.

Renz, H. H. (1948). Stratigraphy and fauna of the Agua Salada group, State of Falcon, Venezuela. *Geological Society of America Memoirs*, *32*, 129.

Retallack, G. J. (2001). *Soils of the past. An introduction to paleopedology* (2nd edn). Oxford, UK: Blackwell Science, 404 pp.

Rivier, F., & Calvo, C. (1988). Terciario del sur del Valle Central: Seccion estratigrafica del Cerro Caraigres, Provincia de San Jose, Costa Rica. *Revista Geológica de América Central*, *9*, 61–74.

Rogers, R., Karason, H., & van der Hilst, R. (2002). Epeirogenic uplift above a detached slab in northern Central America. *Geology*, *30*, 1031–1034. https://doi.org/10.1130/0091-7613(2002)030<1031:EUAADS>2.0.CO;2

Rogers, R. D., & Mann, P. (2007). Transtensional deformation of the western Caribbean-North America plate boundary zone. In P. Mann (Ed.), *Geologic and tectonic development of the Caribbean plate in northern Central America*. *Geological Society of America Special Papers*, *428*, 37–64. https://doi.org/10.1130/2007.2428(03)

Rogers, R. D., Mann, P., & Emmet, P. A. (2007). Tectonic terranes of the Chortis block based on integration of regional aeromagnetic and geologic data. In P. Mann (Ed.), *Geologic and tectonic development of the Caribbean plate in northern Central America*. *Geological Society of America Special Paper*, *428*, 65–88. https://doi.org/10.1130/2007.2428(04)

Rogers, R. D., Mann, P., Emmet, P. A., & Venable, M. E. (2007). Colon fold belt of Honduras: Evidence for Late Cretaceous collision between the continental Chortis block and intra-oceanic Caribbean arc. In P. Mann (Ed.), *Geologic and tectonic development of the Caribbean plate in northern Central America*. *Geological Society of America Special Paper*, *428*, 129–149. https://doi.org/10.1130/2007.2428(06)

Rogers, R. D., Mann, P., Scott, R. W., & Patino, L. (2007). Cretaceous intra-arc rifting, sedimentation, and basin inversion in east-central Honduras. In P. Mann (Ed.), *Geologic and tectonic development of the Caribbean plate in northern Central America*. *Geological Society of America Special Paper*, *428*, 89–128. https://doi.org/10.1130/2007.2428(05)

Rosencrantz, E., Ross, M. I., & Sclater, J. G. (1988). Age and spreading history of the Cayman Trough as determined from depth, heat flow, and magnetic anomalies. *Journal of Geophysical Research*, *93*, 2141–2157. https://doi.org/10.1029/JB093iB03p02141

Rutten, M. G. (1935). Larger Foraminifera of northern Santa Clara Province, Cuba. *Journal of Paleontology*, *11*, 527–545.

Ryan, H. F., & Scholl, D. W. (1989). The evolution of forearc structures along an oblique convergent margin, central Aleutian Arc. *Tectonics*, *8*, 497–516. https://doi.org/10.1029/TC008i003p00497

Sadeghi, R., Vaziri-Moghaddam, H., & Taheri, A. (2011). Microfacies and sedimentary environment of the Oligocene sequence (Asmari Formation) in Fars sub-basin, Zagros Mountains, southwest Iran. *Facies*, *57*, 431–446. https://doi.org/10.1007/s10347-010-0245-x

Saginor, I., Gazel, E., Carr, M., Swisher, C. III, & Turrin, B. (2011). New Pliocene-Pleistocene 40Ar/39Ar ages fill in temporal gaps in the Nicaraguan volcanic record. *Journal of Volcanology and Geothermal Research*, *202*, 143–152. https://doi.org/10.1016/j.jvolgeores.2011.02.002

Saginor, I., Gazel, E., Condie, C., & Carr, M. J. (2013). Evolution of geochemical variations along the Central American volcanic front. *Geochemistry, Geophysics, Geosystems*, *14*, 4504–4522. https://doi.org/10.1002/ggge.20259

Sak, P. B., Fisher, D. M., Gardner, T. W., Marshall, J. S., & La Femina, P. C. (2009). Rough crust subduction, forearc kinematics, and Quaternary uplift rates, Costa Rican segment of the Middle America Trench. *Geological Society of America Bulletin*, *121*, 992–1012. https://doi.org/10.1130/B26237.1

Sallarès, V., Meléndez, A., Prada, M., Ranero, C. R., McIntosh, K., & Grevemeyer, I. (2013). Overriding plate structure of the Nicaragua convergent margin: Relationship to the seismogenic zone of the 1992 tsunami earthquake. *Geochemistry, Geophysics, Geosystems*, *14*, 3436–3461. https://doi.org/10.1002/ggge.20214

Saller, A., Richard, A., La Ode, I., & Glenn-Sullivan, C. (1993). Sequence stratigraphy of aggrading and backstepping carbonate shelves, Oligocene, central Kalimantan, Indonesia. In *Carbonate sequence stratigraphy: Recent developments and applications* (Eds R.G. Loucks & J.F. Sarg), *AAPG Memoirs*, 267–290.

Sanchez, J., Mann, P., & Emmet, P. A. (2015). Late Cretaceous–Cenozoic tectonic transition from collision to transtension, Honduran Borderlands and Nicaraguan Rise, NW Caribbean Plate boundary. In M. Nemcok, S. Rybar, S. T. Sinha, S. A. Hermeston & L. Ledvenyiova (Eds.), *Transform margins: Development, controls and petroleum systems*. *Geological Society of London Special Publications*, *431*, 273–297.

Sandwell, D. T., & Smith, W. H. F. (1997). Marine gravity anomaly from Geosat and ERS 1 satellite altimetry. *Journal of Geophysical Research*, *102*, 10039–10054. https://doi.org/10.1029/96JB03223

Sartorio, D., & Venturini, S. (1988). *Southern tethys biofacies*. San Donato Milanese: Agip, 235 pp.

Schellart, W. P. (2008). Overriding plate shortening and extension above subduction zones: A parametric study to explain formation of the Andes Mountains. *Geological Society of America Bulletin*, *120*, 1441–1454. https://doi.org/10.1130/B26360.1

Schmidt-Effing, R. (1974). El primer hallazgo de amonites en América Central Meridional y notas sobre facies cretácicas en dicha región. *Informe Semestral, IGN*, *1*, 53–61.

Seno, T. (2007). Collision versus subduction: From a viewpoint of slab dehydration. In T. H. Dixon & J. C. Moore (Eds.), *The seismogenic zone of subduction thrust faults* (Part III, pp. 601–623). New York, NY: Columbia University Press.

Seyfried, H., & Sprechmann, P. (1985). Acerca de la formación del puente-istmo Centroamericano Meridional, con énfasis en el desarrollo acaecido desde Campanénse al Eoceno. *Revista Geologica de America Central*, *2*, 63–87.

Sharp, I. R., Gawthorpe, R. L., Underhill, J. R., & Gupta, S. (2000). Fault-propagation folding in extensional settings: Examples of structural and synrift sedimentary response from the Suez rift, Sinai, Egypt. *Geological Society of American Bulletin*, *112*, 1877–1899. https://doi.org/10.1130/0016-7606(2000)112<1877:FPFIES>2.0.CO;2

Spikings, R., & Simpson, G. (2014). Rock uplift and exhumation of continental margins by the collision, accretion, and subduction of buoyant and topographically prominent oceanic crust. *Tectonics*, *33*, 635–655. https://doi.org/10.1002/2013TC003425

Sprechmann, P., Astorga, A., Calvo, C., & Fernández, A. (1994). Stratigraphic chart of the sedimentary basins of Costa Rica, Central America. In H. Seyfried & W. Hellmann (Eds.), *Geology of an evolving Island arc: The isthmus of Southern Nicaragua, Costa Rica and Western Panamá*. *Profil (Stuttgart)*, *7*, 427–433.

Stephens, J. H. (2014). Tectonic and depositional history of an active forearc basin, Sandino basin, offshore Nicaragua. PhD thesis, University of Texas, Dallas, 128 pp.

Stephens, J. H., Fulthorpe, C., & McIntosh, K. (2007). Seismic stratigraphy and tectonics of the Sandino forearc basin, offshore Nicaragua. In National Science Foundation (NSF) Margins Meeting Abstracts. San José, Costa Rica. http://www.nsf-margins.org/CostaRica2007/all_abstracts.pdf.

Struss, I. (2008). The petroleum potential of the Sandino Forearc Basin. PhD thesis, Universität Hannover, 176 pp.

Struss, I., Artiles, V., Cramer, B., & Winsemann, J. (2008). The petroleum system in the Sandino forearc basin, offshore western Nicaragua. *Journal of Petroleum Geology*, *31*, 221–244. https://doi.org/10.1111/j.1747-5457.2008.00418.x

Struss, I., Brandes, C., Blisniuk, P. M., & Winsemann, J. (2007). Eocene deep-water channel-levee deposits, Nicaragua: Channel geometries and internal deformation patterns of six outcrops. In T. H. Nilsen, R. D. Shew, G. S. Steffens & J. R. J. Studlick (Eds.), *Atlas of deep-water outcrops*. *AAPG Studies in Geology*, *56*, 31 pp. CD-ROM.

Székely, S.-F., & Filipescu, S. (2015). Taxonomic record of the Oligocene benthic foraminifera from the Vima Formation (Transylvanian Basin, Romania). *Acta Palaeontologica Romaniae*, *11*, 25–62.

Taylor, F. W., Mann, P., Bevis, M. G., Edwards, R. L., Cheng, H., Cutler, K. B, … Recy, J. (2005). Rapid forearc uplift and subsidence caused by impinging bathymetric features: Examples from the New Hebrides and Solomon arcs. *Tectonics*, *24*, TC6005. https://doi.org/10.1029/2004tc001650

Todd, R., & Low, D. (1976). Smaller foraminifera from deep wells on Puerto Rico and St. Croix. *USGS Professional Paper*, *863*, 32.

Turner, H. L., La Femina, P., Saballos, A., Mattioli, G., Jansma, P., & Dixon, T. (2007). Kinematics of the Nicaraguan forearc from GPS geodesy. *Geophysical Research Letters*, *34*, L02302. https://doi.org/10.1029/2006GL027586

Uchman, A., & Wetzel, A. (2012). Deep-sea fans. In D. Knaust & R. G. Bromley (Eds.), *Trace fossils as indicators of sedimentary environments*. *Developments in Sedimentology*, *64*, 643–671. https://doi.org/10.1016/B978-0-444-53813-0.00021-6

Van Wyk de Vries, B. (1993). Tectonics and Magma Evolution of Nicaraguan Volcanic Systems. PhD dissertation, Milton Keynes, UK, Open University, 328 pp.

Vaughan, T. W. (1918). Geological history of Central America and the West Indies during Cenozoic time. *Geological Society of America Bulletin*, *29*, 615–630. https://doi.org/10.1130/GSAB-29-615

Vogt, K., & Gerya, T. V. (2014). From oceanic plateaus to allochthonous terranes: Numerical modelling. *Gondwana Research*, *25*, 494–508. https://doi.org/10.1016/j.gr.2012.11.002

Walther, C. H. E., Flueh, E. R., Ranero, C. R., Von Huene, R., & Strauch, W. (2000). Crustal structure across the Pacific margin of Nicaragua: Evidence for ophiolitic basement and a shallow mantle sliver. *Geophysical Journal International*, *141*, 759–777. https://doi.org/10.1046/j.1365-246x.2000.00134.x

Weinberg, R. F. (1992). Neotectonic development of western Nicaragua. *Tectonics*, *11*(5), 1010–1017. https://doi.org/10.1029/92TC00859

Wetzel, A., & Uchman, A. (2001). Sequential colonization of muddy turbidites: Examples from Eocene Beloveza Formation, Carpathians, Poland. *Palaeogeography, Palaeoclimatology, Palaeoecology*, *168*, 171–186. https://doi.org/10.1016/S0031-0182(00)00254-6

Weyl, R. (1980). *Geology of Central America*. Berlin: Gebruder Borntraeger, 371 pp.

Whattam, S. A., Gazel, E., Yi, K., & Denyer, P. (2016). Origin of plagiogranites in oceanic complexes. A case study of the Nicoya and Santa Elena terranes, Costa Rica. *Lithos*, *262*, 75–87. https://doi.org/10.1016/j.lithos.2016.06.017

Whattam, S. A., Montes, C., McFadden, R. R., Cardona, A., Ramirez, D., & Valencia, V. (2012). Age and origin of earliest adakitic-like magmatism in Panama: Implications for the tectonic evolution of the Panamanian magmatic arc system. *Lithos*, *142–143*, 226–244. https://doi.org/10.1016/j.lithos.2012.02.017

Wiedenmayer, F. (1977). Shallow-water sponges of the Bahamas. *Experientia Supplementum*, *28*, 329. Springer, Basel.

Wilson, T. C. (1941a). Structure and stratigraphy of the San Rafael-El Carmen area, Department of Managua, Nicaragua, Unpublished.

Wilson, T. C. (1941b). Reconaissance geology of the southern portion of Léon Department, Nicaragua. Unpublished.

Wilson, T. C. (1942). Geology of Pacific Coast area, Nicaragua, summary report. Geological Survey of Nicaragua, Managua. Unpublished.

Wilson, J. L. (1975). *Carbonate facies in geologic history*. Berlin: Springer-Verlag, 471 pp. https://doi.org/10.1007/978-1-4612-6383-8

Wilson, D. S. (1996). Fastest known spreading on the Miocene Cocos-Pacific plate boundary. *Geophysical Research Letters*, *23*, 3003–3006. https://doi.org/10.1029/96GL02893

Winsemann, J. (1992). Tiefwasser-Sedimentationsprozesse und -produkte in den Forearc-Becken des mittelamerikanischen Inselbogensystems: Eine sequenzstratigraphische Analyse. *Profil (Stuttgart)*, *2*, 218.

Wray, J. L. (1977). Calcareous algae. *Developments in Paleontology and Stratigraphy*, *4*, 185.

Yuan, P. B. (1991). Comparative sedimentology of shallow-water limestones developed in active tectonic regions: Examples from Costa Rica, Central America and eastern Taiwan. In J. Cosgrove, & M. Jones (Eds.), *Neotectonics and resources* (pp. 43–64). London and New York: Belhaven Press.

Zoppis Bracci, L., & Del Giudice, D. (1958). Geologia de la costa del Pacifico de Nicaragua. *Boletín del Servicio Geológico Nacional de Nicaragua*, *2*, 19–68.

SUPPORTING INFORMATION

Additional Supporting Information may be found online in the supporting information tab for this article.

How to cite this article: Andjić G, Baumgartner-Mora C, Baumgartner PO, Petrizzo MR. Tectonostratigraphic response of the Sandino Forearc Basin (N-Costa Rica and W-Nicaragua) to episodes of rough crust and oblique subduction. *Depositional Rec*. 2018;4:90–132. https://doi.org/10.1002/dep2.40